# Characterization of the *LATERAL SUPPRESSOR* Promoter and the New Regulator of Axillary Meristem Formation *ENHANCER OF LATERAL SUPPRESSOR 5*

Inaugural - Dissertation

zur

Erlangung des Doktorgrades

der Mathematisch-Naturwissenschaftlichen Fakultät

der Universität zu Köln

vorgelegt von

Bodo Raatz

aus Paderborn

Köln 2009

Die vorliegende Arbeit wurde am Max-Planck-Institut für Züchtungsforschung in der Abteilung für Pflanzenzüchtung und Genetik (Direktor Prof. Dr. Maarten Koornneef) angefertigt.


Berichterstatter: Prof. Dr. Klaus Theres
Prof. Dr. Wolfgang Werr

Tag der mündlichen Prüfung: 17.11.2009

# Table of contents

# 1. Introduction

## 1.1. Meristem activities shape the development of plant architecture

The postembryonic development of flowering plants is based on the activity of meristems, groups of pluripotent cells from which all organs develop. During embryogenesis two groups of meristematic cells are established, the shoot apical meristem (SAM) and the root apical meristem (RAM), giving rise to the major axis of growth.

The RAM will form the main root and later develop lateral roots originating from the pericycle. The SAM will give rise to all aerial structures of the plant, initiating at first leaf and subsequently flower primordia. Lateral meristems develop in the axils of leaves, thereby establishing new growth axis. The controlled outgrowth of these lateral meristems and further SAM activity leads to the vast diversity observable in plant architecture.

### 1.1.1. Genetic regulation of meristem organization

The SAM is laid out during embryogenesis and consists of a group of self sustaining pluripotent cells. Various genes act in concert to maintain the number and identity of the meristem cell population. Knotted-like homeobox (*KNOX*) genes keep cells in an undifferentiated state. One of these, *SHOOT MERISTEMLESS* (*STM*), is expressed in the *Arabidopsis* shoot apex and is required for meristem initiation and maintenance (Barton & Poethig, 1993). Its vital importance can be deduced from *stm* mutants that fail to produce a SAM or true leaves.

The maintenance of the stem cell population relies on the *WUS*-*CLV* loop (Schoof *et al.*, 2000). The homeodomain transcription factor *WUSCHEL* (*WUS*) is expressed in the organizing centre, specifying the overlaying cells as stem cells. These are marked by *CLAVATA3* (*CLV3*) expression, a secreted protein expressed in stem cells, acting as a diffusible extracellular signal. The *CLV* signaling pathway also comprises the *CLV1 CLV2* receptor kinase complex expressed overlapping with *WUS*. They negatively regulate *WUS* expression upon binding of their ligand *CLV3*. *WUS* on the other hand activates the *CLV* pathway completing the feedback loop controlling the stem cell population. Accordingly

*wus* mutants loose meristematic activity leading to a stop-and-go growth characterized by terminating and reinitiating of meristems, whereas *clv* mutants show enlarged meristems (Laux *et al.*, 1996, Clark *et al.*, 1993).

AMs are formed in the axils of leaf primordia. Leaf primordia initiate at the flanks of the SAM, in a spatially and temporally precisely controlled fashion. Early markers of incipient leaf primordia are auxin response maxima, in which auxin flux in the L1 layer is directed towards a convergence point and subsequently inwards, forming a reverse fountain (deduced from intracellular localization of *PINFORMED 1*, Benkova *et al.*, 2003, Heisler *et al.*, 2005). Other early markers of incipient primordia development are the absence of *STM* transcript and the expression of leaf identity genes like *ASSYMMETRIC LEAVES 1* and *AINTEGUMENTA* (Byrne *et al.*, 2000, Elliot *et al.*, 1996).
At early stages in primordia development, preceding any morphological changes, genes involved in lateral meristem initiation like *REGULATOR OF AXILLARY MERISTEMS 1* (*RAX1*), *REGULATOR OF BRANCHING* (*ROB*/*bHLH140*), *CUP SHAPED COTYLEDON 1* (*CUC1*) and *LATERAL SUPPRESSOR* (*LAS*) are starting to be expressed at, or adjacent to, the position of forming primordia and later on at their adaxial side. Formation of new meristems can be linked to the activity of these proteins, as mutations in these genes show various defects in this process as described below.

At a later stage, around P16 in vegetative Columbia (Col) plants, lateral meristem development has progressed to a stage at which the meristematic marker *STM* shows a new focused expression (Greb *et al.*, 2003). Establishment of expression domains of other markers of meristem identity like *WUS* and *CLV* indicates the formation of a new meristem, which will then commence formation of new leaf and flower primordia.
The exact mechanism promoting axillary meristem fate of a specific cell group is poorly understood. One of the required signals is presumably to keep cells in an undifferentiated state. The nature of the signals leading to new cell identities, that may originate from the primordia, the SAM, or organ boundaries, remain to be uncovered.

### 1.1.2. Members of the GRAS Gene family control meristem initiation and organization

The plant specific GRAS gene family has been shown to play a role in different developmental processes, from meristem maintenance to hormone signaling (Bolle, 2004). The family is named after the prominent members *GAI*, *RGA* and *SCR*. Specific domains identifying GRAS proteins are a VHIID motif, roughly conserved in all members of the family, the two leucine-rich domains of approximately 100 AA residues length, and homologies near the C-terminus.

The GRAS proteins SCARECROW (SCR) and SHORT ROOT (SHR) are involved in root and shoot radial patterning. Mutants in either gene show, among a range of defects, that cortex and endodermis cell files are not properly established (Sabatini *et al.,* 2003, Helariutta *et al.,* 2000). SHR protein acts non–cell-autonomously and has been shown to upregulate and physically interact with SCR.

A mutation in the petunia gene *HAIRY MERISTEM* (*HAM*), which belongs to a different subfamily of GRAS genes, leads to the termination of the SAM and AMs. After cessation of meristem activity a layer of differentiated cells covers the tip of the shoot (Stuurman *et al.,* 2002).
A triple mutant of the homologous *Arabidopsis* genes *SCARECROW-LIKE 22* (*SCL22*), *SCL27*, and *SCL6* also displays SAM termination and side shoot formation defects. It could be shown in *Arabidopsis* that the mutations lead to a loss of meristem organization and polarity, as cell groups with meristematic identity are found displaced in lower cell layers (Schulze, 2007). These genes are targeted by miR171, accordingly *MIR171* overexpressor plants resemble *scl22 scl27 scl6* mutants.

GRAS proteins also act as signal transducers of GA, a plant hormone involved in many developmental processes. GA acts mostly as a differentiation signal, effecting e.g. growth habit, floral development, flowering time and seed germination (Fleet & Sun, 2005).
The DELLA-domain-containing proteins *GAI*, *RGA*, and *RGA-LIKE 1-3* are negative regulators of GA response. In the presence of GA these proteins are degraded via the ubiquitin/proteasome pathway, resulting in the derepression of target genes and thereby triggering the GA response.

The *Arabidopsis* GRAS gene *LAS* is an important regulator of AM development. The *las* mutant phenotype is characterized by a lack of AM formation during the vegetative phase, while side-shoots develop normally during the reproductive phase (Fig. 1A). During this work only the *las-4* allele was used, which carries a 20 bp deletion 365 bp after the ATG, henceforward referred to as *las*. *LAS* is expressed in very specific band-shaped domains adaxial of initiating leaf primordia (Greb *et al.*, 2003, Fig. 1C D). The expression domain coincides or lies closely adjacent to those cells, which will later give rise to AMs. As a close homolog of the DELLA domain proteins *GAI*, *RGA*, and *RGL1-3*, *LAS* may act on the same target genes. As *LAS* does not contain a DELLA domain, it will not be degraded upon presence of GA. Hence, a possible function of *LAS* could be to repress the GA response, which primarily means to keep cells in an undifferentiated state in presence of GA.

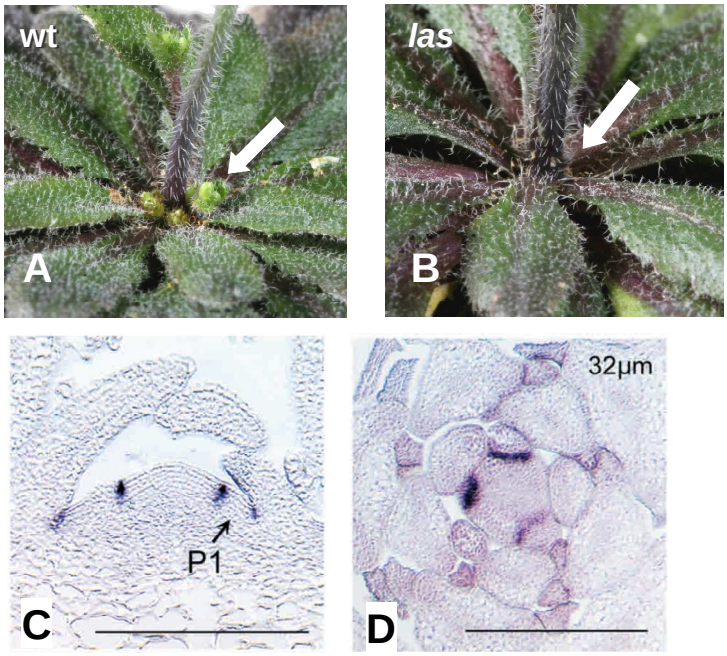


**Figure 1. Phenotype and expression profile of *LAS***

**A**, **B**, axillary bud formation observed in rosettes of wt (**A**) and *las* (**B**) plants. White arrows point towards buds or barren axils, respectively.
**C**, longitudinal and **D**, transverse sections showing *LAS* mRNA accumulation pattern by in situ hybridization, in a 28 d old vegetative Col (**C**) or Ler (**D**) plant. Pictures from Greb *et al.,* (2003), bars 200 µm.

### 1.1.3. Regulators controlling lateral meristem development

Next to the GRAS genes mentioned above, several *R2R3 MYB* genes have been shown to be involved in side shoot development. A mutation in the *RAX1* gene results in defects in axillary meristem development during the vegetative phase (Müller *et al.,* 2006). The triple mutant with the close paralogs *rax2* and *rax3* displays increased lateral meristem formation defects, also affecting cauline leaf axils. The lack of focused *STM* expression in the axils of later leaf primordia suggests that lateral meristem initiation is compromised early in development. Interestingly the *rax* mutants are aphenotypic in long day conditions, and mentioned defects only appear when plants have been grown in short days.

*ROB/bHLH140* could also be shown to be a regulator of branching, similar to the maize and rice homologs *BARREN STALK* and *LAX PANICLE*. *rob* mutants show minor defects in AM initiation in the rosette but enhance the mutant phenotypes of *las* and *rax1* (Yang, 2007). In concert with the supposed role in aiding AM development, *ROB* is expressed in specific expression domains adaxial of leaf primordia and *ROB* overexpressing plants develop accessory side shoots. Experiments indicate that *ROB* physically interacts with *RAX1*, which also shares the same expression domains (Yang, 2007).

Another group of genes that show specific expression domains in axils of leaf primordia are the NAC domain factors *CUC1, 2,* and *3*. A loss of function of *CUC3* was reported to lead to defects in axillary meristem development (Raman *et al.,* 2008). miR164 is a negative regulator of the close homologs *CUC1* and 2 (Rhoades *et al.,* 2002). miR164 overexpression enhances the *cuc3* phenotype, revealing redundant functions, while a loss of miR164 function leads to accessory bud formation, interpreted as deregulated, elevated activity of lateral meristems (Raman *et al.,* 2008).

The *eol5* mutant was discovered in a screen, designed to find modifiers of the *las-4* phenotype (Clarenz, 2004). *las-4* mutant seeds were mutagenized with EMS and M2 populations were analyzed for alterations of *las-4* phenotype. Two classes of mutants were isolated during this screen, the so called and *enhancers of lateral suppressor* (*eol*), in which the AM defects were extended into the cauline leaf axils, and the *suppressors of lateral suppressor* (*sol*), whose phenotype was modified to appear more similar to the wild-type (Clarenz, 2004, Raman, 2006).

This second-site mutagenesis screen was expected to identify mutations in genes that act in some way redundant with *LAS*, in the same or a different pathway. The limitations of a genetic screen are always lethal mutations and the redundancy of regulatory networks. A second-site screen is designed to partially overcome the problem of redundant factors that might mask low phenotypic changes of single mutants. As *las* constitutes a sensitized background, mutations could be detected, whose phenotypic changes would be too weak to be spotted in a screen in the wild-type background.
The *eol5* mutant was discovered during this second-site mutagenesis screen, as it increases the *las* loss of function phenotype. When grown in short days, side shoot formation is strongly reduced in cauline leaf axils, while no enhancement of the *las* phenotype is observable in long day conditions. Additionally, the *eol5 las* double mutant is reported to accelerate flowering and to develop longer inflorescences (Schulze, 2007).

### 1.1.4. Strategies to discover new regulators of AM initiation acting upstream of known genes

In order to uncover the genetic network controlling a process like AM initiation, the first step undertaken is usually the analysis of mutants, either derived from screens designed to detect a specific mutant phenotype, or from fortuitous observations. These approaches led to the discovery of various genes involved in AM formation. The currently available information about the process is gathered from their characterizations and interaction studies.

Yet many players cannot be identified this way, due to lethality or to redundancy preventing observable phenotypic alterations in mutants. Applying methods like yeast two-hybrid studies can identify interacting partners. Downstream targets are routinely sought-after utilizing expression arrays, detecting transcript changes caused by mutations.

Identifying transcriptional upstream regulators binding to the promoter of an investigated gene, is a more challenging task and therefore less common. One way to address this problem is to devise entirely new screens, e.g. utilizing gene-of-interest reporter gene constructs, or looking for reversions of gain-of-function mutations. Other techniques like yeast one-hybrid studies or DNA affinity purification aim to identify proteins binding to a

specific promoter fragment. These techniques require knowledge of the promoter regions of the investigated gene. Understanding promoter structure and function can give valuable insight in the process the gene is involved in. Information about timing and position of binding proteins improves understanding of the genetic processes.

Computational methods are not "yet" universally useful in understanding promoters. Most approaches are based on transcription factor binding motifs, which have aided understanding in various cases (e.g. auxin responsive genes, Chapman & Estelle, 2009). While some binding motifs are well described, others are either not known, or a description of protein-DNA interaction at a sequence level, based on single binding motifs, simply does not reflect the complexity of the underlying process (Florquin *et al.*, 2005).

With reasonable knowledge of the investigated promoter regions, yeast one-hybrid experiments are a suitable choice to find upstream regulators (Li and Herskowitz, 1993). While broad promoter regions can be used to search for interacting factors, many studies indicate that repeats of short sequences are favorable to produce the desired results (Deplancke *et al.*, 2004, BD Biosciences MATCHMAKER User Manual, 1998). Therefore a detailed promoter study, identifying the essential regions, is a suitable starting point to find upstream interactors and thereby increase understanding of the regulatory network.

In the case of *LAS*, upstream regulators are of special interest, as *LAS* is expressed in specific domains, including or neighboring those cells that will later give rise to AMs, and whose cell fate is affected in *las* mutants. Hence it is plausible that the function of *LAS* might be largely regulated on transcript expression level. This emphasizes the importance of understanding the establishment of the specific RNA accumulation pattern, i.e. investigating the *LAS* promoter and finding upstream regulators. Thus, promoter studies are applied to identify important elements that can later be utilized to find interacting factors by yeast one-hybrid experiments.

#### 1.1.4.1. Previous work on the *LAS* promoter

*Lateral suppressor (Ls)* was first studied in tomato, displaying a similar lack of side shoot formation in the *ls* mutant as described above for *Arabidopsis*. Additionally, defects occur during flower development, like a lack of petals and reduced flower numbers (Schumacher *et al.*, 1999).

Complementation experiments showed that comparatively large promoter regions are necessary for gene function. 1411 bp of 5' and 2667 bp of 3' regulatory sequences driving the *Ls* open reading frame (ORF) were found to be sufficient to produce a wild-type phenotype when transformed into the *ls* mutant. In contrast, a shorter construct with only 570 bp of 3' sequences did not lead to complementation (Schumacher *et al.*, 1999; Schmitt, 1999). The *Ls* gene was also shown to be functional in tomato, if the 3' regulatory sequences were in reverse orientation, a property typical for enhancer elements.

In order to individually complement the lack of AMs or the flower phenotype, transgenic constructs were produced, in which the 5' promoter was exchanged with the *PLENA* promoter, active in inflorescence meristems (Bradley *et al.*, 1993), or with the CET4 promoter (Amaya *et al.*, 1999), only active in the vegetative meristem. *ls* mutant plants transformed with these constructs exhibited no complementation. Only constructs carrying also the 3`sequences of *Ls* were able to confer complementation, leading to restoration of both phenotypes, irrespective of the 5' promoter (Gregor Schmitz, personal communication). This indicated that the 3' regulatory sequences are the decisive factor for a functional promoter.

Andrea Eicker (2005) showed that also in *Arabidopsis* the 3' promoter of *LAS* plays an important role. To identify important promoter regions, *las Arabidopsis* plants were transformed with numerous deletion constructs. In a first experiment constructs with 5' sequences of varying length were analyzed, all including 4000 bp of 3' sequences of the *LAS* gene. Secondly, different sized 3' promoter fragments were examined for their ability to complement. (In the 5' promoter distances always refer to the ATG, while 3' promoter sizes are measured from the stop codon.)
Fig. 2 summarizes the deletion construct analysis results (Eicker, 2005), illustrating that 820 bp upstream and 3547 bp downstream of the *LAS* gene are necessary for promoter function, whereas shortening of these sequences to 800 bp or 3133 bp respectively, resulted in the loss of complementation ability. These promoter regions shown to contain essential elements are depicted in red in Fig. 2. Additionally, partial complementation could be obtained, also with a short 3' region (488 bp), when using 2910 bp of 5' sequences, leading to ~ 60 % of rosette axils sustaining bud formation. These results indicate the presence of an enhancer element between 1447 and 2910 bp upstream of the ATG, which is partially redundant to the one downstream of the ORF.

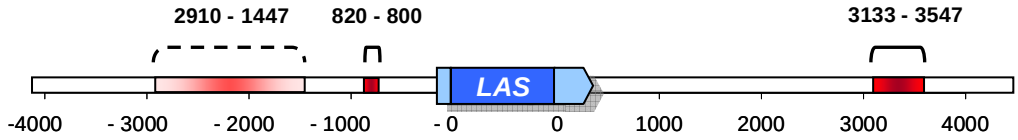


**Figure 2. Overview of relevant *LAS* promoter regions determined by deletion construct analysis.**

*LAS* CDS is depicted in blue, UTRs in light blue, regions shown to contain essential promoter elements in red. Numbers above parentheses state distance in bp between the indicated regions and the start, respectively stop codon of the *LAS* ORF. Dashed parenthesis indicates region leading to partial complementation in the absence of long 3' sequences.

## 1.2. Transcriptional control of gene expression

Transcriptional activation of genes is dependent on gene promoters, regions of DNA that lead to spatially and temporally specific activation of mRNA formation. That means these sequences result in the assembly of a transcription initiation complex at the transcription start site (TSS). This contains the DNA Polymerase II (PolII), which is responsible for transcribing mRNAs and some small RNAs (Pedersen *et al.*, 1999).

Promoters are commonly divided into 3 parts: the core promoter, the proximal, and the distal promoter (Abeel el al. 2008). The Core promoter usually extends 50 bp around the TSS and provides the platform to assemble the transcription initiation complex. In plants specific core promoter sequence elements seem less conserved than in animals. The most prominent is the TATA box, located ~ 30 bp upstream of the TSS, present at the TSS of ~ 30 % of *Arabidopsis* genes (Molina & Grotewold, 2005). Initiator elements (Inr) around the TSS have also been reported in several promoters (Shahmuradov *et al.*, 2003). In general no sequence conservation was found that could be used to predict a large number of core promoters (Molina & Grotewold, 2005). The lack of sequence conservation might be replaced by structural information, as Florquin *et al.*, (2005) described different classes of core promoters, based on structural properties. Structural characteristics, like DNA bending properties, may affect positioning of nucleosomes, providing easier access of proteins to certain DNA elements, and histones may aid specific DNA binding proteins by providing binding platforms.

In order to initiate transcription, core promoters need additional elements that provide binding sites for proteins. The proximal promoter is usually considered to include a region

of a few hundred bp upstream of the TSS, containing various binding motifs for transcription factors. Eukaryotic promoters usually contain binding sites for several TFs that positively or negatively affect formation and activation of the transcription initiation complex (Pedersen *et al.*, 1999).

Distal promoter elements can be localized at distance of several thousand bp and comprise additional regulatory elements named enhancers or silencers. Proteins binding to these elements are assumed to interact with proteins at the core or proximal promoter by looping of DNA. Enhancer or silencer elements can usually act independent of orientation and of their position ahead or behind the transcribed region of the gene. As all regulatory sequences behind the gene belong to the distal promoter, these regions will be referred to as 3' promoter in this work.

The actual activity of a promoter depends on different aspects. Obviously the number and location of motifs play an important part but only in combination with the composition of TFs present at a certain time. Proximal and distal promoters might also be defined by structural elements like DNA bending properties, influencing the nucleosome positioning and thereby TF binding stability. Another important factor is the chromatin state, limiting the accessibility of DNA to proteins, which is dependent on DNA methylation and histone modifications, as described below. (Pedersen *et al.*, 2005).

### 1.2.1. Chromatin modifications and their role in plant development

Substantial parts of the genome are in a densely packed state called heterochromatin, in which DNA is inaccessible to TFs. Heterochromatin is inherited through cell divisions. While large parts of the heterochromatin, like telomeric and centromeric regions, remain in this state, other regions of densely packed chromatin can convert to euchromatin in response to developmental cues. Derepression of DNA by unfolding of chromatin is an important part of gene regulation (Pedersen *et al.*, 1999). Chromatin state depends on chromatin marks, such as methylations of DNA and histones,

Histone and DNA methylation marks require further proteins that translate this information to induce heterochromatin formation. The HETEROCHROMATIN PROTEIN 1 (HP1), originally described in *Drosophila*, leads to heterochromatin formation and gene repression (Bannister *et al.,* 2001). HP1-like proteins are found in most eukaryotes ranging from *S. pombe* (Swi6) to human (HP1h) and plants (*LHP1*) (Berger & Gaudin, 2003).
The *Arabidopsis* gene *TFL2* e.g. is an HP1 homolog that recognizes H3K9 K27 methylation, leading to the formation of inactive chromatin (Steimer *et al.*, 2004). The *tfl2* mutant phenotype shares some similarities with the *curly leaf* (*clf*) mutant phenotype (see below), misexpressing homeotic genes and thus, appears to be one of the genes involved in translating histone methylation patterns into repressed chromatin state. Numerous other proteins can be expected to be involved in mediating chromatin condensation in response to heterochromatic methylation marks.

#### 1.2.1.1. Role of DNA and histone methylations in plants

DNA methylation plays a major role in maintaining genome integrity. Accordingly transposons and other repeat elements comprise most of the methylated DNA (Chan *et al.,* 2005). Transcribed regions are usually found to be, if at all, less methylated, e.g. shown for the CpG islands (regions of low CpG methylations) described in vertebrates. CpG islands have also been reported in *Arabidopsis* but do not seem to play a major role (Shamuradov *et al.*, 2005).
So far DNA methylation has not been shown to play a role in plant development (Schubert *et al.,* 2005). Mutants affected in DNA methylation occasionally show developmental phenotypes, like the *AGAMUS (AG)* and *SUPERMAN* mutants, but methylation of these loci has not been shown to play a role in vivo. An exception to this concept are the *PHABULOSA* and *PHAVOLUTA* genes, which can be methylated due to the regulation by the miR165 and miR166 (Bao *et al.*, 2004).

Nucleosomes are the fundamental repeating units of chromatin, consisting of 146 bp of DNA wrapped around histones. Histones are subject to various modifications like acetylation, phosphorylation, methylation, ubiquitination, or sumoylation, which can be reversible and associated with regulation of individual genes (Völkel *et al.,* 2007). Histone methylations belong to these reversible marks, acting as a cellular memory of transcriptional status, as they are heritable over cell divisions. Proteins that methylate

histones, and thereby affect chromatin state, play a role in many developmental processes like meristem maintenance, phase transition, and embryogenesis (Reyes, 2006).

One of the best studied epigenetic systems in eukaryotes is the Polycomb group (PcG) of proteins and their antagonists the Trithorax group proteins, which are involved in the maintenance of repressed and active transcriptional states, respectively (Bantignies & Cavalli, 2006). These protein complexes produce epigenetic marks by methylating histones. The effect of histone marks depends on the number of methyl groups and the affected amino acids.
While H3K4 (Lysine 4 of Histone 3), H3K36, and H3K79 methylations are usually associated with expressed genes, H3K9, H3K27, and H4K20 methylations constitute repressive marks (Völkel *et al.*, 2007). Complicating the histone code, lysine residues can carry one, two, or three methyl groups, linked to different enzymes and responses. In wild-type *Arabidopsis*, monomethyl H3K27 (meH3K27) and dimethyl H3K27 ($me_2$H3K27) are concentrated preferentially in heterochromatin, whereas trimethyl H3K27 ($me_3$H3K27) appears to be mostly euchromatic (Schubert *et al.*, 2005).

PcG proteins mediate the cellular memory of transcriptional states over many cell divisions (Steimer *et al.*, 2004). Conserved to their function in animals, PcG proteins elicit tri-methylations of H3K27 on their direct target genes, which is correlated with stable, long-term repression (Farrona *et al.*, 2008). The *Arabidopsis* genome contains several homologs of members of the conserved Polycomb Repressive Complex 2 (PRC2), well described in animals. The protein group comprises homologs of four genes, first described in *Drosophila*: *Enhancer of Zeste* (E[Z]), *Suppressor of Zeste 12* (Su[z]12), *Multicopy suppressor of Ira* (MSI), and *Extra sex combs* (ESC). In *Arabidopsis* these proteins are represented in small gene families (Farrona *et al.*, 2008).

E[Z] homologs contain a SET domain (Su(var)3-9, Enhancer-of-zeste, Trithorax), conferring histone methyl transferase (HMT) activity (Berger & Gaudin, 2003). Known *Arabidopsis* homologs are *MEDEA* (*MEA*) involved in seed development (Grossniklaus *et al.*, 1998, Luo *et al.*, 1999), *CURLY LEAF* (*CLF*) and *SWINGER* (*SWN*), redundantly regulating leaf and floral development, and floral transition (Goodrich *et al.*, 1997).
*CLF*, *SWN*, and *MEA* show a large functional overlap, displaying mainly additive mutant effects. The *swn* mutation does not cause visible alterations alone but enhances the effect

of *clf* and *mea* mutants. However, there are also specific regulatory functions, e.g. a MEA containing PcG complex acts on *PHERES 1* gene during seed development. Known targets for a CLF containing PcG repressive complex include the *KNOX* genes, which are found misexpressed in mutants (Schubert *et al.,* 2005).

Su[z]12 homologs are characterized by C2H2 zinc finger motifs, assumed to confer unspecific DNA binding ability (Steimer *et al.*, 2004). FERTILIZATION INDEPENDENT SEED 2 acts in a complex with MEA during seed development (Luo *et al.*, 1999), while EMBRYONIC FLOWER 2 (EMF2) and VERNALIZATION 2 (VRN2) have been shown to affect floral transition (Yoshida *et al.*, 2001, Gendall *et al.*, 2001).
VRN2 has been described to implement stable repression of *FLC* after cold treatment. *FLC* is a negative regulator of floral induction, which is itself repressed by the vernalization pathway or the autonomous pathway to enable flowering (Farrona *et al.*, 2008). *FLC* is strongly activated by *FRIGIDA* (*FRI*). As Col or Ler accessions do not possess an active FRI gene, vernalization is not required for flowering. Nevertheless, *FLC* levels influence floral induction as it is regulated by, and regulates, a large number of genes (Farrona *et al.*, 2008). In wild-type plants, but not in *vrn2* mutants, *FLC* remains repressed after vernalization (Schubert *et al.,* 2005), however, *vrn2* mutation does not affect flowering in Ler wild-type background (Gendall *et al.*, 2001).
Mutations in the homologous *EMF2* gene flower early under both long days and short days and lead to small, dwarfed plants, indicating participation in a different complex (Chanvivattana *et al.,* 2004). Interestingly, *emf2 vrn2* double mutants are not early flowering, showing otherwise additive, pleiotropic phenotypes (Schubert *et al.,* 2005).

*FERTILIZATION INDEPENDENT ENDOSPERM* (*FIE*) is an ESC homolog, containing a characteristic WD40 repeat. *FIE* has been reported to repress floral homeotic genes (Schubert *et al.,* 2005) and to be involved in seed development (Ohad *et al.,* 1999, Chaudhury *et al.*, 1997).
In animals, PRC2 complexes were shown to include the WD40 gene *MSI*. There are five homologs (*MSI1-5*) in *Arabidopsis,* but so far no experimental data provides evidence that they are part of PcG complexes (Farrona *et al.*, 2008).

#### 1.2.1.2. Plant SET domain proteins

SET domain proteins form the largest group of lysine HMTs, having different functions in *Arabidopsis* (Berger & Gaudin, 2003). SET domain proteins can be divided into seven families based on their conserved domains (Ng *et al.*, 2007). The previously mentioned *CLF*, *SWN*, and *MEA* constitute the first family and are the best studied SET proteins, as they are part of the PRC2 homologs. Yet, in recent years also the remaining SET proteins, which have not been associated with these complexes, have attracted attention.

*KRYPTONITE* (*KYP*), the first HMT identified in plants, was shown to be involved in DNA methylation control (Berger & Gaudin, 2003). *kyp* mutations cause a reduction of methylated H3K9, a loss of DNA methylation, and subsequently reduced gene silencing (Jackson *et al.*, 2004). This indicates that *KYP* mediated methylation of histones results in DNA methylation.
Redundant functions have been reported for *KYP/SUVH4* and its homologs *SUVH5* and *SUVH6*, which together control activity of the DNA methyltransferase *CMT3* (Ebbs *et al.*, 2006).
*CAROTENOID CHLOROPLAST REGULATORY 1* (*CCR1/SDG8*) is another SET domain protein, reported to be involved in plant development (Dong *et al.*, 2008, Cazzonelli *et al.*, 2009). *ccr1* mutants show increased outgrowth of lateral branches, possibly due to altered carotenoid composition.

Another SET domain protein belonging to the same subfamily as *KYP* is *CZS*, named after its conserved protein domains C2H2 zinc finger and SET. *CZS* was identified by its interaction with *SWP1*, a SWIRM (Swi3p, Rsc8p, Moira) domain Polyamine oxidase (PAO)-like protein (Krichevsky *et al.*, 2007). *czs* mutants, just like *swp1* mutants, show a mild delay in flowering correlated with an upregulation of *FLC*. Chromatin immunoprecipitation (ChIP) experiments showed that $me_2$H3K9 and $me_2$H3K27 marks at the *FLC* locus are reduced, suggesting that a role of *CZS* may be to directly repress *FLC* expression.
PAO containing co-repressor complexes have been shown to be transcriptional regulators in animals (Jepsen and Rosenfeld, 2002). They specifically silence neuronal genes in non-neuronal cells. In animals these complexes have been shown to contain LSD1 (lysine-specific demethylase 1), a protein containing a SWIRM domain and PAO domain that may

act as a histone H3 lysine demethylase, the TF REST (Repressor element 1), adapter proteins, histone deacetylases, and a SET domain HMT (Krichevsky *et al.*, 2007b). A homologous complex may be present in plants, as another LSD1 homolog *FLOWERING LOCUS D* (*FLD*) represses *FLC* by histone acetylation, as part of the alternative pathway of flowering regulation. A hypothesis is that *CZS* and *SWP1* act together in a PAO containing co-repressor complex, silencing target genes like *FLC* (Krichevsky *et al.*, 2007b).
Studies of the close *CZS*/*SUVR5* homologs *SUVR4*, *SUVR1*, and *SUVR2* revealed that they locate to the nucleus, and that *SUVR4* has an in vitro HMT activity, generating $me_2$H3K9 with a substrate preference for monomethylated H3K9 (Thorstensen *et al.*, 2006).

## 1.3. Aim of this work

The aim of this project was to obtain a deeper understanding of the process of AM initiation by first, analyzing the *LAS* promoter and second, the characterization of a new regulator of AM initiation.

The *LAS* gene was chosen for a detailed promoter analysis because it is a key regulator in AM development. *LAS* is expressed in very specific domains adaxial of initiating primordia in - or very near to - those cells later giving rise to AMs. This indicates that *LAS* function might be largely dependant on transcription, emphasizing the importance of understanding the mRNA accumulation pattern, i.e. to understand the composition and localization of the regulatory sequence motifs. The promoter was analyzed by deletion constructs and *in silico* tools to identify important elements. Additionally, fusion constructs with other promoters were produced to elucidate the relevance of specific promoter regions, and promoter GUS fusions enabled direct visualization of the expression patterns of modified promoter assemblies. Information about position and importance of promoter elements can then be used in yeast one-hybrid studies to identify upstream regulators of *LAS*, which generate the specific expression pattern.

In a second approach, the gene underlying the *eol5* mutant phenotype was to be identified and characterized. The *eol5* mutant was previously obtained in a second-site mutagenesis screen and reported to enhance the phenotypic defect of *las*. A map based cloning strategy

was applied for the identification of the underlying gene. The subsequent goal was to characterize the *eol5* and *eol5 las* mutant phenotype, particularly in regard to the effect on lateral meristem initiation, meristem maintenance, and flowering time.

To shed light on the function of the *EOL5* gene, RNA expression changes in the mutant were analyzed by real-time PCR. Double mutants with known players in AM initiation were analyzed in order to position the gene function in known regulatory pathways. Furthermore, homologs of *EOL5* were examined for defects in side shoot formation, in order to reveal a possible general role of HMT containing complexes.

# 2. Materials and Methods

## 2.1. Materials

### 2.1.1. Chemicals

The main sources of chemicals used in this work are the following:

Ambion, Austin, USA

Amersham Pharmacia Biotec, Braunscheig, Germany

Biozym, Hess. Oldendorf, Germany

Carl Roth GmbH, Karlsruhe, Germany

Invitrogen GmbH, Karlsruhe, Germany

MBI Fermentas GmbH, St. Leon-Rot, Germany

Merck KgaA, Darmstadt, Germany

New England BioLabs GmbH, Schwalbach/Taunus, Germany

Operon, Cologne, Germany

QIAGEN, Hilden, Germany

Roche, Basel, Switzerland

Sigma Chemical Co., St.Lois, USA

### 2.1.2. Enzymes

Enzymes used during this work were obtained from following suppliers:

Invitrogen GmbH, Karlsruhe, Germany

New England BioLabs GmbH, Schwalbach/Taunus, Germany

MBI Fermentas GmbH, St. Leon-Rot, Germany

Roche, Basel, Switzerland

Sigma Chemical Co., St.Lois, USA

Novagen, Toyobo, Japan.

### 2.1.3. Vectors

The following vectors were utilized during the course of this work.

pCR®-Blunt-II-TOPO®: Cloning of PCR products, Invitrogen.

pGEM4Z: Cloning by restriction sites and construct assembly, Promega GmbH, Mannheim, Germany.

pGPTVbar AscI: Binary vector for plant transformation (Überlacker & Werr, 1996).

### 2.1.4. Antibiotics

Antibiotics during this work were used to select for transformed bacteria in the following final concentrations:

Ampicillin (Amp) 100 µg/L

Gentamycin (Gent) 50 µg/L

Kanamycin (Kan) 50 µg/L

### 2.1.5. Bacteria

The *Escherichia Coli* strain used for amplification of plasmid DNA was:

DH5α (Hanahan, 1983): F- end A1 hsdR17 (rk-, mk+) gyrA96 relA1 supE44 L- recA1 80dlacZM15 Δ ( lacZY AargF) U196

Plants were transformed using the following *Agrobacterium tumefaciens* strain:

GV3101: Virulence plasmid: pMP90 (Koncz und Schell, 1986)

Selection markers: Rifampicin, Gentamycin and Kanamycin.

### 2.1.6. Plant material

This work was carried out using the model plant *Arabidopsis thaliana.*

**Table 1: Mutant alleles used in this work**

| Allele name | Allelic variation | Background | Source |
|---|---|---|---|
| *las-4* | deletion | Col | Greb *et al.,* 2003 |
| *eol5* | SNP | Col | Clarenz, 2004 |
| *czs-1* | T-DNA insertion | Col | SALK N661919 |
| *czs-2* | T-DNA insertion | Col | GABI 500A10 |

| | | | |
|---|---|---|---|
| *rob-2* | T-DNA insertion | Col | SALK N52476 |
| *mir164a-4* | T-DNA insertion | Col | SM333570 |
| *mir164b-1* | T-DNA insertion | Col | SALK N636105 |
| *mir164c* | transposon insertion | Col | Baker *et al.,* 2005 |
| *suvh1* | T-DNA insertion | Col | SALK N859507 |
| *suvr1* | T-DNA insertion | Col | SALK N860017 |
| *suvr3* | T-DNA insertion | Col | SALK N662712 |
| *swn-7* | T-DNA insertion | Col | SALK obtained from Daniel Schubert |
| *clf-28* | T-DNA insertion | Col | SALK obtained from Daniel Schubert |
| *emf2-10* | 18 bp deletion, weak allele | Ws | Chanvivattana *et al.,* 2004 |
| *vrn2-1* | SNP | Ler | Gendall *et al.,* 2001 |
| *swp1-1* | T-DNA insertion | Col | SALK N642477 |
| *FRI FLC* | active *FRI* introgressed from San Feliu-2 accession | Col / Sf-2 | Searle *et al.,* 2006 |

### 2.1.7. Oligonucleotides

Primers were mainly supplied by Invitrogen and Operon

**Table 2: Oligonucleotides used in different subprojects**

**Genotyping and sequencing of plasmids**

| | | | |
|---|---|---|---|
| pGPTV-FOR4 | caagaccggcaacaggat | pGPTV-FOR2 | aactgaaggcgggaaacgac |
| pGPTVfor3 | aggacgtaacataagggactgac | T-DNA-R | caatacgcaaaccgcctctc |
| pGPTV-rev2 | tccataaaaccgcccagtc | pGPTVrev3 | gaagcttgcatgcctgcag |
| Plasmid-Forward | cacgacgttgtaaaacgacggccag | Plasmid-Reverse | cacacaggaaacagctatgaccatg |

**Genotyping and cloning of *LAS* constructs**

| | | | |
|---|---|---|---|
| *35S-F_SacI* | gatgagctctctccactgacgtaag | 35S-R_AvrII | ggtcctaggtcctctccaaatgaa |
| AtLs1411F_SacI | tgggagctccggcatcagaatctcaac | AtLs7116R_SbfI | caacctgcaggaaaccagagtcttgtcttc |
| AtLs1831F_XhoI | atactcgagaatgtaatgattcacttttctaaaatcat | AtLs2019F_XhoI | atactcgagcaacttcatctctatccataaaactatgt |
| AtLs2135R_AvrII | tatcctaggcctttacctgaaggtatattg | AtLs1631F_XhoI | atactcgaggtgaatttttatttaattagtatcatttgc |
| AtLs2593muR | tggttcgaaacaagaactagt | AtLs2599F | cagtgtatgcaaagaacagttc |
| AtLs3070R | aacacaattgacggcaatgg | AtLs2349F | acctccgtcgtcttcttttc |
| AtLs3530F | taggagctccaaaatcgtcccctcttctcc | AtLs2952R | agacctaaagagtcagcgaacc |
| AtLs4051R_SbfI | aatcctgcagggacgatttcaatcaatttag | AtLs7116R_SacI | aacgagctcaaaccagagtcttgtcttctc |
| AtLs4940 F | ctaactagtctaaggtttagaggatgatc | AtLs5697F_XmaI | ttgcccgggataaaacaaaagggtgtgc |
| AtLs5396F_BamHI | aatggatccttagggttagtgtcgacaga | AtLs1411F_BstBI | tggttcgaacggcatcagaatctcaac |
| AtLs5614R_XmaI | ccccccgggaatccctttttttacccca | AtLs5672R_XmaI | gctcccgggtcatccgacaaatcg |
| AtLs5739R_BamHI | ataggatcctataacataagtctaaataagcac | AtLs6625F_KpnI | agaggtaccatttagggttttaggtg |
| AtLs6798R_SbfI | aatcctgcaggtgatcacaaactttggatag | AtPI-598-F_SacI | tttgagctcaattaattatatacatacacgagtaagc |
| AtLsREV | gagacaaagaggacggtcac | AtLs4975R | tcgcagagatcatcctctaaac |
| AtPI-1-R_AvrII | tctcctaggctttctctctatctct | AtLs3569_AvrII | tggcctaggtccaaagagaaggacaa |
| LAS-5UTR -6.2f | cgcggatccggcatcagaatctcaac | | |

**Mapping primers**

| | | | |
|---|---|---|---|
| cer429966_F | ggctcttgagccgaagaaat | cer429966_R | acgtttcagaccttcgtcgt |
| cer429971_F | tcgagagatgttgccatgag | cer429971_R | cgtgattgttgtcgtcgatt |
| cer44411A_F | cggatcagaccgattcaaac | cer44411A_R | ctccccaaaaagaaacgaca |
| cer44411B_F | gttgttgttcggttcggttt | cer44411B_R | caccgggaaactaccagcta |
| cer445734_F | ttgcacctttgccatcatac | cer445734_R | tgtcaaaacaaaatgacaatgc |

| | | | |
|---|---|---|---|
| cer445742_F | ccggagccatcgtagaagta | cer445742_R | tggttttccacaaaattcca |
| cer44613B_F | atcaatatgttgaaaaagctacaccag | cer44613B_R | cgccaccacaaatctccatc |
| cer44613F | aaaataatgggtggggaaatcg | cer44613R | ttcgaaacacgttggaaaatgac |
| MASC02463F | gagtgtcaaaggttacgggttct | MASC02463R | gcttgaatggtttacacttgacag |
| MASC02627F | atgtggttgattcaaagggtg | MASC02627R | tgaaattgggaggaggattg |
| MASC02866F | tagaatttccctgccaacatc | MASC02866R | gggcttgaagctgttgagac |
| MASC02949F | gtttttgaaagtccccggat | MASC02949R | catggagctggtggtttagc |
| MASC03021F | actccgattccaaacacatca | MASC03021R | ggtatgtgaaatgggttttggt |
| MASC07353F | aagcattgctctgtttatcgtc | MASC07353R | ttcttcttctatagcttttggtctc |

**Sequencing primers**

| | | | |
|---|---|---|---|
| at2g23347_F | cctgataaaagcagcgtcct | at2g23347_R | agctcctgcacgaagttactg |
| at2g23450_986F | tgtttgtttggtggttcaatg | at2g23450_2505R | aacattgtggtactggttgaaaga |
| at2g23450-499F | ccactgggcacgtatcttct | at2g23450_1007R | cattgaaccaccaaacaaaca |
| at2g23460_2077F | tatgagcaggagatgcgaaa | at2g23460_3620R | ccttggagccaatagaacca |
| at2g23460_648F | ccgcagacgaaaggtaagaa | at2g23460_2195R | accccaagatttccagcag |
| at2g23460-670F | aattcgacccctgacacac | at2g23460_789R | ccttccttcaggcatagaacc |
| at2g23520_1236F | cttgacggattggttggtct | at2g23520_2775R | ttaccctccttccatttcca |
| at2g23520-178F | tcttctcttccgtgaaagtcg | at2g23520_1374R | cacatccctcacttgagctg |
| at2g23530_717F | agacttgtcaccaatgcaggt | at2g23530_2232R | aacagagagggtcatgtcgaa |
| at2g23530-696R | tctctcaagtcaattcaaatcca | at2g23530_848R | ccatcgtcttctgcctgtaag |
| at2g23640_F | tctggtctaagttatcaaattccaa | at2g23640_R | gacacaggtaaagtcgaccaa |
| at2g23700_1354F | cggcatttcaatcaagaaga | at2g23700_3258R | aacccttcccaagacaatca |
| at2g23700-113F | cccaactaagagattcttcttcttc | at2g23700_1449R | tcgaattgtcgaacaccaga |
| at2g23755-903F | gattgatgaaccatttgccata | at2g23755_633R | ggaactattgatcttccttcaagc |
| at2g23770_287F | cccttctggtcaacaagtca | at2g23770_1987R | tgaccaactccaacacaaca |
| at2g23770-1254F | tgtgaaataaatggtgcgtgt | at2g23770_405R | gtcgttagcaatggcgaaat |
| at2g23780-671F | actaatcgatcggcgttcac | at2g23780_997R | gcatctatcaaccttaaagaatcaaa |
| at2g23790_1140F | tggggatggattgattgact | at2g23790_2684R | aatgatgccaaaagctcgtt |
| at2g23790_-301F | tcacctctaccaacccgaac | at2g23790_1250R | cctccaccaccttcttttga |
| at2g23800-F | ccacgaaaagccgttaagtt | at2g23800-R | cgtccactgctacgtccata |
| at2g23810_406 | ggagttgtcttgtggagagca | at2g23810_1856R | gaaccttcttcattatgtttgatg |
| at2g23810-916F | ggctaaggtatgcttttcaaac | at2g23810_618R | aaaggatcaaaaagctcaatctc |
| at2g23820_896F | attgtcaagcttggctgcat | at2g23820_2396R | ccgtgcaaaatcttgaaaca |
| at2g23820-524F | tcaaaacgacatcgtgttaaat | at2g23820_1018R | gacaaacttcacatcttcaaggatt |
| at2g23830_F | ttgcacgggttaaaagttga | at2g23830_R | gcaagagacatcgctaagagtg |
| at2g23834_F | atacatgcctgccgaggac | at2g23834_R | agaacaccgggatctcagaa |
| at2g23840_829F | ttctcctacgggttcgttct | at2g23840_2463F | cttcgaccgttgcatcttct |
| at2g23840-638F | caggttctgcaacttttgg | at2g23840_926R | gcttcaaactggcaacaaga |
| at2g23860_514F | taacaaagaatcggggcatc | at2g23860_1954R | tcgagacgatatagttgaaataatga |
| at2g23860-903F | aaaaattcagcatttcattacattt | at2g23860_739R | cgagttttgctctggcaatc |
| at2g23910_1134F | ctcattttggtcaagattcaatg | at2g23910_2651R | tcgtggatgcatttgagatt |
| at2g23910-219F | ttccaccggtcaatggatta | at2g23910_1282R | gagcatgccacaactgtgat |
| at2g23920_F | tcaggattgtgaagcaggatt | at2g23920_R | ttcaccacaacatcaaaaatga |
| at2g23930_F | acaattggccgcattagaac | at2g23930_R | tcaaagcagtggatccagagta |
| at2g23950_1457F | tggtttatgtaatttgattttgtttg | at2g23950 _2985R | ttgctttcacaggacctcaa |
| at2g23950-200F | gcgtaggagagacattgcag | at2g23950_1506 | ccaaaacaaaatactttagacaacaaa |
| at2g23980_1509F | gggcttgaaaccagcacata | at2g23980_2989R | ggaagcaatggcagactctc |
| at2g23980_160F | tggactcaaggtactcgcaaa | at2g23980_1610R | acctgcatgtttccaatgag |
| at2g23980-1217F | ttcggcaacgattactctcc | at2g23980_260R | gatgctttgcttccttgagc |
| at2g23985_F | gacgccgtgattgtgtgtaa | at2g23985_R | caattgggtgatgaatgttttg |
| at2g24030_18F | atggcgatacgacgagtttc | at2g24030_1543R | ggtctctctaatggcattggttat |
| at2g24030-1363F | aaaaatcgtttgaaattctcactt | at2g24030_137R | tgtctgaaaaagttgttgaactg |
| at2g24080_F | ttagcggtgtactgcggttt | at2g24080_R | aacacttagcaatgtcaaatcttca |
| atCLF2299_F | gagttgctgagcgagttcct | atCLF3857_R | taagaaagctccccaaccag |
| atCLF3690_F | tgctcctgaaacaacaacaaa | atCLF5170_R | tagtgcgcgaatcaaatcag |
| atCLF-495_F | tcgaaaagctgttgctgaaa | atCLF969_R | tctccttcgacccactacaga |
| atCLF800_F | catgggtttttctggacagg | atCLF2400_R | atcgctgggtgaacaacttc |
| atICK1_F | aacgggaccactaaaacacg | atICK1_R | agcgtttagggcggtaagat |
| atLBD10_-361_F | aaaaatgctaaagaatggggtat | atLBD10_1856_R | tcatttgcttgctttggttg |
| atmiR831a_F | gttggggctcagtcatcatc | atmiR831a_R | tttcgtagtcttggataaaatcagc |
| atSAW2_1615_F | aaacgaactaatcacttgaggttt | atSAW2_2947_R | tgatgaataatgacagaagaaattg |
| atSAW2_2856_F | tgtcagtggtacagtttcattgg | atSAW2_4182_R | cattaaatatggttttgattgtttttg |
| atSAW2_361_F | cgcagcaacaacaacacttt | atSAW2_1753_R | tcgcagtagtggttgtaccg |
| atSAW2_3992_F | tctcaaaggaaacacatgtatcataa | atSAW2_5355_R | tgttaataagtcgatcgggtacg |
| atSAW2_-898_F | atggtggtggtttggttcat | atSAW2_441_R | gtggacggttccgatcata |

**CZS sequencing, genotyping, and cloning of constructs**

| | | | |
|---|---|---|---|
| at2g23740_1113F | ctgagtctccaatgcaacca | at2g23740_2649R | ggctgccacaaggaatacac |
| at2g23740_19F | agttggttcttgacgtggatg | at2g23740-456F | cctgggtttgttgattggtc |
| at2g23740_2507F | tggtcgtttagtggatttgc | at2g23740_3961R | tgggaatctacacctcatgga |
| at2g23740_3847F | agctgtcgcagttcagtgtg | at2g23740_5303R | tcaatccttccaaagagtttcaa |
| at2g23740-1502F | tcgctaacataacctgcaca | at2g23740-61R | tctgcaataagaacaggggaat |
| at2g23740-185F | tgacttcgtatgtctgaaaatgc | at2g23740_1220R | ctgtgctatttcgccaacac |
| at2g23740-AscIF | ataggcgcgcctcgctaacataacctgcaca | at2g23740_SbfIR | atacctgcaggtcaatccttccaaagagtttcaa |
| atCZS-156F | cttccgtgacctagcctttg | atCZS_182R | ggctcagaaggtgacgactc |
| atCZS-1668F | cttcgtaacaaattttcgctga | at2g23740_358R | tttcgcacatcttattccagc |
| atCZS-1668F_AscI | ataggcgcgcccttcgtaacaaattttcgctga | atCZS_5378R_SbfI | atacctgcagggcttccatggttctgcaact |
| atCZS-641R | ataaagtgggaacacgaaacaca | atCZS_3168R | gagcatctgttacgccatca |
| atCZS-929F | tacatgcccaaataccgatg | atCZS_5378R | gcttccatggttctgcaact |

**Real-time PCR primers**

| | | | |
|---|---|---|---|
| ANAC83_490F | atgcacgaatatcgcctctc | ANAC83_679R | tcgttcttgttaccggctct |
| atCZScDNA_3938F | tcacagctgctcaccaaatc | atCZS_4928R | tctcgggtgatctcttctcct |
| atCZScDNA_510F | gaccagttcccttcagaggtt | atCZS_795R | cttcacaagcattatcccaaga |
| AtLs3233F | atggcgatctttgattcgtt | AtLs3297R | ccaccgttgctctagggtta |
| AtPP2C_1543F | atgggaacagatgagcaacc | AtPP2C_1730R | tgccatcttcaccagtctcc |
| DRN_837F | gatcgctacgggaattttca | DRN_935R | tttcttgataccccactcg |
| DRNL_732F | ccagagagcggttttcagac | DRNL_832R | cagcccaacctaactctcca |
| FLCcDNA_4156F | agccaagaagaccgaactca | FLC_4508R | cctggttctcttctttcagca |
| LB25_56F | acctttttcttgttgcgatcc | LB25_1296R | agtctgacgtgcatttacgc |
| miR164B_9F | agggcacgtgcattactagc | miR164B_70R | ccgcatatatacacgcatttg |
| PP2A_F | taacgtggccaaaatgatgc | PP2A_R | gttctccacaaccgcttggt |
| STM_2056F | tggagccgtcactacaaatg | STM_2802R | gccgtttcctctggtttatg |

**Primers for genotyping mutants**

| | | | |
|---|---|---|---|
| atSWP1_934F | gtgatggtgttgaggcaatg | atSWP1_1916R | ctggaacagagggcttgaac |
| bHLH140-EcoRIfo | gatgaattcatggatgatttcaatcttcgtagc | bHLH140-1931R | caaatttacattaaaacgcctgtttatc |
| clf-28F | ctgccagttcaggaatggtt | clf-28R | gaagggagctctctgcttgat |
| emf2-10F | gccaggcattcctcttgtta | emf2-10R | ttgtaagcaaccccacaaca |
| LB-T-DNA | tgaaaagaaaaaccaccccag | JL_202 | cattttataataacgctgcggacatctac |
| miR164A_171R | cacaaacaacgaagagctagtca | miR164A-463F | cgtgaccggcttcatagg |
| miR164B-263F | tgacataaacaacactcgcactt | miR164B_196R | acacttgaaccctcgtcgtc |
| miR164C-544F | aattacgtcgtgagggttgg | miR164C_267R | aacacaaaaagtggagtaacaatca |
| SWN_1539F | ggataagcagaataccgaggaa | SWN_2422R | attgggacctcacgctttc |
| VRN_2323F | tgcgttcattaagtaggcaaca | VRN_2523R | aaggtctttttgtgtgtgttcaag |

### 2.1.8. Growth media and buffers

Culture media used in this work were prepared as described by Sambrook & Russell (2001). *Agrobacterium tumefaciens* was incubated in YEP medium (1 % Pepton, 1 % Yeast Extract, 0,5 % NaCl, 0,5 % Saccharose). For growth on solid medium 1 % agarose was added to LB or YEP media. All culture media and buffers were made with highly purified Milli-Q-water (Millipore Waters GmbH, Neu -Isenburg). When required, solutions were autoclaved for 20 min at 121°C. For plants grown in sterile conditions, seeds were placed on MS Medium (Murashige and Skoog, 1962) with vitamins but without addition of sugar.

### 2.1.9. Software and databases

The following software tools were used in the course of this work:

Sequence processing, planning of cloning strategies and restriction analyses, annotation of genomic sequences, sequence alignments, and assembly and analysis of sequencing results were performed using the DNASTAR® software package.

Primers for PCR and sequencing were designed using primer3 online tool (Rozen & Skaletsky (2000); http://primer3.sourceforge.net/).

NCBI (National Center for Biotechnology Information; http://www.ncbi.nlm.nih.gov/) database was used for BLAST analyses and acquiring sequences.

TAIR (The Arabidopsis Information Resource; www.arabidopsis.org) database was used to obtain DNA sequences and information about *Arabidopsis* genes.

GBrowse (Generic Genome Browser Version 1.70; http://gbrowse.arabidopsis.org/cgi -bin/gbrowse/arabidopsis/) was used to visualize genomic sequences and aligned ESTs and high throughput transcriptome sequences.

SMART (a Simple Modular Architecture Research Tool; Schultz *et al.* (1998); http://smart.embl-heidelberg.de/) allows the identification and annotation of domain architectures of proteins.

TDNA express (Alonso *et al.* (2003); http://signal.salk.edu/cgi-bin/tdnaexpress) is a genome browser revealing locations of T-DNA insertions.

CREDO (Cis-Regulatory Element Detection Online, Hindemitt & Mayer (2005), http://mips.helmholtz-muenchen.de/proj/regulomips/credo.htm) is a web-based tool for computational detection of conserved sequence motifs, integrating results from a variety of algorithms: AlignACE (Hughes *et al.,* 2000), DIALIGN (Morgenstern, 1999), FootPrinter (Blanchette and Tompa, 2002), MEME (Bailey & Elkan, 1994), and MotifSampler (Thijs *et al.*, 2001).

FIMO (Find Individual Motif Occurrences; http://meme.sdsc.edu/meme/fimo-intro.html) uses motif information from MEME output files to compare these to further sequences.

BAR (Bio-Array Resource, Winter *et al.* (2007); http://www.bar.utoronto.ca/efp/cgi-bin/efpWeb.cgi,) provides an *Arabidopsis* browser for visualization of large-scale expression data.

Bioinformatics Toolkit (Dep. of Protein Evolution at the Max-Planck Institute for Developmental Biology, Tübingen, http://toolkit.tuebingen.mpg.de/t_coffee) was used for alignments and to construct phylogenetic trees.

UCSC Genome Browser on *A. thaliana* (Jan. 2004 Assembly at UCLA; http://epigenomics.mcdb.ucla.edu/H3K9m2/, Bernatavichute *et al.*, 2008) shows data of ChIP chip experiments, providing a high-resolution, genome-wide map of several H3 methylations and DNA methylations.

## 2.2. Methods

General molecular biology laboratory methods were carried out as described by Sambrook & Russell (2001), unless otherwise stated.

### 2.2.1. Incubation conditions for bacteria

*E. coli* cultures were incubated on LB medium at 37°C over night (Sambrook & Russell, 2001). *Agrobacterium tumefaciens* cultures were incubated on YEP medium at 28°C for 2-3 days with appropriate antibiotics.

### 2.2.2. Plant growth conditions

*Arabidopsis* seeds were stratified for 2-3 days at 4°C on soil before transfer to green house or growth chambers. For phenotyping, plants were grown in greenhouse conditions, in Grobanks (Mobylux GroBanks, CLF Plant Climatics, Emersacker, Germany), or Percival (Percival Scientific, Inc., Perry, USA) growth chambers. Plants were either grown in short days (8 h light, 16 h darkness) or long days (16 h light, 8 h darkness).
In greenhouse, short day conditions were achieved by covering benches after the 8 h of light period. During day time, additional artificial light was occasionally supplied. For long day conditions artificial light was supplied for up to 16 h a day. In Grobanks climate chambers temperature was 22°C during day and 17°C - 18°C at night. In Percival growth chambers day and night temperatures were 22°C and 16°C respectively, temperatures

changed over a 15 min period. In both growth chambers red light (from light bulbs) was supplied for an extra 15 min before and after activation of fluorescent tubes.
For sterile growth seeds were surface sterilized () and placed on Agar plates. After stratification for 2 nights plates were transferred to Grobanks growth chambers.

### 2.2.3. Crossing *Arabidopsis* plants

Flowers from preferably young inflorescences were selected for crosses; usually the 2 – 3 oldest flowers of each inflorescence that had not yet opened. The inflorescence meristem, younger buds, and any open flowers were removed. Flower buds were opened with fine forceps, and sepals, petals, and stamens were removed. Fertilization with pollen from young flowers of the pollen donor was accomplished by dusting anthers of the pollen donor on the naked stigma. These were covered with plastic film for a few days to avoid desiccation. Seeds were harvested when siliques opened upon touching.

### 2.2.4. Isolation of DNA

DNA isolation of a small number of samples was accomplished using the quick protocol described by Edwards *et al.*, (1991) with minor adaptations. 500 µl of extraction buffer were used to which 150 µl of 5M KAc were added before the first centrifugation. Subsequently the supernatant was added to 400 µl of isopropanol. Large scale DNA isolations for mapping, genotyping, and cloning were carried out using the DNeasy® 96 Plant Kit (Qiagen) with the BioSprint® 96 automated workstation (Qiagen).

### 2.2.5. Isolation of plasmid DNA

Plasmid DNA from *E. coli* was isolated using the Plasmid Mini Kit (Qiagen).

### 2.2.6. Purification of PCR products

PCR products were cleaned using Quiaquick PCR Purification Kit (Qiagen).

### 2.2.7. Polymerase chain reaction (PCR)

Generally, PCR reactions were set up according to the following protocol: 5 µl 10x PCR Buffer (Sambrook und Russel, 2001), 2 µl of 50 mM MgCl, 0.5 µl dNTP (100 mM), 0.3 µl Taq-Polymerase, 1 µl of each Primer (10 µM), and 0.1 – 2.0 µl of described DNA preparations as template, adding $H_2O$ to reach a reaction volume of 50 µl. Taq polymerase was produced as described by Pluthero (1993). Reactions were generally carried out in the Mastercycler® epgradient (Eppendorf, Hamburg, Germany) using the following standard program. 94°C for 3 min, 35 cycles of 94°C for 15 sec, ~ 60°C for 30 sec, and 72°C for 1 min/kb product, followed by 5 min at 72°C.
PCRs for cloning and all problematic PCRs were carried out using the KOD hot start DNA polymerase (Novagen), using the following standard program. 94°C for 2 min, 35 cycles of 94°C for 15 sec, ~ 60°C for 30 sec, and 68°C for 30 sec/kb product, closing with 2 min at 72°C.

### 2.2.8. Cloning of constructs

Restriction enzymes were used according to the manufacturer's instructions.

Prior to ligation linearized vectors were mostly dephosphorylated with Calf Intestine Alkaline Phosphatase (CIAP, MBI Fermentas) according to the manufacturer's instructions.

Ligations were carried out using T4 DNA Ligase (MBI Fermentas) according to the manufacturer's instructions.

TOPO cloning was performed utilizing the Zero Blunt® TOPO® PCR Cloning Kit (Invitrogen) according to the manufacturer's instructions.

Constructs for plant transformation were assembled in pGEM4Z background and transferred into a binary plant transformation vector with pGPTVbar AscI background by cutting with AscI and SbfI and subsequent cloning of the insert into pBR51. Arrow "⇒" denotes the new name of the plasmid after transfer of insert into pBR51. Unless otherwise mentioned, PCR products were amplified from genomic DNA.

pBR51 (pGPTVbar AscI without GUS ORF): pGPTVbar AscI and pAE25 (pGEM4Z with AscI site; Eicker, 2005) were cut with AscI and SacI, mixed and ligated. pBR51 was selected for with Kanamycin.

pBR36 (⇒ pBR37): Genomic *LAS* fragment was amplified from pES22 (Eicker, 2005) using AtLs1411F_SacI and AtLs7116R_SbfI primer pair. PCR product was cut with SstI and SbfI and cloned into pAE25 (pGEM4Z with AscI site; Eicker, 2005).

pBR23 (⇒ pBR38): PCR products from AtLs3530F / AtLs5614R_XmaI and AtLs5697F_XmaI / AtLs7116R_SbfI primer pairs, both amplified from pES22, were cut with XmaI, ligated, and reamplified with AtLs3530F and AtLs7116R_SbfI primer pair. PCR product was cut with SpeI und SbfI and cloned into pBR36.

pBR24 (⇒ pBR39): PCR product from AtLs3530F / AtLs6798R_SbfI primer pair, amplified from pES22, was cut with SpeI und SbfI and cloned into pBR36.

pBR26 (⇒ pBR41): PCR product of 35S-F_SacI / 35S-R_AvrII (on pBAR35S, from Peter Huijser) and AtLs2135R_AvrII / AtLs2952R (on pES22,) primer pairs were cut with XmaJI, ligated, and reamplified. PCR product was cut with SstI and AgeI and cloned into pBR36.

pBR27 (⇒ pBR42): PCR product of AtLs2599F and AtLs4051R_SbfI primer pair, amplified from pES22, was cut with AgeI and SbfI and cloned into pBR26.

pBR28 (⇒ pBR43): PCR product of AtPI-598-F_SacI and AtPI-1-R_AvrII primer pair was cut with SstI and XmaJI and cloned into pBR26.

pBR29 (⇒ pBR44): PCR product of AtLs2599F and AtLs4051R_SbfI primer pair, amplified from pES22, was cut with AgeI and SbfI and cloned into pBR28.

pBR30 (⇒ pBR45): GUS ORF containing LAS UTRs was amplified by AtLs2135R_AvrII and AtLs4975R primer pair (on pES44, Fig. 11, from Andrea Eicker). PCR product was cut with XmaJI and SpeI and cloned into pBR26.

pBR31 (⇒ pBR46) GUS ORF containing LAS UTRs was amplified by AtLs2135R_AvrII and AtLs4975R primer pair (on pES44, Fig. 11, from Andrea Eicker). PCR product was cut with XmaJI and SpeI and cloned into pBR28.

pBR32 (⇒ pBR47): PCR product of AtLs1411F_SacI and AtLsREV primer pair, amplified from pES22, was cut with SstI and SmiI and ligated into pBR30.

pBR33 (⇒ pBR48): PCR products of AtLs3530F / AtLs5614R_XmaI and AtLs5697F_XmaI / AtLs7116R_SbfI primer pairs, both amplified from pES22, were cut

with XmaI, ligated, and reamplified with AtLs3530F and AtLs7116R_SbfI primer pair. PCR product was cut with SpeI und SbfI and cloned into pBR32.

pBR34 (⇒ pBR49): PCR products of AtLs7116R_SacI / AtLs5396F_BamHI and LAS-5UTR -6.2f / AtLs2952R primer pairs, both amplified from pES22, were cut with BamHI, ligated, and reamplified with AtLs7116R_SacI and AtLs2952R primer pair. PCR product was cut with SstI and cloned into pBR27.

pBR54 (⇒ pBR57): PCR product of AtLs1631F_XhoI and AtLs2952R primer pair was cut with XhoI and AgeI and cloned into pBR36.

pBR55 (⇒ pBR58): PCR product of AtLs1831F_XhoI and AtLs2952R primer pair was cut with XhoI and AgeI and cloned into pBR36.

pBR56 (⇒ pBR59): PCR product of AtLs2019F_XhoI and AtLs2952R primer pair was cut with XhoI and AgeI and cloned into pBR36.

pBR60 (⇒ pBR61): PCR product of at2g23740-AscIF and at2g23740_2649R primer pair was cut with AscI and XmaI and cloned into pAE25 (pGEM4Z with AscI site; Eicker, 2005) forming pBR60I. PCR product of at2g23740_1113F and at2g23740_SbfIR primer pair was cloned into pCR-Blunt II-TOPO vector by topocloning forming pBR60F. pBR60I was cut with XmaI, PspXI, and SacI and ligated to pBR60F, which was cut with XmiI and PspXI. After ligation and transformation pBR60, containing the complete *CZS* ORF including 1502 bp upstream and 286 bp downstream sequences, was selected for with ampicillin. Positive clones were identified by colony PCR using T-DNA-R and at2g23740_3847F primers.

### 2.2.9. Sequencing

Sequencing reactions were carried out either on plasmid DNA or on PCR products treated with ExoSAP-IT® (USB Corporation, Cleveland, USA) according to manufacturer's instructions. Sequencing was carried out by the MPIZ service unit Automatic Isolation and Sequencing (ADIS) using Abi Prism 377 und 3700 sequencers (Applied Biosystem, Weierstadt) by means of BigDye-terminator chemistry.

### 2.2.10. Transformation of bacteria

Transformations *E.coli* with plasmid DNA was carried out via heat-shock treatment of chemical competent cells as described by Hanahan (1983).
In order to transform *Agrobacterium,* competent cells were mixed with ~ 500 ng of DNA and incubated for 5 min on ice, and subsequently in liquid nitrogen. After a heatshock for 5 min at 37°C, 500 µl of YEP medium was added and cells were incubated on a shaker at 28 °C for 1.5 – 3 h. Subsequently, cells were plated out on solid YEP medium containing gentamycin and kanamycin.

### 2.2.11. Transformation of *Arabidopsis*

Transgenic plants were established using *Agrobacterium*-mediated transformation, following the floral dip method described by Clough and Bent (1998). To select for transgenic plants, T1 seedlings were sprayed with 250 mg/L glufosinate (BASTA®, Hoechst) 2 - 3 times.
To sort out multicopy insertions in one locus, PCRs with outwards directed T-DNA border primers were carried out. If a PCR product could be generated the line was evicted, as this indicates T-DNA tandem insertions. Homozygous lines were selected by spraying T3 seedling populations with Basta.

### 2.2.12. Southern blot

To detect transgene sequences in genomic DNA alkali DNA blotting and subsequent radiolabeled detection was performed as described by Sambrook and Russell (2001). Blotting was performed using Hybond XL nylon membranes (Amersham Biosciences). A 482 nt radiolabeled probe targeted to the LAS 3’ UTR was utilized to detect transgenic and endogenous DNA fragments in transformed plants.

### 2.2.13. GUS staining

GUS stainings were carried out as described by Sessions *et al.,* (1999). Tissues were embedded in Paraplast+ (Kendall, Mansfield, USA) in the ASP300 tissue processor (Leica,

Wetzlar, Germany). Plant tissues were sectioned and dewaxed by changing through two consecutive 5 min steps of 100 % xylol, two consecutive 5 min steps of 100 % ethanol, 1 min steps of 90 %, 70 %, 50 %, and 30 % ethanol and a 5 min wash step in water. Slides were immediately mounted in 30% glycerol and photographed through a brightfield microscope.

### 2.2.14. Positional Cloning

A mutation can be identified by map based cloning if it causes a significant and reliable aberration of phenotype. The first step is to cross the mutant with a different accession that can be distinguished on a genomic level by DNA markers. The F2 population of this cross is first analyzed on phenotypic level to distinguish the homozygous mutants from the phenotypically wild-type plants (segregation ratio for recessive mutations 1:3). Next, the genomes of these plants are analyzed by markers to determine which chromosomal area in each plant originates from which parent, resulting from the recombination events during meiosis. In *Arabidopsis* usually 4-5 markers per chromosome provide a sufficient information density for rough mapping. The position of the mutation is determined by comparing phenotypes and genotypes of each plant. In plants exhibiting a mutant phenotype, a marker close to the mutated gene will show an increased frequency of the mutated parent's allele, because the locus of the mutation has to be homozygous for this accession to produce this phenotype. Wild-type looking plants on the other hand will bear an increased frequency of the other parent's allele at this marker compared to the statistical expectation.

After the locus has been roughly mapped to a chromosomal area, more markers are applied in this region in the processes of fine mapping to narrow down the position of the mutation. Analysis of recombinants and matching phenotype and genotypes between markers should bring forth a small region including the gene of interest in which candidate genes can be selected and sequenced until the mutation causing the phenotypic deviation is found.

#### 2.2.14.1. CAPS marker

The genotyping during fine mapping was accomplished utilizing mostly CAPS markers, which are available in large numbers for most chromosomal regions between Col and Ler.

PCR products were cut with the appropriate enzyme by adding 10 µl of PCR to 10 µl of master mix, containing 2 µl of the appropriate restriction buffer, 0.5 µl of enzyme, and 7.5 µl of $H_2O$, followed by incubation at (usually) 37°C for 1 h, and subsequent separation on a suitable agarose gel.

### 2.2.15. Isolation of RNA from plants

RNA was extracted using the RNeasy Plant Mini Kit (Qiagen) and eluted in 0.5 x TE buffer.

### 2.2.16. cDNA synthesis

For cDNA synthesis RNA was first subjected to DNase digestion using DNA-free™ Kit DnaseI (Applied Biosystems / Ambion, Darmstadt, Germany), according to the manufacturer's protocol.
First strand cDNA was synthesized using the RevertAid™ H Minus First Strand cDNA Synthesis Kit (Fermentas) according to manufacturer's instructions. About 1 µg of RNA was used in a 20 µl reaction.

### 2.2.17. Real-time PCR

Quantitative real-time PCR was performed using the Power SYBR® Green PCR Master Mix kit, according to the manufacturer's instructions. The SYBR Green dye binds to double-stranded DNA, thereby providing a fluorescent signal that reflects the amount of double-stranded PCR product generated during the reaction. Real-time PCR reactions were carried out and monitored by the Mastercycler® ep realplex (Eppendorf). The relative expression was determined by the standard curve method (Applied Biosystems, User Bulletin #2, 2001) and was normalized with the parallel measured expression of 2PPA (Czechowski *et al.*, 2005).

## Abbreviations

| | |
|---|---|
| A | adenine |
| AA | amino acid |
| AM | Axillary meristem |
| *BRC* | *BRANCHED* |
| BC2F2 | backcross two, following generation two |
| bHLH | basic helix loop helix |
| BLAST | Basic Local Alignment Search Tool |
| bp | base pair |
| CaMV | cauliflower mosaic virus |
| ChIP | chromatin immunoprecipitation |
| *CLV* | *CLAVATA* |
| Col | Columbia |
| *CUC* | *CUP SHAPED COTYLEDONS* |
| *CZS* | *C2H2 ZINC FINGER SET DOMAIN PROTEIN* |
| *DRN* | *DORNRÖSCHEN* |
| *DRNL* | *DORNRÖSCHEN-LIKE* |
| *E. coli* | *Escherichia coli* |
| EBI | European Bioinformatics Institute |
| EMBL | European Molecular Biology Laboratory |
| *EMF2* | *EMBRYONIC FLOWER 2* |
| EST | expressed sequence tags |
| *FLD* | *FLOWERING LOCUS D* |
| FIMO | Find Individual Motif Occurrences |
| *FLC* | *FOWERING LOCUS C* |
| G | guanine |
| GA | gibberelic acid |
| GAI | *GIBBERELIC ACID INSENSITIVE* |
| GFP | green fluorescent protein |
| GUS | β-glucuronidase |
| HA | human influenza hemagglutinin |
| het | heterozygous |
| HMT | histone methyl transferase |
| hom | homozygous |
| H3K9 | lysine nine on histone three |
| JGI | Joint Genome Institute |
| kb | kilo base pairs |
| KNOX | *KNOTTED LIKE HOMEOBOX* |
| *LAS* | *LATERAL SUPPRESSOR* |
| ld | long day |
| Ler | Landsberg |
| *LFY* | *LEAFY* |
| LN | natural logarithm |
| *LOM* | *LOST MERISTEMS* |
| *Ls* | *Lateral suppressor* from tomato |

| | |
|---|---|
| LSD | Lysine-specific demethylase |
| *MEA* | *MEDEA* |
| $me_3H3K9$ | tri-methylated lysine nine of histone three |
| miR | micro RNA |
| MYB | protein domain first described in an avian myeloblastosis virus oncogene |
| NASC | Nottingham Arabidopsis Stock Centre |
| NCBI | National Center for Biotechnology Information |
| nt | nucleotide |
| ORF | open reading frame |
| PAO | Polyamine oxidase |
| PcG | Polycomb group |
| *PEP1* | *PERPETUAL FLOWERING 1* |
| PID | percent identity |
| PolII | RNA polymerase II |
| PRC2 | Polycomb repressive complex 2 |
| QTL | quantitative trait locus |
| *RAX1* | *REGULATOR OF AXILLARY MERISTEMS* |
| *RGA* | *REPRESSOR OF ga1-3* |
| *RGL* | *REPRESSOR OF ga1-3-like* |
| *ROB* | *REGULATOR OF BRANCHING* |
| R2R3 | repeats 2 and 3 of the MYB domain |
| SAM | shoot apical meristem |
| *SCL* | *SCARECROW_LIKE* |
| *SCR* | *SCARECROW* |
| sd | short day |
| SET | Su(var)3-9, Enhancer-of-zeste, Trithorax |
| *SHR* | *SHORT ROOT* |
| SMART | Simple Modular Architecture Research Tool |
| SNP | single nucleotide polymorphism |
| STD | standard deviation |
| *STM* | *SHOOT MERISTEMLESS* |
| *SOC1* | *SUPPRESSOR OF OVEREXPRESSION OF CONSTANS 1* |
| *SUVH* | Su(var) homologs |
| *SUVR* | Su(var) homologs |
| SWIRM | Swi3p, Rsc8p, Moira |
| *SWP1* | *SWIRM DOMAIN PAO DOMAIN-LIKE PROTEIN 1* |
| TAIR | The Arabidopsis Information Resource |
| T-DNA | transfer DNA |
| TF | transcription factor |
| TSS | transcription start site |
| UTR | untranslated region |
| *VRN2* | *VERNALIZATION 2* |
| Ws | Wassilewskija |
| wt | wild-type |
| *WUS* | *WUSCHEL* |
| *YAB1* | *YABBY 1* |

# 3. Results

## 3.1. Part 1: Characterization of the *LATERAL SUPPRESSOR* promoter

Aerial architecture of flowering plants is based on the activities of axillary meristems (AM). Among various genes that have been reported to play a role in the initiation of these AMs, *LAS* was shown to be a key regulator. *LAS* is expressed in very specific band-shaped domains at the adaxial side of leaf primordia (Greb 2003, Fig. 1C, D). This *LAS* expression pattern is including or adjacent to those cells, which will later develop into meristems and which fail to do so in the *las* mutant. This suggests that the function of *LAS* may be largely regulated by its RNA accumulation pattern, leading to the important question of how these specific RNA expression domains are established.
To address this question, a promoter analysis to identify essential elements in the promoter of *LAS* was initiated. Understanding promoter structure and function can give valuable insights into the process the gene is involved in. Detailed knowledge of the promoter is also a suitable starting point to find upstream interactors, e.g. by yeast one-hybrid experiments.

### 3.1.1. Deletion analysis of the 5' *LAS* promoter

Previous work on tomato and *Arabidopsis* has shown that large promoter regions are necessary for a functional *LAS*/*Ls* promoter. In *Arabidopsis*, first results indicated that 820 bp upstream and 3547 bp downstream of the *LAS* gene are sufficient for complementation, whereas further shortening abolishes promoter activity (Eicker, 2005). Additionally, 2910 bp of 5' sequences are partially able to replace the 3' region (Fig. 2). (In the 5' promoter distances always refer to the ATG, while 3' promoter sizes are counted from the stop codon.).

Due to time constraints, the constructs pAE70 and pAE84, shown in Fig. 3, had not been analyzed in as much detail as the others mentioned. The complementation results were obtained by decapitation followed by examination of side shoot outgrowth. These lines

were now subjected to closer inspection by checking every leaf axil under the binocular microscope for the presence or absence of axillary buds. All constructs were analyzed in plants homozygous for the *las-4* allele. As only the *las-4* allele was used in this project it will henceforward be referred to as *las*.

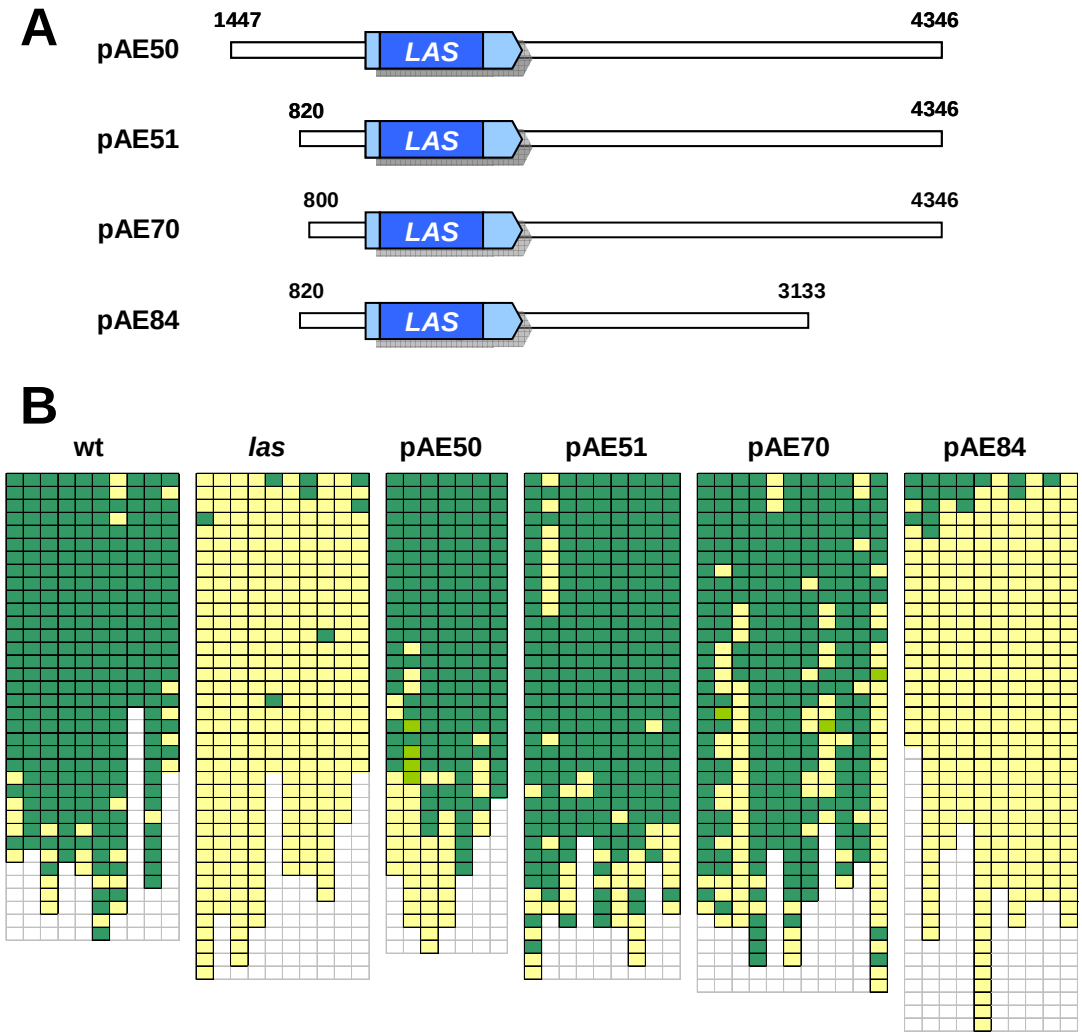


**Figure 3. Analysis of *LAS* promoter deletion constructs.**

**A**, schematic diagram of constructs analyzed. ORF shown in blue, UTRs in light blue. Numbers indicate distances in the 5' region from the start codon, in the 3' region from the stop codon of *LAS*. **B**, analysis of bud formation in rosette leaf axils of plants transformed with constructs shown above and controls, grown for 6 weeks in sd before shift to ld. Every column represents one plant, every box one rosette leaf axil from youngest (top) to oldest. Green indicates an axillary bud, yellow an empty leaf axil, light green an axillary meristem.

pAE70 includes 800 bp of 5' sequences in front of the ATG and a long 3' region of 4346 bp behind the stop codon (Fig. 3A). In pAE84, on the other hand, the *LAS* gene is preceded by 820 bp, shown to be sufficient for complementation, but the 3' sequences are shortened to 3133 bp. The constructs pAE50 and pAE51, which have previously been reported to

confer complementation (Eicker, 2005), were analyzed as controls. They differ from pAE70 in the length of 5' sequences upstream of the *LAS* gene containing 820 bp and 1447 bp respectively.

Analysis of four independent lines each of pAE50 and pAE51 revealed that plants transformed with these constructs indeed display a phenotype comparable to the wild-type, as shown in Fig. 3B. Out of six pAE70 lines examined, originating from 3 independent transformation events, only two could be unequivocally identified by PCR as carrying the complete pAE70 construct, whereas in the remaining lines some transgene sequences could not be amplified. Detailed phenotypic analyses of plants harboring the correct construct showed either partial or nearly complete complementation, one line differing only marginally in phenotype from pAE50 and pAE51 plants (Fig. 3). This indicated that the utilized promoter fragment still contains all essential elements. Four independent pAE84 lines completely resembled *las* mutants in phenotype (Fig. 3), thereby validating the presence of an important element between 3133 and 3547 bp in the 3'region.

To determine the sequences necessary for the function of the *LAS* 5'promoter, a new set of deletion constructs was designed and analyzed for their ability to complement the *las* phenotype. The constructs pBR59, pBR58, and pBR57 include 212, 400, and 600 bp upstream of the ATG and 3550 bp of the 3' regulatory sequences (Fig. 4A).

*las* plants were transformed with these constructs and analyzed by southern blot hybridization to identify single copy lines. For some constructs no single copy lines could be found, hence, lines showing the least bands on the southern blot were chosen for analysis. Homozygous lines were identified by spraying T3 seedling populations with Basta. For pBR57 two, for pBR58 four, and for pBR59 three independent lines were analyzed. Lines carrying the same construct produced equal phenotypes, apart from one pBR58 line, which also exhibited minor leaf damages and growth retardations upon Basta spraying, indicating reduced transgene cassette activity.

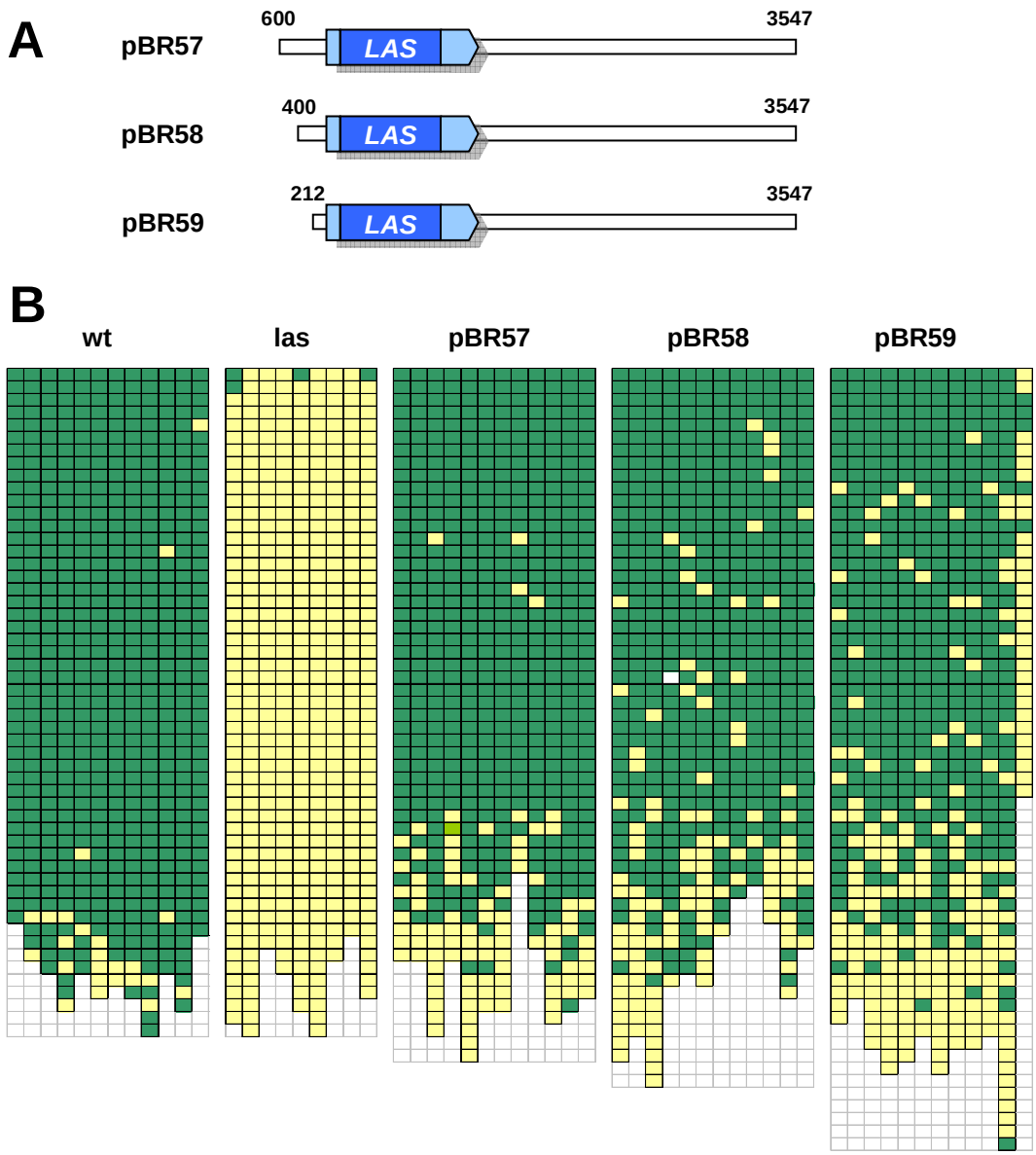


**Figure 4. Deletion construct analysis of the *LAS* 5' promoter.**

**A**, schematic diagram of constructs analyzed. ORF shown in blue, UTRs in light blue. **B**, analysis of bud formation in rosette leaf axils of plants transformed with constructs shown above and control plants, grown for 6 weeks in sd before shift to ld. Every column represents one plant, every box one rosette leaf axil from youngest (top) to oldest. Green indicates an axillary bud, yellow an empty leaf axil, light green an axillary meristem.

The construct pBR57 led to a phenotype indistinguishable from the wild-type, while plants harboring the constructs pBR58 and pBR59 displayed very minor defects in AM initiation (Fig.4B). The mild phenotypic differences between pBR57 plants and the other lines indicated the presence of a promoter element of marginal importance situated between position 400 and 600. Overall, no line manifests a strong reduction in AM initiation, illustrating that no essential 5' promoter element is localized ahead of the first 212 bp, 95

bp of which are transcribed 5'UTR sequence. This corroborates the idea that 3' sequences are of major relevance for correct *LAS* expression.

### 3.1.2. Phylogenetic promoter analysis

#### 3.1.2.1. *LAS* orthologs in different species

Another method to identify important promoter elements is phylogenetic footprinting, i.e. comparing promoter sequences of orthologous genes from different species with the aim to detect conserved regions. Orthologs of the *Arabidopsis LAS* gene were identified using BLAST algorithms on various sequence databases (TAIR, NCBI, JGI, EMBL EBI). Sequences homologous to the *LAS* protein sequence could be obtained from the close homolog *Capsella rubella*, more distantly related species like tomato and poplar, and also different monocots. Sequences from *C. rubella* and barley were described by Rossberg *et al.*, (2001) and Eicker (2005), respectively.
*LAS* sequences of 11 species were aligned with *Arabidopsis LAS* using the ClustalW algorithm, and a neighbor joining tree was constructed, depicted in Fig. 5. The closest relatives of *LAS* in the *Arabidopsis* genome, the *SCL28*, *4*, *7* and *26* genes (Bolle, 2004) as well as *SCR* and *GAI* were also included as a comparison. The phylogenetic tree shows that all genes from the different species show more identity to *LAS* than the closely related *SCL* genes, indicating that the foreign genes are orthologs or co-orthologs of *LAS*.

All grasses shown here appear to have two co-orthologs of *LAS* that evolved before speciation of maize, barley and rice. Poplar has three *LAS* paralogs, all others only one. The *LAS* alignment only roughly reflects the expected relationship of species based on their assumed evolutionary development. All grass genes form a separate clade, but asterids and rosids do not group together. This is not resolved by comparing only the considerably more conserved C-terminal halves. Nevertheless, the sequence comparison showed that there is a set of clear *LAS* orthologs, whose regulatory sequences can be used for phylogenetic analyses.

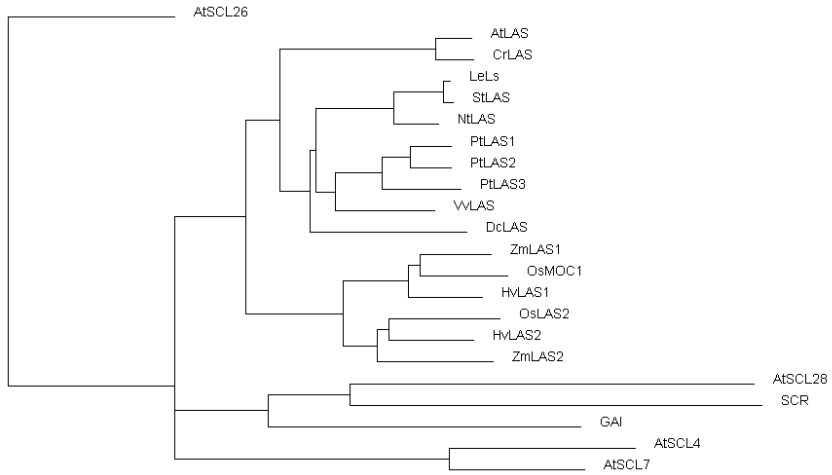


**Figure 5. Phylogenetic tree of *LAS* homologs.**

Phylogenetic tree is based on an alignment of full length protein sequences. *LAS* homologs were aligned by Bioinformatics Toolkit using ClustalW algorithm (Thomson *et al.,* 1994), shown is a neighbor joining tree using PID. Pt: *Populus trichocarpa* (poplar), Vv*: Vitis vinifera* (grape vine), Dc*: Daucus carota,* Sl*: Solanum lycopersicum* (tomato), St*: Solanum tuberosum* (potato), Nt*: Nicotiana tabacum,* Cr*: Capsella rubella,* At*: Arabidopsis thaliana, Os: Oryza sativa* (rice), Zm*: Zea mays* (maize), Hv*: Hordeum vulgare* (barley), SCL*: SCARECROW LIKE* genes from *Arabidopsis*.

#### 3.1.2.2. Phylogenetic footprinting analysis of *LAS* promoters

The available promoter regions of *LAS* and its orthologous genes were compared using the Credo 1.1 CREDO software, a web-based tool for computational detection of conserved sequence motifs. It integrates different algorithms (AlignACE, DIALIGN, FootPrinter, MEME and MotifSampler, see materials and methods) to analyze noncoding sequences (Hindemitt & Mayer, 2005).

Ample promoter sequences were available from: *Arabidopsis*, *C. rubella*, tomato, rice, barley, grapevine and poplar. A comparison of 5' promoter sequences did not reveal any highly conserved elements. An analysis of 3' regions of tomato, *Arabidopsis*, and *C. rubella* resulted in the identification of two regions with noticeable homology, referred to as region A and B (Fig. 6). Numerous short, weakly conserved motifs that were detected all along the 3' sequences, appeared in the same order, indicating a general homology of these sequences (depicted as red dots in Fig. 6). Regions A and B, however, stand out as sharing homologies of high significance (Fig. 7).

Analyses including all available sequences revealed that region A is conserved in all investigated species (Fig. 7). High similarities extend over an 82 bp stretch (in

*Arabidopsis*) conserved in every species examined so far. In all cases it was found downstream of the *LAS* gene, however, in some species less conserved copies appear 5' of the gene as well (rice: *MOC1*, poplar: *PtLAS2*). The region A does not show any open reading frame as various out-of-frame deletions or insertions are found between species. A probe against this region did not show hybridization on an RNA blot (Gregor Schmitz, personal communication) and transcriptome analysis as described by Lister *et al.*, (2008) did not reveal any transcript traces at the complete *LAS* locus, including the ORF (analysis of inflorescence tissue). This suggests that this sequence is not transcribed and the observed conservation may be due to a regulatory function. The region B was only found to be conserved in the 3' sequences shown in Fig. 6, and comprises two adjacent elements. Homologies are much less pronounced in region B than in region A, but as half of this region is deleted in pAE70, the longest non-complementing construct (Fig. 3), a role in promoter function is suggested.

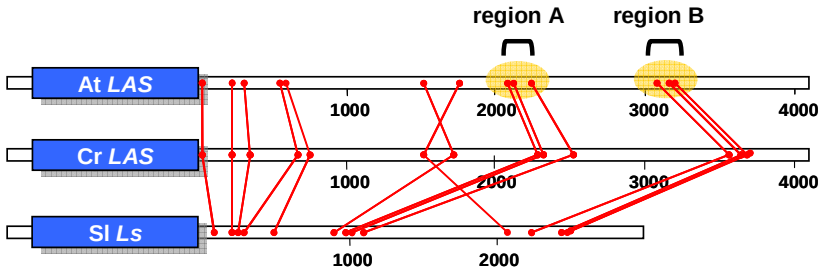


**Figure 6. Phylogenetic comparison of *LAS* 3' regions**

*LATERAL SUPPRESSOR* ORFs and 3' promoter sequences from *Arabidopsis* (At), *C. rubella* (Cr) and tomato (Sl). ORF shown in blue, red dots indicate homologous motifs as detected by CREDO software. Regions of higher homology A and B are highlighted in yellow. Numbers state distances from stop codon.

A phylogenetic footprinting analysis of 5`and 3`promoters of the genes *LAS*, *CUC1*, *CUC3*, *ROB*, *DRN*, and *RAX1*, which show similar expression profiles marking mostly incipient primordia and axils of primordia, discovered some motifs showing conservation between these sequences. However, comparing the resulting motif matrices showing the highest p-values with the available 3' regions of *LAS* orthologs, using the FIMO software tool, no well conserved motifs are found. Thus, no elements in common have been found, which are clearly associated with mRNA expression in axils of leaf primordia.

In summary, phylogenetic footprinting revealed two conserved regions in the 3' promoter. One of these shows high homologies in all investigated species, indicating that not only the *LAS* gene but also its regulatory regions are highly conserved between species.

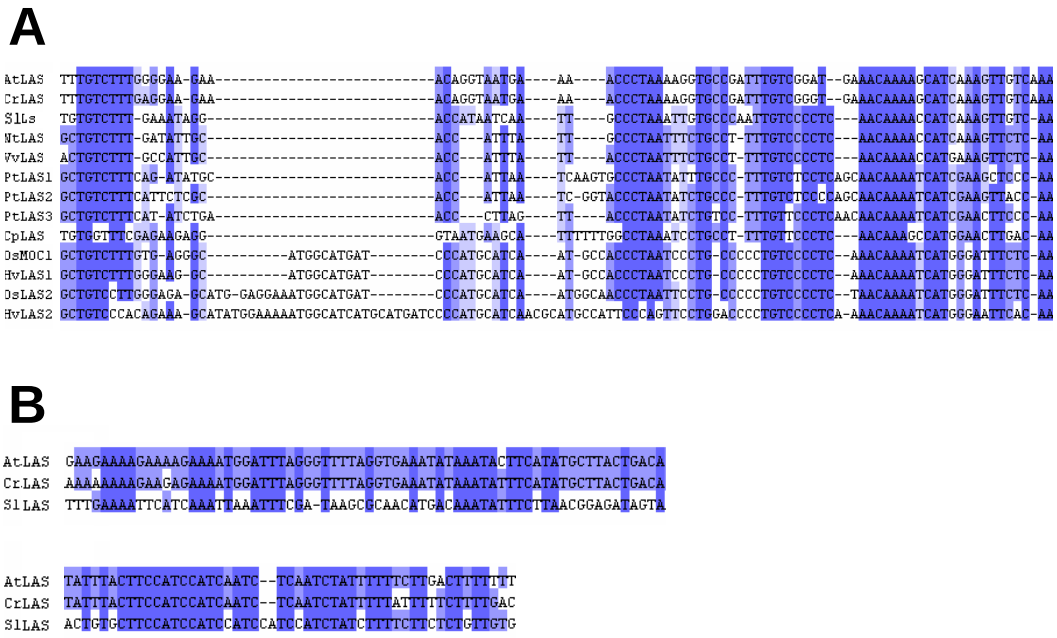


**Figure 7. Sequence alignment of *LAS* 3' promoter regions A and B of various species.**

**A**, alignment of orthologous sequences of the identified promoter region A, aligned by Bioinformatics Toolkit using MUSCLE algorithm (Edgar, 2004). The following list shows abbreviations and the distances of depicted sequences from the stop codon of the respective *LAS* ortholog. At*: Arabidopsis* (2046bp), Cr*: Capsella rubella* (2356 bp), Sl*: Solanum Lycopersicum* (tomato, 914 bp), Nt*: Nicotiana tabacum* (tobacco, 798 bp), Vv*: Vitis vinifera* (grape vine, 809 bp), Pt*: Populus trichocarpa* (poplar, *PtLAS1:* 1330 bp, *PtLAS2*: 644 bp, *PtLAS3*: 1299 bp), Cp*: Carica papaya (*1010 bp), Os*: Oryza sativa* (rice, *MOC1:* 1207 bp, *OsLAS2*: 1092 bp), Hv*: Hordeum vulgare (*barley, *HvLAS1:* 1103 bp, *HvLAS2*: 1567 bp). **B**, alignment of orthologous sequences of the promoter region B. Shown sequences appear in a distance oft 52 bp in *Arabidopsis* and 112 bp in tomato.

### 3.1.3. Tomato promoter sequences are functional in *Arabidopsis*

To test the hypothesis that the identified regions A and B are important regulatory sequences, and to further analyze the degree of conservation between species, a set of constructs containing tomato regulatory sequences behind the *Arabidopsis LAS* ORF was designed to drive *LAS* expression in *Arabidopsis*.

A genomic DNA fragment, harboring the *Arabidopsis LAS* ORF, as well as 2.9 kb of 5' sequence and 2.1 kb of 3' sequence, was previously shown to complement the tomato *ls* phenotype, indicating that there is a high functional conservation between the two genes (Greb *et al.*, 2003). This finding was substantiated by the complementation of the *las* mutant with the *Arabidopsis LAS* gene combined with 1798 bp of tomato 3' sequences

(Eicker, 2005). These promoter sequences were also shown to be functional when inserted in front of the gene.

As illustrated in Fig. 8A, tomato promoter 3´sequences were cloned behind the *Arabidopsis LAS* gene including the UTRs, 820 bp 5' and 488 bp 3'sequences. The tomato promoter fragments are deficient either in the region A, half of region B or a larger promoter part including the complete region B. The pAE128 construct carries the tomato 3' sequences in reverse orientation in front of the *LAS* gene to confirm the enhancer properties of this region. *las* mutants were transformed with these constructs and assessed for complementation. At least three independent transgenic lines each were analyzed barring pAE128, for which only one line could be established.

The construct pAE127 carrying 1306 bp of tomato 3' sequences led to a phenotype indistinguishable from the wild-type, demonstrating that this part of the tomato *Ls* promoter is able to drive *LAS* expression in *Arabidopsis*. Nevertheless regulatory sequences do not appear to be completely conserved, as pAE127 is able to confer complementation, even though it is lacking the second half of the region B. The non-complementing construct pAE84, made up of comparable *Arabidopsis* sequences, is also lacking half the 3'region B (in both cases the genomic sequences end in between the two aligned sequences shown in Fig. 7), indicating that this region in dispensable in tomato but not *Arabidopsis* sequences.

The constructs pAE123 and pAE125 confer only partial complementation of the *las* phenotype. pAE123 includes the largest 1728 bp tomato promoter fragment but is lacking the complete 3' region A, while pAE125 still contains this region, but is shortened down to 754 bp from the 3' end. The inability to confer complete complementation demonstrates that the missing regions are necessary for the tomato promoter to be completely functional. pAE128 plants display an almost wild-type phenotype, demonstrating that this tomato promoter fragment is functional independent of its position and of its orientation.

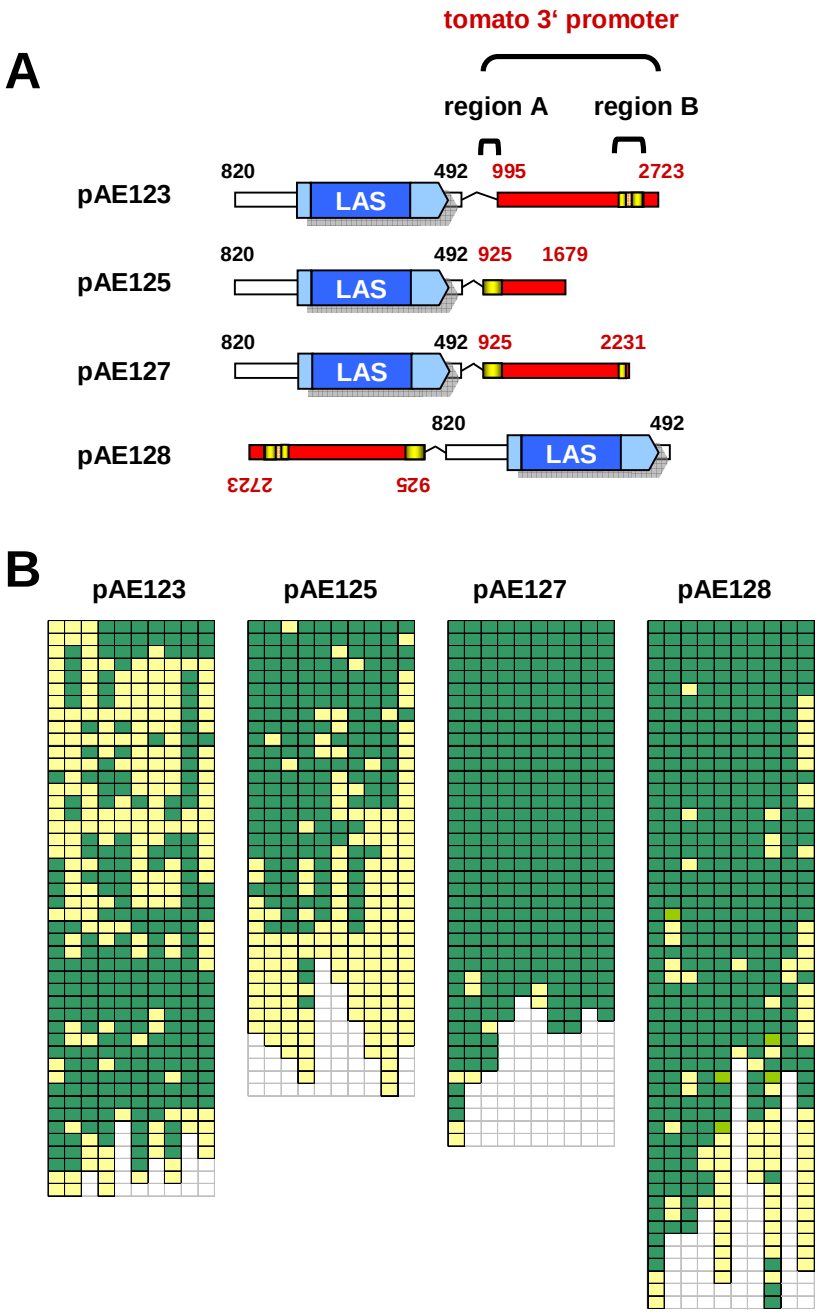


**Figure 8. Tomato promoter sequences driving *LAS* gene expression in *Arabidopsis***

**A**, schematic diagram of constructs analyzed. *LAS* ORF shown in blue, UTRs in light blue, tomato sequences in red, promoter regions A and B in yellow; *Arabidopsis* promoter sequences in white. Black numbers indicate distances from *AtLAS* start and stop codon, respectively. Red numbers indicate distances in the tomato promoter between shown sequences and the *Ls* stop codon.
**B**, axillary bud formation in rosette leaf axils of plants transformed with constructs shown above. Each column represents one plant, every box one rosette leaf axil from youngest (top) to oldest. Green indicates an axillary bud, yellow an empty leaf axil, light green an axillary meristem.

### 3.1.4. Determining the significance of selected promoter regions

To verify the importance of the different promoter regions investigated so far, transgenic lines were established, in which defined parts of the *LAS* promoter were either deleted or modified. The hypothesis that the 5' promoter region is only required to provide basal and unspecific activity was investigated by replacing it with both a flower specific *PISTILLATA* (*PI*) promoter fragment and with a 35S CaMV minimal promoter. These promoter assemblies contain the *LAS* gene including the UTRs in combination with either 3550 bp of 3' sequences, shown to be sufficient for complementation, or with insufficient 483 bp of 3' sequences, in order to examine the impact of this 3` region on *LAS* expression (Fig. 9A). In order to determine the importance of the 3'regions A and B the constructs pBR38 and pBR39 were devised, in which either the region A is deleted or the construct ends just behind region B (Fig. 10A). pBR49 carries 820 bp of upstream sequences, a short insufficient downstream promoter, and additionally 1723 bp of 3' sequences in reverse orientation in front of the gene, including regions A and B. It was designed firstly to prove that the important 3'regulatory elements have characteristics of enhancer elements, being independent of orientation and position in regard to the gene. Secondly, as this construct lacks the bp 483 to 1827 of the 3' promoter, it can also reveal if this region plays an essential role in promoter function.

As mentioned in the previous chapter, identification of single copy lines by southern blot hybridizations was not successful for all lines. In these cases lines showing as few bands as possible on the southern blot were chosen for analysis. For constructs pBR38 and pBR49 four independent lines were analyzed, for pBR37, pBR39, pBR41, pBR42, and pBR44 three lines, for pBR43 two lines. Lines of the same construct displayed mostly consistent phenotypes, apart from one line of each pBR37 and pBR49 showing no complementation at all and one pBR41 line exhibiting complementation only in the lower rosette.

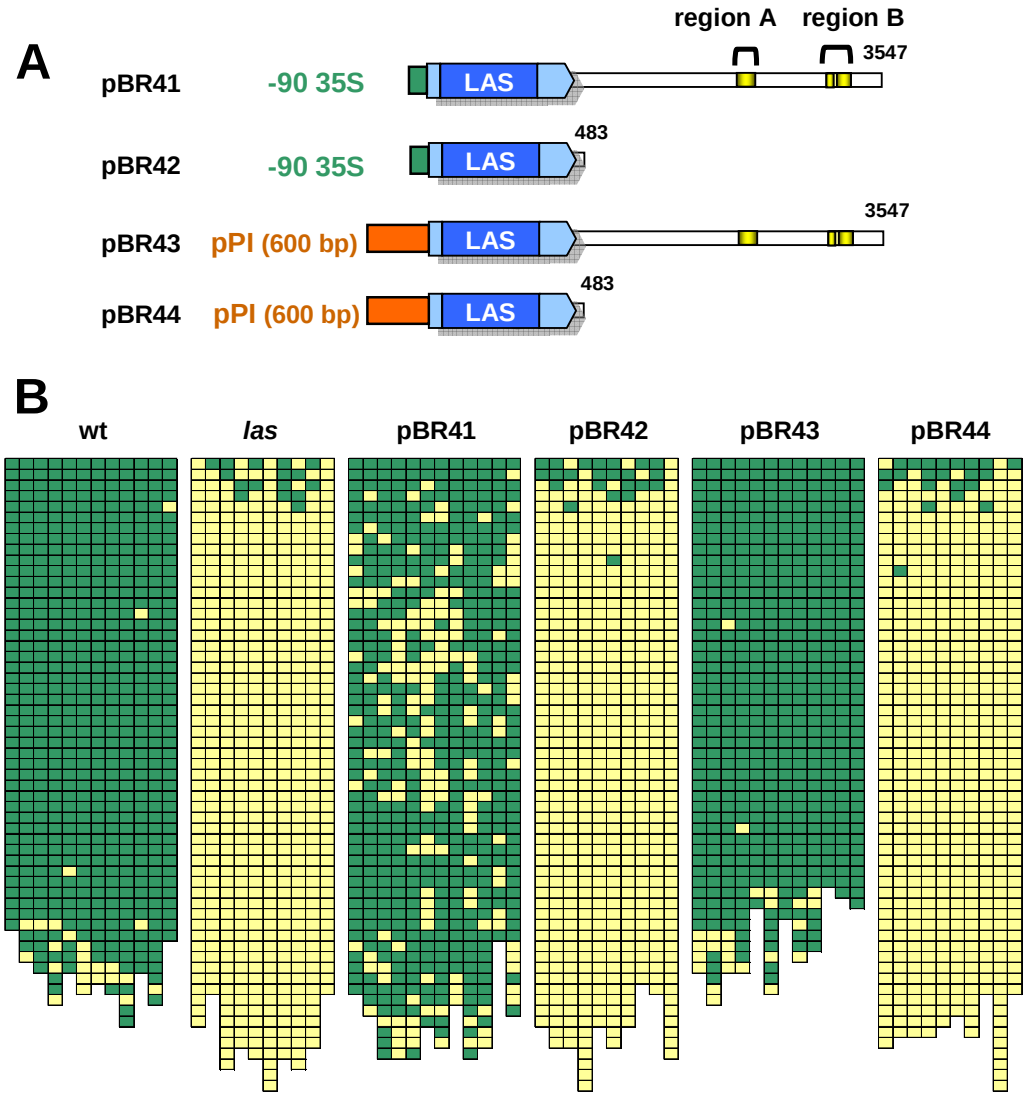


**Figure 9. Analysis of *LAS* promoter swapping constructs.**

**A**, Schematic diagram of the constructs analyzed. LAS ORF depicted in blue, UTRs in light blue, promoter regions A and B in yellow, -90 bp 35S minimal promoter in green, 600 bp *PI* promoter fragment in orange.
**B**, axillary bud formation in rosette leaf axils of populations transformed with constructs shown above, grown for 6 weeks in sd before shift to ld. Every column represents one plant, every box one rosette leaf axil starting from youngest (top) to oldest. Green indicates an axillary bud, yellow an empty leaf axil.

pBR43 carries a *PI* promoter fragment of 600 bp (Fig. 9A), which was shown to promote expression in flower primordia (Honma and Goto, 2000), but not in inflorescence meristems (Fig. 12C). In combination with the *LAS* 3' regions it activates the *LAS* gene sufficiently to confer full complementation, as the population shown in Fig. 9B was indistinguishable from wild-type plants.

pBR41 is merely equipped with a 90 bp 35S minimal promoter (Benfey *et al.*, 1989, Honma and Goto 2000) and also led to almost complete complementation, with plants

showing only mild defects in AM initiation. This demonstrates that no specific promoter elements are required in front of the TSS of the *LAS* gene, as long as the shown 3' sequences are present. The lack of side shoots seemed to be most pronounced in the middle of the rosette, whereas other promoter lines showing partial complementation tended to exhibit most empty axils in the oldest rosette leaves. This suggests a zonal variation in the activity of the -90 35S promoter, which is supported by a third analyzed pBR41 line grown at a later time point. Complementation was only partial but restricted to the lower rosette (data not shown).

The mostly complete complementations elicited by pBR43 and pBR41 constructs are contrasted by the lines transformed with the constructs pBR42 and pBR44, which are lacking a long 3' region. Plants carrying these constructs phenocopy *las* mutants, confirming that the *LAS* 3' regulatory sequences are essential for correct expression of *LAS*.

The pBR37 plasmid, carrying 820 bp 5' and 3547 bp 3' sequences, was designed as a positive control in the vector used for all constructs during this work and resembles a promoter assembly previously shown to confer complementation (Fig. 10). Accordingly plants transformed with pBR37 were indistinguishable from wild-type plants.

The pBR38 construct has an 83 bp deletion of the complete 3' region A starting from 2055 bp after the stop codon. Complementation ability of theses constructs is unaffected, as pBR38 plants shown in Fig. 10 did not differ significantly in phenotype from those carrying the pBR37 construct.

pBR39 contains 3239 bp of 3'sequences, thus carrying a complete 3'region B. That means it is 106 bp longer than the non-complementing construct pAE84, in which half the 3' region B is missing. Hence, complementation ability should be reconstituted if region B is the crucial element. Contrasting this expectation, Fig. 10 illustrates that pBR39 amends the *las* phenotype no more than pAE84 (Fig. 3), thereby narrowing down the location of the essential element required for promoter function to the region between 3239 bp and 3547 bp.

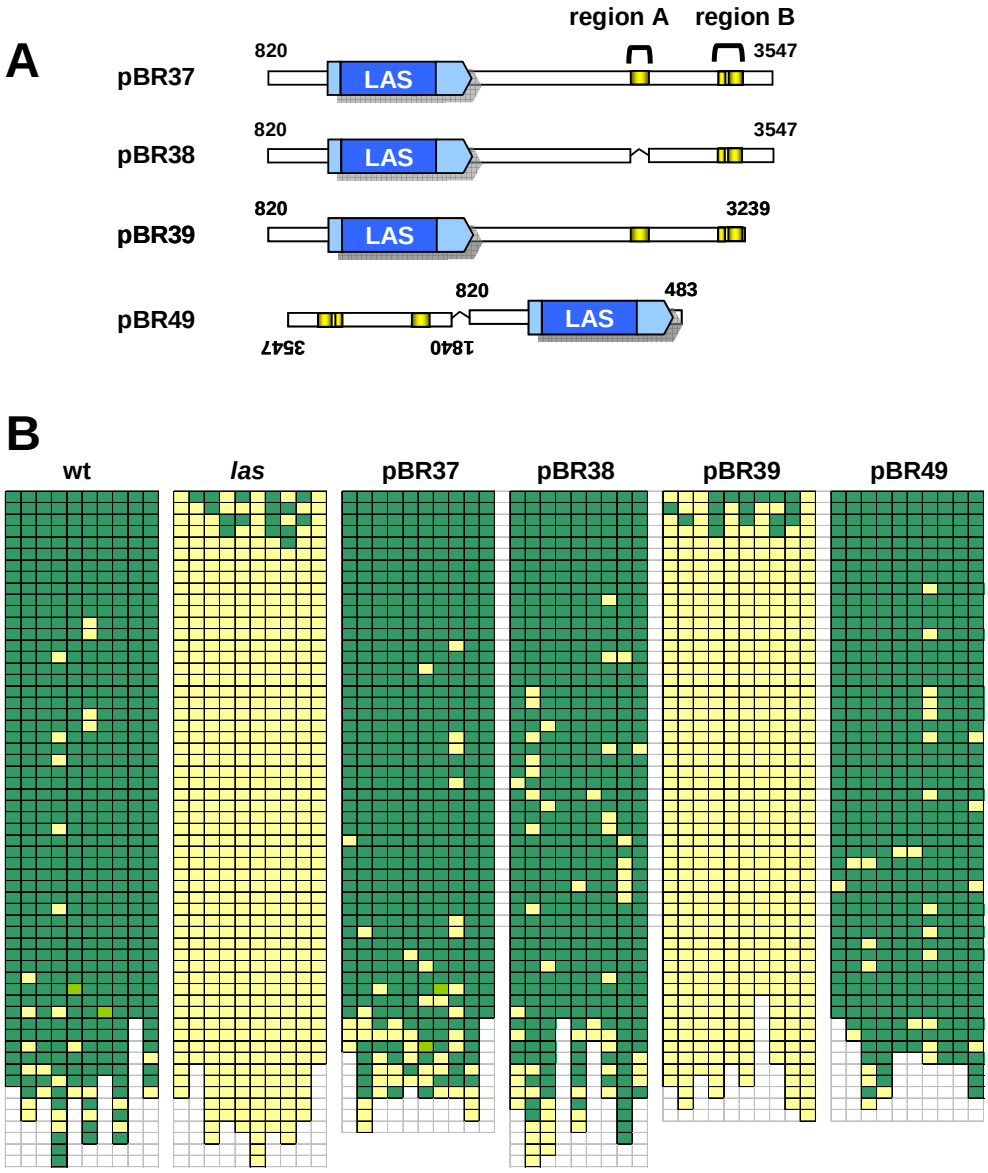


**Figure 10. *LAS* promoter deletion analysis investigating specific regions.**

**A**, Schematic diagram of the constructs analyzed. *LAS* ORF depicted in blue, UTRs in light blue, promoter regions A and B in yellow.
**B**, axillary bud formation in rosette leaf axils of populations transformed with constructs shown above, grown for 6 weeks in sd before shift to ld. Every column represents one plant, every box one rosette leaf axil starting from youngest (top) to oldest. Green indicates an axillary bud, yellow an empty leaf axil.

pBR49 led to a full restoration of the wild-type phenotype, which demonstrates that the 3' region is functional independent of location and orientation in respect to the *LAS* ORF (Fig. 10). This also demonstrates that the missing 3' sequences from bp 483 to 1827 do not contain any motifs of fundamental importance for promoter function.

### 3.1.5. Visualization of promoter activities by GUS stainings

The various modifications of the *LAS* promoter led to altered gene expressions, resulting in the different degrees of complementation described above. To visualize the exact expression patterns leading to the various states of functionality of the *LAS* gene, different promoter assemblies were combined with the GUS reporter gene.

pES44 contains ample *LAS* promoter areas of over 4 kb upstream and nearly as much downstream of the reporter gene (Fig. 11). As shown in Fig. 12A, all other GUS constructs represent the promoter assemblies previously examined for complementation, depicted in Fig. 9 and Fig. 10. In every construct the GUS ORF is combined with the *LAS* UTRs to yield the identical expression pattern, as in the complementation experiments. Constructs pBR45 – 48 were analyzed in the *las* mutant background. For each of these constructs three to four independent lines were examined, some lines exhibited weaker signals but no deviating expression patterns.

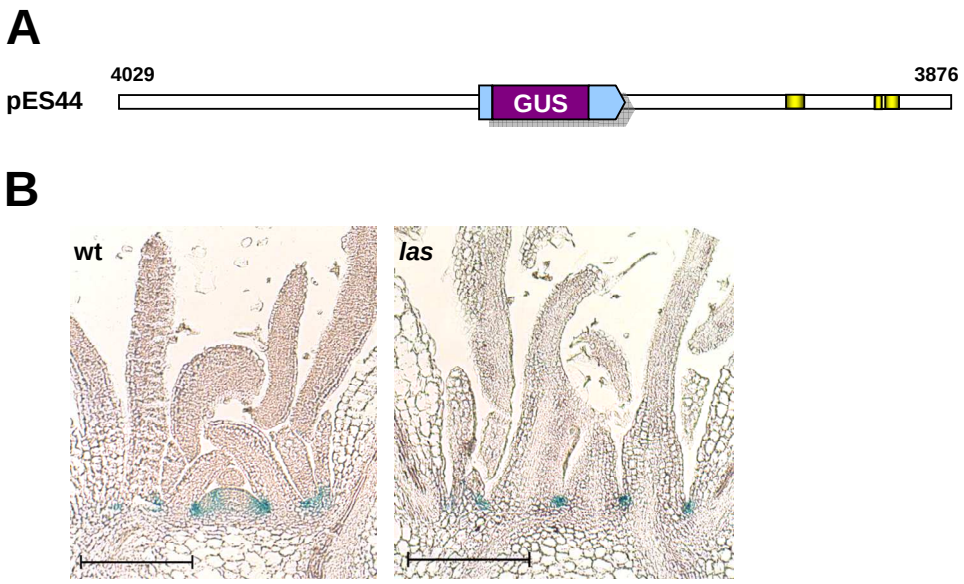


**Figure 11. LAS::GUS expression in wt and *las* plants.**

**A**, schematic representation of pES44 construct. GUS ORF in violet, LAS UTRs in light blue, conserved regions A and B in yellow. **B**, GUS signals in vegetative apices conferred by pES44 in wt and *las* mutant plants. Bars: 200µm.

In plants transformed with the pES44construct, which contains large promoter regions, GUS signals appeared in the axils of leaves (Fig. 11A and B). The pattern resembled that determined by RNA in situ hybridization shown in Fig. 1C. Signal strength appeared similar in wild-type and *las*, although previous in situ hybridization studies indicated

reduced mRNA levels in the *las* mutant (Greb, 2003). Quantitative cDNA analysis confirms that *LAS/las* mRNA levels do not differ significantly between mutant and wild-type (see chapter 3.2.4.2).

GUS signal conferred by pBR47 (Fig. 12F) showed the same pattern as observed in pES44 plants or *LAS* RNA in situ hybridizations (Fig. 1). pBR47 contains all the *LAS* promoter regions shown to be sufficient for complementation (compare to pBR37, Fig. 10) and promotes expression in the axils of rosette leaves, cauline leaves, and flowers (Fig. 12F). Hence, the complementation that was shown using these promoter regions (Fig. 10) is associated with the endogenous *LAS* expression pattern. Fig. 12H and I depict two early flower primordia in stage 3-4 (Smyth *et al.*, 1990). At this stage the earliest GUS signals in flowers started to appear in the axils of sepals. Later on during flower development expression is found in boundary regions separating all organs. This includes expression between sepals and petals and between carpels, which has not been reported before (Fig. 12J).

pBR45 plants, carrying the same 35S minimal 5' promoter as the partially complementing pBR41 line, showed GUS signals similar to the endogenous *LAS* expression in the axils of leaves, flowers, and in flowers (Fig. 12K). Additionally GUS signals were detected in the outer cell layers of the hypocotyl, more intense in the zone between hypocotyl and rosette, and strongly enhanced around emerging lateral organs, probably adventitious roots (Fig. 12O).

The *PI* 5' promoter in combination with the *LAS* 3' sequences produced a GUS expression pattern composed of both activities. Fig. 12L and N illustrate the *LAS*-like expression in the axils of leaves and flowers as well as between floral organs, explaining the complementation ability of pBR43 (Fig. 9). Fig. 12N represents a stage 9 flower clearly illustrating the expression between sepals and petals. The early stage 3 flower primordium in Fig. 12M, however, displayed a strong signal, which did not appear in pBR47 plants shown in Fig. 12H, I. Interestingly this expression also did not completely resemble the previously published expression pattern caused by the inserted 600 bp *PI* promoter fragment (Honma and Goto, 2000; Fig. 12C), but instead appeared similar to the expression pattern caused by a 500 bp fragment of *PI* (Fig. 12D). During later stamen development the GUS expression did not remain activated, as in both the 600 bp and 500

bp *PI* promoter lines (Fig. 12E), but instead vanished from stamens as observed in pBR47 plants.

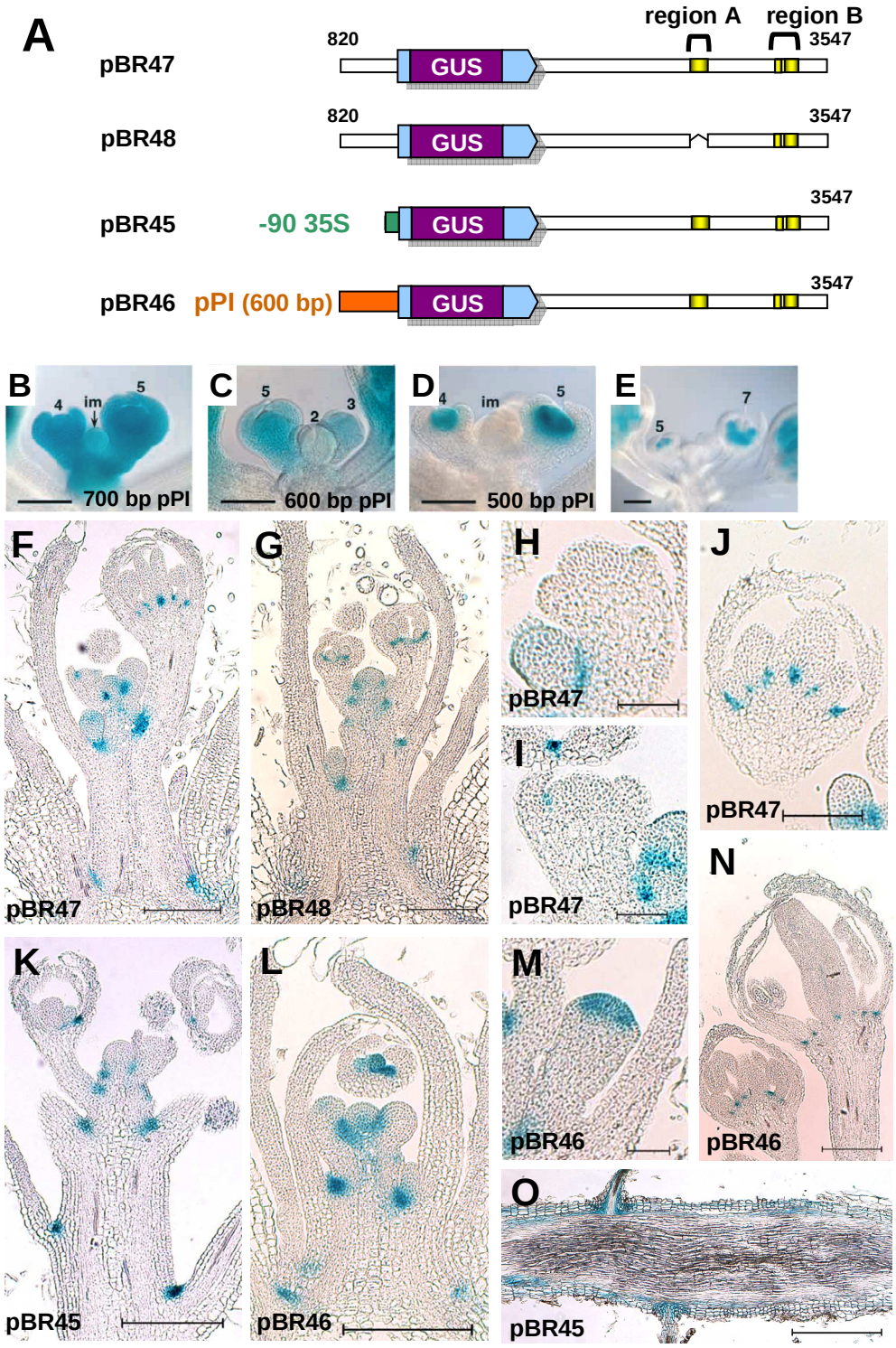


**Figure 12. GUS stainings of promoter deletion and promoter swapping constructs.**

**A**, schematic representation of analyzed constructs. GUS ORF in violet, LAS UTRs in light blue, conserved regions A and B in yellow, -90 bp 35S minimal promoter in green, 600 bp *PI* promoter fragment in orange.
**C - E**, GUS expression generated by different *PI* 5' promoter fragments fused to the GUS gene. Pictures from Honma and Goto (2000), bars 100µm. **F**, **H**, **I**, **J**, GUS expression observed in pBR47

plants in the reproductive apex (**F**), two flower primordia (stage 3 – 4) beginning to show signals in the axils of sepals (**H**, **I**), and in a stage 6 flower (**J**). **G**, GUS signals in the reproductive apex of pBR48 plants. **K**, **O**, GUS expression generated by the pBR45 construct in a side shoot (**K**) and the hypocotyl (**O**). **L, M**, **N**, GUS signals conferred by pBR46 in the reproductive apex (**L**), early stage 3 flower (**M**), stage 9-10 flower (**N**). Bars F, G, K, L, N 200µm; J 100 µm; H, I, M, 50µm; O 500µm. ld grown plants out of the T2 generation were treated with Basta and harvested at a time around the onset of flowering.

The pBR48 plants (Fig. 12G) are lacking the promoter region A like pBR38 (Fig. 10). In line with the result that pBR39 plants complement the *las* phenotype, the GUS expression pattern was identical to the one observed in pBR47 plants, resembling the endogenous *LAS* expression.

In summary, analysis of GUS lines revealed that all constructs harboring the *LAS* 3' sequences can confer an expression pattern similar to the known *LAS* mRNA accumulation pattern. In each case GUS signals were observed in small domains in the axils of rosette and cauline leaves and floral primordia and between floral organs. Only the constructs harboring a minimal 35S promoter or a *PI* promoter fragment exhibited additional signals according to their own specificities.

## 3.2. Part II: Characterization of a new player of axillary meristem formation

In order to obtain a deeper understanding of AM initiation it is of major importance to discover more of the players involved in the genetic network controlling this process. An efficient technique to identify new factors is a genetic screen, searching mutagenized populations for mutants, in which side shoot development is perturbed. Following this strategy a screen, designed to identify modifiers of the *las-4* phenotype, was set up as described by Oliver Clarenz (2004). *las-4* mutant seeds were mutagenized with EMS and M2 populations analyzed for alterations of the *las-4* phenotype. This led to the identification of numerous mutants named *enhancers of lateral suppressor* (*eol*), in which AM formation is compromised also in cauline leaf axils. This second-site mutagenesis screen is expected to produce mutants that act redundantly to *las* on the final process of AM initiation. An advantage of this *las* modifier screen is that it utilizes a background sensitized for AM formation defects. Therefore, it may also detect mutants that exhibit phenotypic deviations too weak to be spotted in a wild-type background.

### 3.2.1. The *enhancer of lateral suppressor 5* (*eol5)* mutant

The *eol5* mutant was identified in the *las-4* second-site mutagenesis screen, for its strong reduction in side shoot development (Clarenz, 2004). Under short day conditions the amount of buds formed in cauline leaf axils was strongly decreased, up to a complete loss of axillary shoot formation (Fig. 13A - C). However, no phenotypic deviations were observed under long day conditions. Only after four weeks of growth under short days and subsequent shift to long days an effect of the *eol5* mutation becomes observable, reaching full penetrance after about six weeks in short days (Clarenz 2004). The phenotypic severity is not only dependant on day length but also on growth conditions and other factors, for details see chapter 3.2.3.3.

During a detailed analysis of *eol5 las* plants, further phenotypic alterations were observed that had not been noticed in previous studies. The double mutant repeatedly exhibited defects in inflorescence meristem function, leading to defective floral primordia and flower development in a zonal fashion along the stem, as illustrated in Fig. 13A. Less pronounced defects led to malformed and infertile flowers, at other times floral primordia only produced reduced structures or appeared to be missing altogether (Fig. 13F and G).
Defective SAM function also manifested in a complete termination of meristem activity (Fig. 13I). When grown under short day conditions *eol5 las* plants showed these meristem arrests at varying frequencies. While in some populations up to 75 % of plants terminated, this effect was not noticed at other times. Meristem arrests were never observed in parallel grown *las* plants. Termination occurred at a later stage of growth after bolting in short day conditions. This is clearly distinguishable from the normal halt of growth at the end of a plants life cycle, which takes place at a later time point, with some flowers arrested at different developmental stages remaining on the apex.

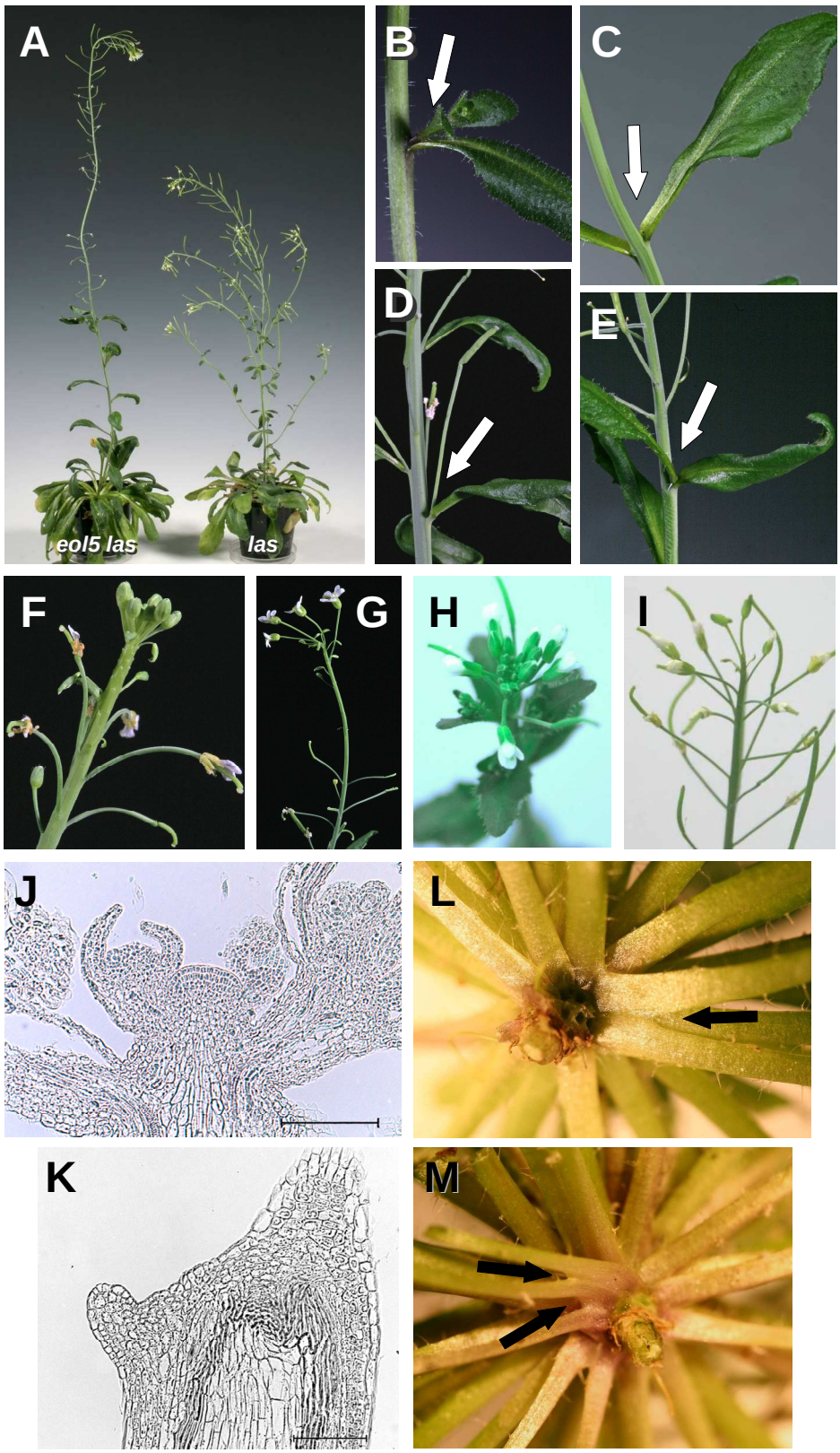


**Figure 13. Phenotype of *eol5 las* double mutants.**

**A**, growth habit of wt and *eol5 las* plants grown in sd. **B** to **E**, cauline leaf axils showing lateral shoot (**B**) as observed in wt or *las* plants, empty leaf axil (**D**) as seen in *eol5 las* plants, flower (**D**), and leaf (**E**) emerging from a leaf axil. White arrows point to affected axils. **F** and **G**, zones of defective floral primordia development, observed in *eol5 las* plants, at an earlier (**F**) and later (**G**) stage, leading to infertile flowers and barren stem segments. **H**, wt inflorescence with flower truss. **I**, terminated *eol5 las* inflorescence. **J** and **K,** sections of late wt (**J**) and terminated *eol5 las* (**K**)

inflorescence apices, harvested at same time point. Bars 100 µm. **L** and **M**, fusions of rosette leaves in *eol5 las* plants. Rosettes are shown from below, the root and the lowest rosette leaves have been removed. Black arrows indicate fusions.

The terminal structures in *eol5 las* apices which ceased growth, ranged from fully developed flowers to reduced flowers, minute leaves, or pin like structures (Fig. 13I). Sections shown in Fig. 13J and K illustrate the cellular morphology of wild-type and terminated *eol5 las* inflorescences. Wild-type apices, measuring 40 to 80 µm in diameter, displayed floral primordia of different developmental stages and small meristematic cells in their expected positions. Terminated *eol5 las* shoot tips, on the other hand, ended growth with enlarged apices of 150 to 300 µm and mostly lacked small undifferentiated cells. Additionally, shoot tips are completely devoid of recognizable flower primordia, instead malformed structures, often made up of differentiated cells, were found adjacent to the termination site. The loss of meristematic identity indicates a role of *EOL5*, possibly in redundancy with *LAS*, in the maintenance of the main meristem.

The uppermost cauline leaves of *eol5 las* plants commonly harbored flowers instead of side shoots in their axils (Fig. 13D), occasionally leaves or other reduced structures (Fig. 13E). Formation of flowers in cauline leaf axils also occurs in *las* single mutants but less frequently, as can be seen e.g. in Fig. 23.

In addition, *eol5 las* mutant plants displayed fusions of rosette leaves as depicted in Fig. 13L and M. The observed fusions merged the base of rosette leaves and occurred in the lower part of the rosette in almost all double mutants, whereas this was virtually never observed between pairs of leaves in *las* plants. In plants grown in short days at two different time points an average of 6.7 ± 4.3 (n = 11+4) leaves per plant were involved in such fusions. Under long day conditions this phenotype was also observable but less pronounced. 50 % of the plants exhibited fusions, with 3.0 ± 1.0 (n = 10) leaves involved. This signifies that *EOL5*, together with *LAS*, is also involved in organ separation.

## 3.2.2. Positional cloning of *eol5*

### 3.2.2.1. Rough mapping of *eol5*: problems and solutions

In order to identify the mutation causing the *eol5* phenotype a map based cloning strategy was adopted, as described in chapter 2.2.14. The *eol5 las* double mutant was crossed to the *Landsberg erecta* (Ler) accession, to be able to utilize the number of known polymorphisms between Col and Ler. For rough mapping of the *eol5* locus, the F2 population was phenotyped and genotyped, as reported by Schulze (2007).

The phenotyping proved to be the challenging element of the mapping process, since the F2 population did not show the segregation ratio of a recessive mutation. Apart from the expected phenotypes, many plants with intermediate levels of bud formation were observed, a problem persisting throughout the whole mapping effort. Nevertheless, rough mapping was carried out, genotyping those plants showing a strong *eol5 las* double mutant phenotype (Schulze, 2007). The analysis revealed a considerable increase in the Col allele frequency on chromosome II and a less pronounced one on chromosome V. This indicated that the *eol5* locus is situated most likely on the lower arm of chromosome II.
Segregation of *las-4* modifiers from the Ler background and their interaction with Col factors were assumed to be the main reason for the distorted segregation ratios and the appearance of intermediate phenotypes. Recent results suggest that also the penetrance of the mutant phenotype and environmental factors play a substantial role (see chapter 3.2.3.3). To facilitate fine mapping, a mapping population exhibiting an unambiguous segregation ratio in a homozygous *las* mutant background is required. For this purpose, a backcross strategy was applied, mainly to reduce the amount of Ler alleles in the background (Schulze 2007). A heterozygous F2 plant was backcrossed twice to the *eol5 las* mutant while retaining a Ler allele at the *EOL5* locus. The F2 population of the second backcross (BC2F2) was used in this work to verify the rough mapping results and to initiate fine mapping. At later stages subsequent generations down to BC2F5 were utilized, as background segregation is reduced in these lines.

### 3.2.2.2. Fine mapping of *eol5*

Analysis of different BC2F2 populations showed that the problems with segregation ratios were all but solved by the conducted backcrosses. Fig. 14C and D illustrate phenotypes obtained from two exemplary mapping populations segregating for *eol5* in a homozygous *las* background. Many plants could not be classified as either *eol5 las* nor as *las* based on bud formation in cauline leaf axils, whereas control populations shown in Fig. 14A and B formed distinct groups. The population in Fig. 14C contained the expected number of *eol5 las* mutants but lacked the anticipated ¾ of *las* looking plants, whereas another population (Fig. 14D) produced many plants with *las* phenotype but no strong *eol5 las* mutants. Genotypic analysis of two markers, later on shown to enclose the *eol5* locus, revealed that the *eol5 las* phenotype co-segregates to a large degree with the homozygous Col genotype, as indicated in Fig. 14C and D below the graphs. This verifies the rough mapping result, proving that the *eol5* locus is situated in this region of chromosome II.

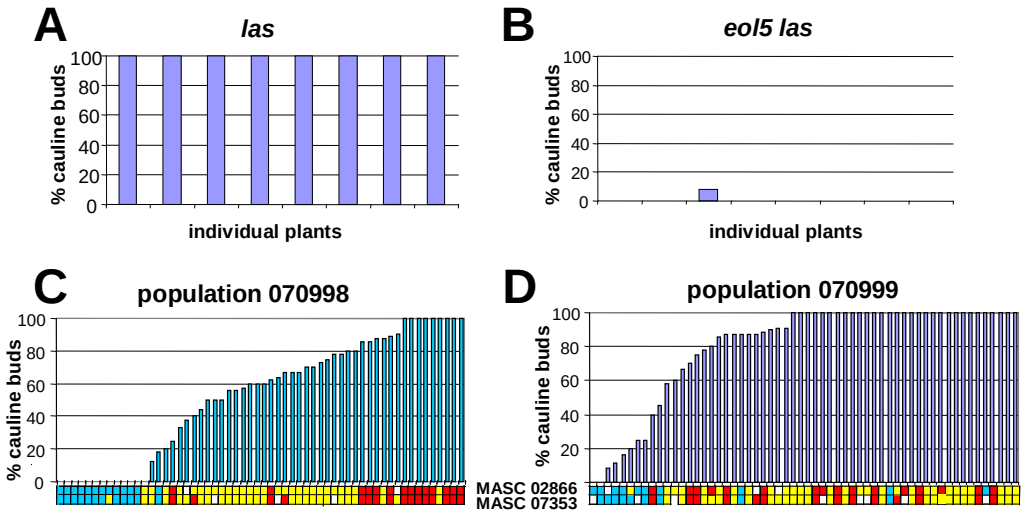


**Figure 14. Axillary bud formation phenotypes of control and exemplary mapping populations.**

**A**-**D**, axillary bud formation in cauline leaf axils presented as percentage of cauline leaf axils that support bud formation. X-axis shows the number of analyzed plants, every column representing one plant, ordered by percentage of bud formation. **A**, **B**, homozygous *las* (**A**) and *eol5 las* (**B**) control populations. **C**, **D,** two exemplary BC2F3 mapping populations. Below graphs genotypes of the respective plant above is stated for the markers MASC07353 and MASC02866. Red: homozygous Ler, yellow: heterozygous, blue: homozygous Col.

Yet numerous plants did not exhibit the phenotype that could be deduced from their genotype, some showing more, others less axillary buds. The first population (Fig. 14C) hints towards a dosage effect of *EOL5*, as mostly heterozygous plants display intermediate phenotypes but the population in Fig. 14D does not substantiate this idea. Indications for a

dosage effect were already reported earlier (Clarenz, 2004). Looking at many populations evidence for such an effect was found on multiple occasions but it never appeared to be reliably reproducible.

The variability of the phenotype poses a big challenge to fine mapping, which usually relies on the correct phenotyping of single plants. Consequently first fine mapping attempts yielded contradictory results. Plants harboring recombination breakpoints in the area of interest, between the markers MASC07353 and MASC02866, were phenotyped and genotyped, resulting in information on which side of the recombination event the mutation is located. Since classifying single plants as either wild-type or mutant, based on their phenotype, is largely prone to errors, as seen in Fig. 14C and D, the directional information produced extensive contradictions. Due to this problem the strategy was modified in a way that offspring populations of interesting recombinants were analyzed, to deduce the parental genotype regarding the *eol5* mutation. Between 12 and 32 plants per population were analyzed, if possible utilizing later generations down to BC2F5 populations, to diminish the amount of segregating modifiers in the background. Following this strategy numerous offspring populations of recombinants were examined with a range of new markers, resulting in the positional information shown in Tab. 3 and Fig. 15.

Contradictions could not be eliminated, but reduced, pointing to a region between marker MASC02463 and MASC445742, which are most likely to enclose the mutation causing the *eol5* phenotype (Tab. 3). Remaining contradictions arose from two lines (080455 and 080462), pointing towards an *eol5* locus left of marker MASC02463, dissented by the positional information obtained from nine lines (080438 to 080057, Tab. 3). On the right side, only one line (080057) indicated that the mutation is right of the marker MASC445742, a position that is in disagreement with nine other lines (080047 to 080462). In between these two markers further contradictions could not be reliably resolved, so that a region of 256 kb, containing 64 annotated genes (Fig. 15), was taken into consideration to contain the *eol5* locus.

**Table 3. Positional information about the location of the *eol5* locus obtained from fine mapping populations.**

Analysis of markers in the chromosomal region investigated by fine mapping. Every row represents one plant, carrying a recombination in the region of interest, whose offspring populations have been examined for co-segregation of the *eol5* phenotype with shown segregating genetic markers. Genotype at the respective markers is depicted by color. Turquoise = Col, yellow = heterozygous and orange = Ler, boxed genotypes have been determined by PCR, others inferred from neighboring markers.
The results shown in the second row denote, whether the offspring populations of this plant showed co-segregation of the *eol5 las* phenotype with the markers segregating in those populations. Derived from this information arrows are drawn pointing towards the expected location of causative mutation. As described above and in chapter 3.2.3.3, a plant's phenotype did not always reflect the genotype at the eol5 locus, thus, difficulties arose judging co-segregation in offspring populations. Strength of arrow indicates confidence in the stated decision on co-segregation.

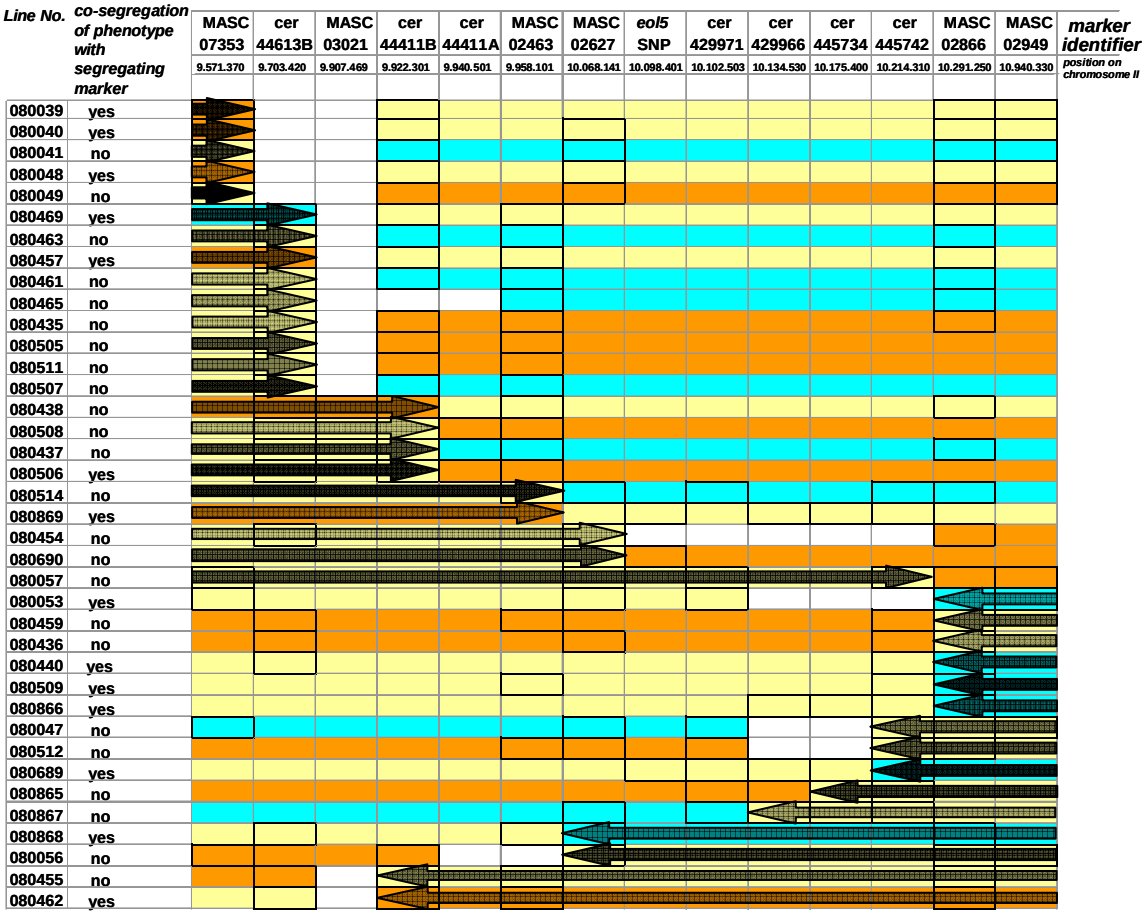


Within this region the ORFs of 39 candidate genes were sequenced, obtaining ≥ 70 kb of sequence information. While the *las* parent line showed no polymorphism to the sequence available at the TAIR database, only one single mutation could be detected by sequencing the *eol5 las* double mutant. The single identified mutation is a G to A exchange in the gene at2g23740. According to the TAIR gene annotation the nucleotide exchange locates to the second exon and leads to a premature stop codon after AA 62, as illustrated in Fig. 16B.

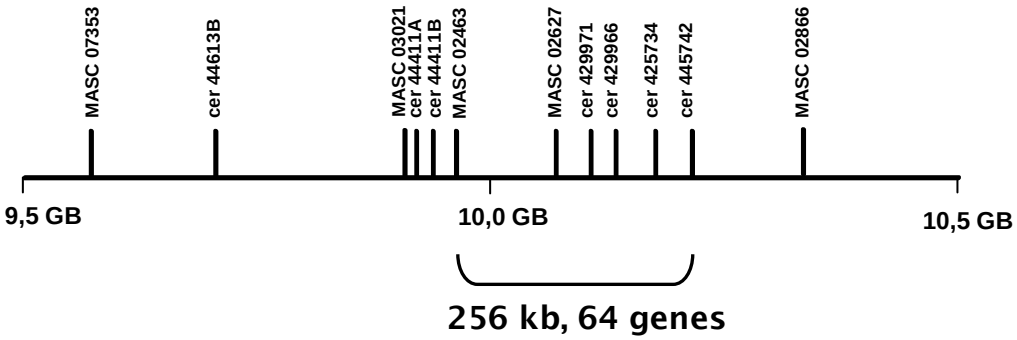


**Figure 15. Physical map of part of the lower arm of chromosome II**

Physical map of the region of interest on chromosome II showing the positions of used markers. Parenthesis indicates the region in which the *eol5* mutation is presumably located according to the fine mapping results.

In 2007 Krichevsky *et al.*, published their work on the gene at2g23740 naming it *CZS*, due to the conserved C2H2 zinc finger and SET domains. *CZS* presumably encodes a histone methyltransferase, a class of proteins involved in epigenetic control of chromatin state by the methylation of lysine residues of histones. The structure of the gene is shown in Fig. 16A and C, exhibiting homologies to four known protein domains. Next to three C2H2 zinc finger domains there is an N-terminal combination of a PreSET domain, a SET domain, and a PostSET domain, known to confer histone methyltransferase activity (Baumbusch *et al.*, 2001).

*CZS* is described to be a negative transcriptional regulator, physically interacting with *SWP1*, a SWIRM PAO domain protein (Krichevsky et al, 2007). The T-DNA insertion allele *czs-1* shows a moderate delay in flowering time and a corresponding upregulation of *FLC*, accompanied by a decrease in H3K9 and H3K27 dimethylation of the *FLC* locus. As yet no reports indicate a role in meristem initiation or maintenance, nor is there an obvious connection to the described *CZS* function.

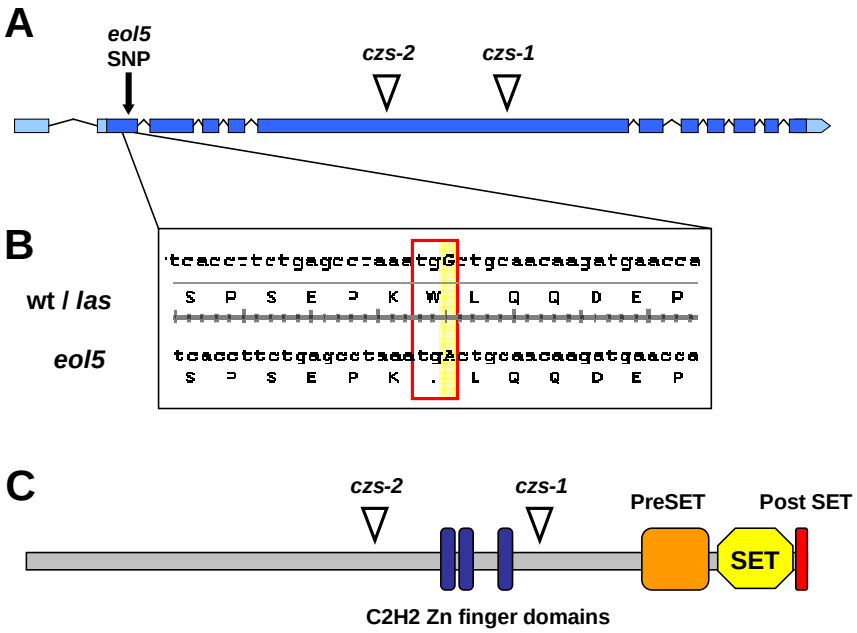


**Figure 16. Gene structure of *CZS*.**

**A**, intron-exon structure of *CZS*, ORF depicted in blue, UTRs in light blue, spaces in between indicate introns. Arrowheads point out positions of *czs-1* and *czs-2* T-DNA insertions in mutant alleles, arrow indicates position of SNP in *eol5* allele. **B**, close up of sequence containing SNP detected in *eol5 las* plants. Nucleotide change highlighted in yellow, AA change leading to premature Stop codon at AA 63 boxed in red. **C**, protein sequence showing known protein domains, as predicted by SMART software tool.

### 3.2.2.3. Annotation of *CZS*

Krichevsky *et al.*, (2007) published a cDNA sequence for *CZS* (GenBank accession number DQ104398), which deviates from the TAIR annotation in a way that a later start codon is suggested, leading to an 804 nt shorter ORF (Fig. 17A).

This reported ORF poses a problem to the fine mapping result of *eol5* (chapter 3.2.2.2), because, according to this published sequence, the identified mutation would in fact not be in the ORF. Instead, it would locate, including the denoted introns, 1124 bp in front of the start codon (Fig. 17A). In such a position a mutation would most likely not cause a serious constraint to the function of *CZS*, hence, not explain the *eol5* phenotype.

In order to provide evidence supporting the TAIR annotation, an alignment of *CZS* to several mRNA derived sequences is shown in Fig. 17. Fig. 17D displays aligned ESTs from the TAIR data base. As ESTs are usually obtained by single Sanger sequencing reads from the ends of cDNAs, they only cover the 5' and 3' parts of *CZS*, due to the large size of the mRNA. Nevertheless, the alignment confirms most of the annotated intron-exon

structure and attests that the 5' end of the TAIR annotated mRNA is transcribed. Sequencing reads from the high throughput transcriptome sequencing (Lister *et al.,* 2008) are aligned in Fig. 17E, also supporting the TAIR annotation. Transcript traces cover the whole gene, confirming transcription and intron-exon structure within the limits of the short read lengths.

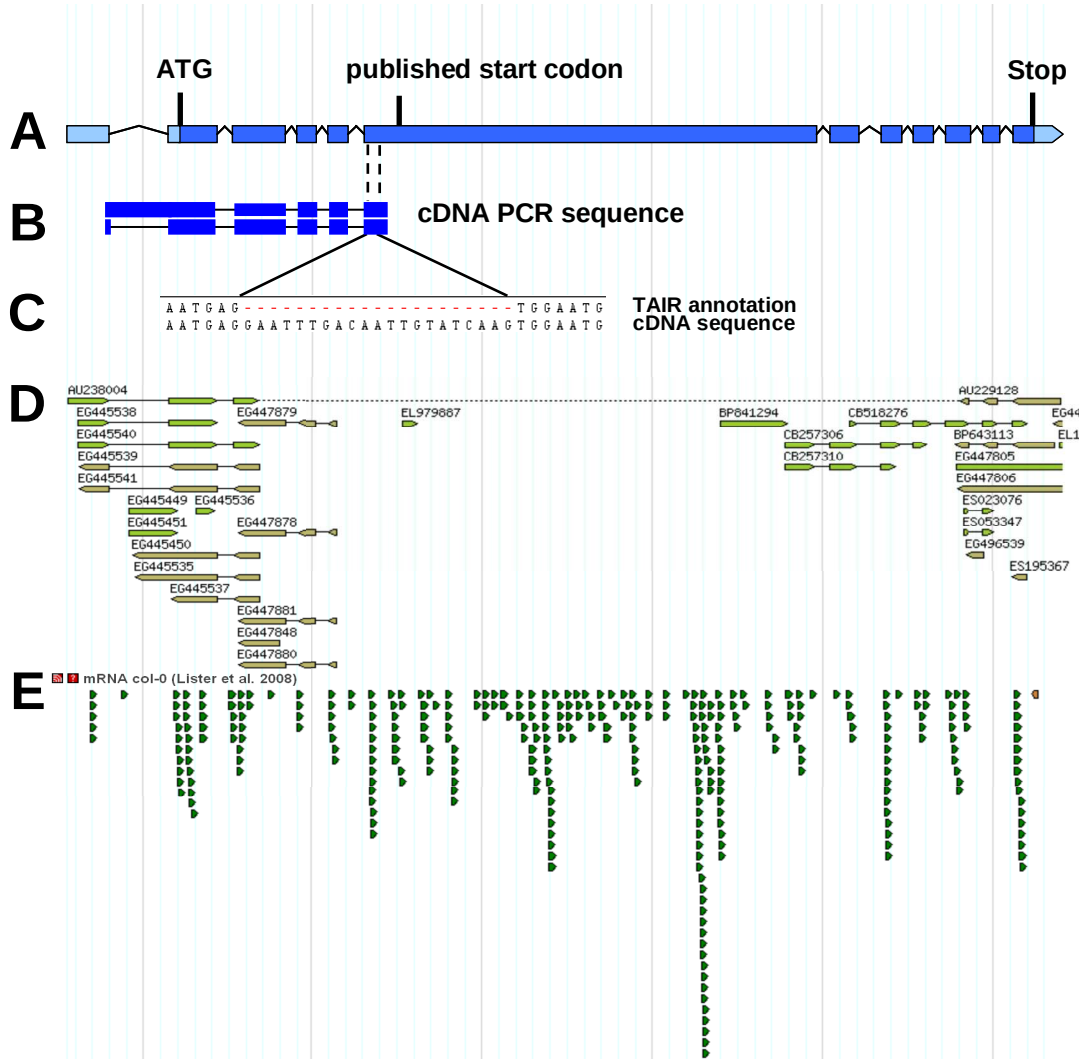


**Figure 17. *CZS* gene aligned to RNA derived sequences.**

**A,** *CZS* Gene structure, ORF in blue, UTRs in light blue. **B**, Alignment of sequenced PCR products obtained from cDNA with one primer pair. **C**, alignment showing close-up of a 21 bp disagreement found between TAIR annotation and cDNA sequencing. **D**, Alignment of EST sequences and **E**, reads of high throughput transcriptome sequencing (Lister *et al.,* 2008). Selection of sequences and alignment in **D** and **E** performed by GBrowse (TAIR).

In order to obtain cDNA sequence information of the complete 5' part of the gene, PCR products were amplified from a cDNA library using gene specific primers and subsequently sequenced. The alignment of some of the obtained sequences is shown in Fig.

17B, verifying that this part of the gene is transcribed. However minor deviations from the expected intron-exon structure were identified. Sequencing showed that the large exon 6 starts 21 bp earlier than annotated by TAIR, a region of the sequence that was not covered by EST data. Furthermore the first intron is frequently part of the extracted mRNA, as was already indicated by some EST reads, giving evidence for alternative splicing variants. As this intron lies in front of the start codon, its presence or absence does not affect the ORF. In summary all RNA derived sequences confirm the *CZS* mRNA sequence annotated by TAIR with the exception of the intron 5 – exon 6 border position..

Having shown that the *CZS* mRNA is indeed completely formed as annotated by TAIR, a protein alignment with homologous proteins from different species was generated to check for protein sequence conservation. Homologies at AA level provide evidence that this sequence is also translated. *BLAST* algorithms on databases NCBI, JGI, EMBL EBI, PlantGDB, etc., were used to find sequences homologous to the *CZS* protein sequence. Complete genomic sequences could be obtained from papaya, poplar lotus, grape vine, rice, *Brachypodium dystachion* and *Physcomitrella*, all, apart from *Physcomitrella*, showing the identical intron-exon structure. Additionally, mRNA sequences could be obtained for *Ricinus communis* and maize.

The alignment presented in Fig. 18 shows strong homologies between all sequences. Numerous domains, distributed along the whole protein, are well conserved, with most identities found near the N- and C-termini of the gene. The conservations also extend to the monocot species and even the distantly related *Physcomitrella* ortholog shares various domains with *Arabidopsis CZS*, even though it is clearly the least homologous sequence. The domain structure of *CZS* is unique in *Arabidopsis* (Baumbusch *et al.*, 2001) and the protein seems to be plant specific. As illustrated in Fig. 16C, the highly conserved SET domains are localized at the C-terminus explaining the high conservation at the end of the gene. The conserved domain near the N-terminus (Fig. 18, AA 290 to 350) has not been described yet, but constitutes one of the most conserved motifs, showing strong homologies also in *Physcomitrella*.

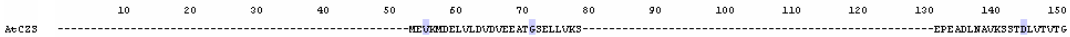
AtCZS
CpCZS
PtCZS
LjCZS
RcCZS
VvCZS
BdCZS
ZmCZS
OsCZS
PpCZS

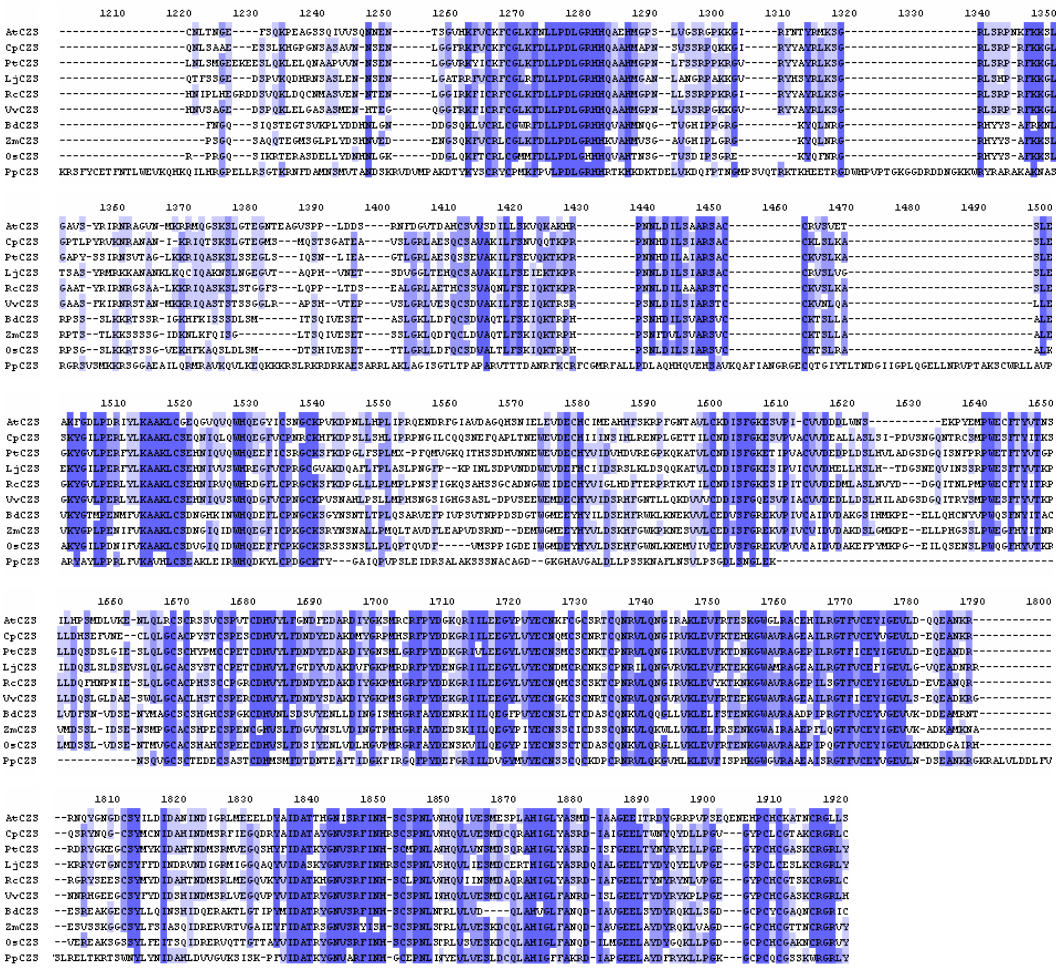

**Figure 18. Protein sequence alignment of *CZS* orthologs.**

CZS homologous sequences from various species were aligned by Bioinformatics Toolkit using MUSCLE algorithm (Edgar, 2004). Papaya sequence is missing the coding exon 4, poplar and papaya are missing the N-terminal ends due to incomplete sequencing effort. Protein start codons were often not known and have been inferred from alignments with *AtCZS* or *OsCZS*. At*: Arabidopsis,* Cp*: Carica papaya,* Pt*: Populus trichocarpa* (poplar), Lj*: Lotus japonicus,* Rc*: Ricinus communis,* Vv*: Vitis vinifera* (grape vine), Bd*: Brachypodium dystachion,* Zm*: Zea mays,* Os*: Oryza sativa,* Pp*: Physcomitrella patens*.

The strongly conserved domain near the N-terminus (Fig. 18, AA 290 to 350) is encoded on exon 2 and 3, thus not part of the ORF annotation published by Krichevsky *et al.*, (2007). High conservation on protein sequence level provides a strong indication that this region is not only transcribed but also translated. Together with the data obtained from the alignments of mRNA derived sequences this provides proof that the mutation found in *eol5* plants causes a nonsense codon near the start of the *CZS* ORF. Alignment analysis and cDNA sequencing resulted in a modified annotation of the *CZS* gene, comprising an ORF of 4149 nt, leading to a protein of 1383 AA.

#### 3.2.2.4. Confirmation of mapping results

In order to confirm that *EOL5* is allelic to *CZS* a complementation experiment was carried out. Krichevsky et al (2007) described that complementation of the *czs-1* flowering phenotype was accomplished using a native promoter with 235 bp upstream and 119 bp downstream sequences, measured from 5' and 3' ends of the TAIR annotated mRNA, respectively.

A construct, containing the *CZS* gene including 1502 bp upstream and 286 bp downstream sequences (*pCZS*::*CZS*) was cloned and tested for complementation. *eol5 las* double mutants were transformed with this construct and the T1 population phenotypically analyzed after selecting for transformants with Basta. As a control, a population of the same seed batch was evaluated, which was not treated with Basta, and therefore is very unlikely to contain transgenic plants.

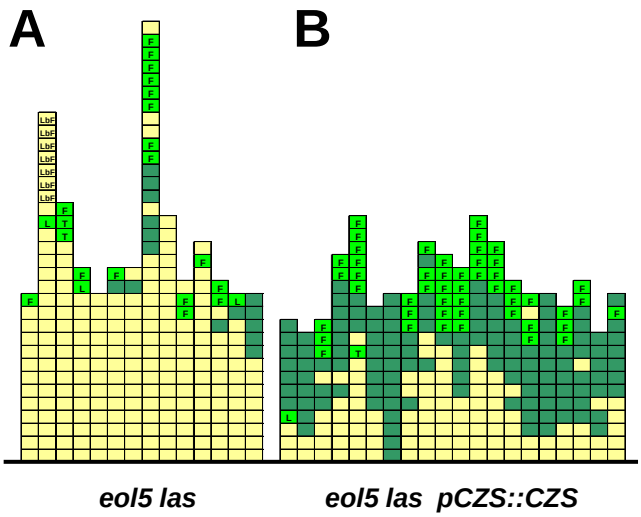


**Figure 19. Complementation of *eol5* with *pCZS::CZS***

Phenotypic analysis of cauline leaf axils of *eol5 las* double mutant populations without (**A)** and with (**B**) complementing *pCZS*::*CZS* construct. Populations are grown from T1 seeds 7 weeks in sd before shift to ld. **A**, untreated, hence unlikely to be transgenic. **B**, sprayed with Basta to select primary transformants. Each column represents one plant, every box one cauline leaf axil from youngest (top) to oldest (bottom). Green indicates an axillary bud, yellow an empty leaf axil, light green the following intermediate axillary structures: F: flower in axil, L: leaf in axil, LbF: tiny leaf between flowers.

The population selected for the presence of the *pCZS*::*CZS* construct was able to form significantly more side shoots in the cauline leaf axils than the control plants (Fig. 19). While only one plant completely resembled the described *las* phenotype, exhibiting no AM initiation defects in the cauline leaf axils, most plants displayed various empty leaf axils, indicating a partial complementation. Whether this is due to a partial activity of the

*pCZS*::*CZS* construct (caused by insufficient regulatory sequences or silencing effects), or merely a result of unusual growth conditions (Basta spraying, different tray type) can not be resolved here, as no *las* controls were grown in parallel. In comparison to other sowings a remarkably large proportion of axils was bearing abnormal structures (mostly flowers), pointing towards unusual growth conditions. In summary, complementation showed that the histone methyltransferase *CZS* is involved in the process of AM formation.

Another strategy to prove that a certain mutation is responsible for an observed aberration of phenotype is to examine different mutant alleles. Therefore, other *CZS* alleles in the *las* background were sought after. During the initial *las* second-site mutagenesis screen more than 30 *eol* mutant lines were selected (Clarenz, 2004). To check whether any of these are allelic to *eol5*, all available lines were sown and the *CZS* locus sequenced. Data for 21 *eol* lines could be obtained, but no mutations in *CZS* were found, indicating that other genes are affected in these mutant lines. An allelism test in order to analyze *czs-1/eol5* plants in the *las* background has been initiated, the analysis of single mutants is described in the following chapter.

### 3.2.3. Characterization of *eol5*

#### 3.2.3.1. Analysis *eol5* single mutant alleles

*eol5* was so far only reported to cause phenotypic deviations from the wild-type in a double mutant combination with *las* (Clarenz, 2004; Schulze, 2007). To determine, whether the *eol5* mutation alone causes any phenotypic abnormalities, *eol5 las* plants were crossed to the wild-type and F2 populations were examined in detail. Phenotypic analysis of backcross populations, as shown in Fig. 20, demonstrated that plants homozygous only for *eol5* displayed a novel degree of bud formation, whereas wild-type plants and the *las* single and double mutants exhibited the previously described phenotypes. All *eol5* plants showed a significant defect in AM formation, revealing a distinguishable *eol5* single mutant phenotype. The reduction in the number of axillary buds varied in magnitude with different sowings. Defects seen in Fig. 20 are less pronounced than e.g. in Fig. 21 or Fig. 31, where even some cauline leaf axils are affected. The phenotype of *eol5* heterozygous

plants, on the other hand, always appeared indistinguishable from the wild-type, as can be seen in Fig. 20 as well as in other backcross populations (data not shown).

Subsequent analysis of lines homozygous for the T-DNA insertion alleles *czs-1* and *czs-2* also revealed axillary bud formation defects, albeit less pronounced. Fig. 21 illustrates a mild increase in the number of barren axils compared to the wild-type, found in the lower rosette in both *czs-1* and *czs-2* plants. The extent of AM initiation defects again differed between sowings, with T-DNA insertion lines shown in Fig. 30B or Fig. 31B displaying stronger phenotypic deviations. In all cases the *eol5* mutant plants exhibited more extensive defects than *czs-1* and *czs-2* plants, indicating that *CZS* function is not completely lost in these alleles. Nevertheless, the same process is affected in all mutants, adding further proof that *CZS* is allelic to *EOL5*.

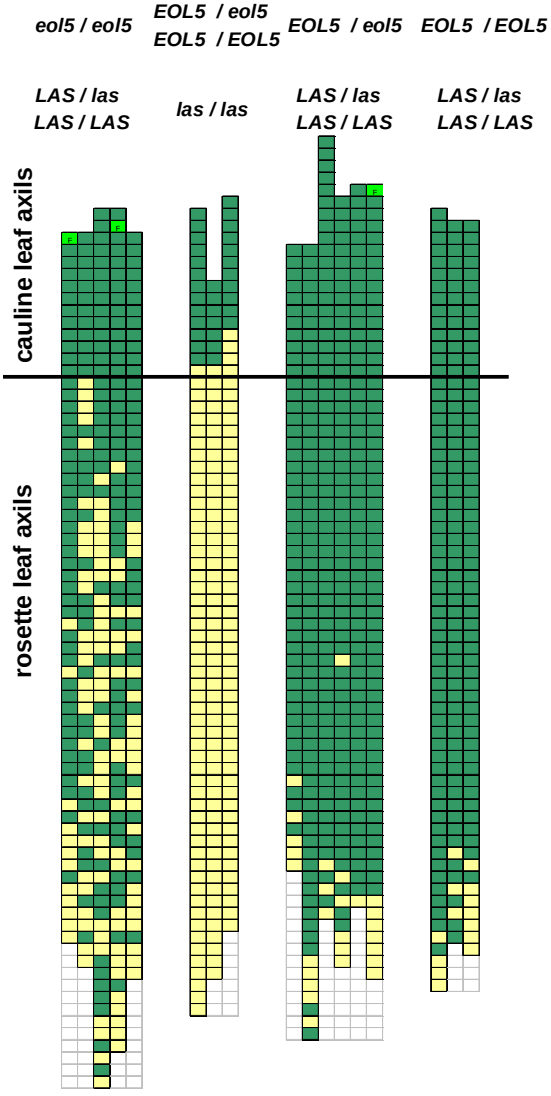


**Figure 20. Phenotypic analysis of the F3 generation of an *eol5 las* X wt backcross population.**

Analysis of axillary bud formation in an *eol5 las* X wt F3 population, segregating for *las* and *eol5*. Four combinations of genotypes are grouped, as indicated above. Plants were grown in sd for 7 weeks, before shift to ld. Each column represents one plant, every box one leaf axil from youngest (top) to oldest. Green indicates an axillary bud, yellow an empty leaf axil, light green: flower in axil.

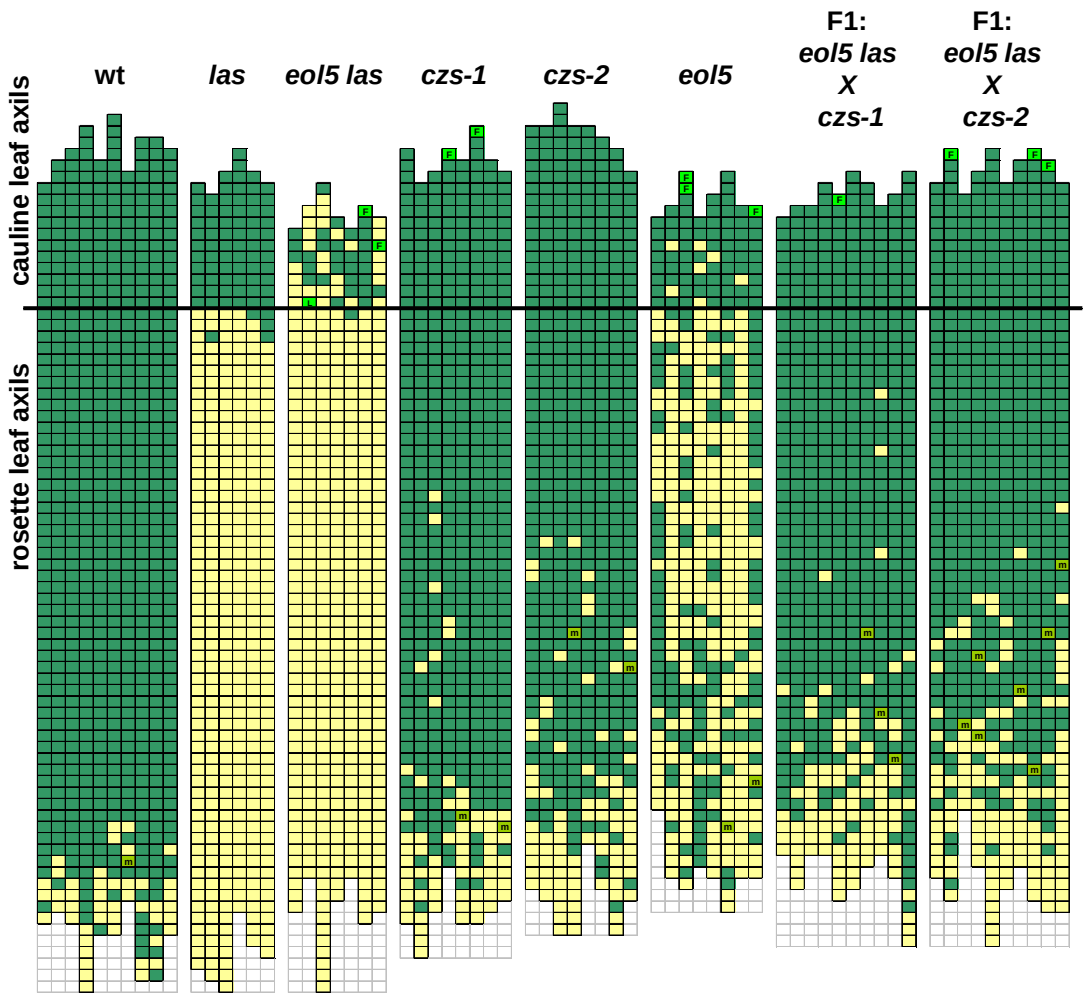


**Figure 21. Phenotypic analysis of the effects of different *czs* mutant alleles**

Analysis of axillary bud formation of plants homozygous for the different *czs* mutant alleles *czs-1*, *czs-2*, and *eol5*, genotypes indicated above. Last two blocks depict F1 populations from *eol5 las* X *czs-1* and *eol5 las* X *czs-2* crosses.
Plants were grown in sd for 7 weeks and subsequently shifted to ld. Each column represents one plant, every box one leaf axil from youngest (top) to oldest. Green indicates an axillary bud, yellow an empty leaf axil, light green the following intermediate structures: F: flower in axil, L: leaf in axil, m: meristem.

Having identified a distinct phenotype of *eol5* single mutants, an allelism test could be carried out to confirm that *EOL5* is allelic to *CZS*, without having to wait for double mutant generation. For this purpose, F1 plants of *eol5 las* double mutants crossed to *czs-1* or *czs-2* plants were analyzed. If both, *eol5* and *czs* mutations, lead to a loss of function of the same gene, the F1 generation should exhibit the same phenotype as the parents. F1 populations of crosses of *eol5 las* to *czs-1* and *csz-2* are defective in AM formation, confirming the allelism of *CZS* and *EOL5* (Fig. 21). Their phenotypes resemble that of the T-DNA insertion lines, and are clearly discernable from *eol5* plants. Similarly, mild phenotypic deviations in such F1 populations have been observed in two other growings

(data not shown). Hence, the *czs*-1 and *czs-2* alleles appear to have a dominant effect over *eol5*.

The analysis of *czs* single mutants in long day conditions revealed that AM formation is also affected in this light regime. Phenotypic deviations appear weaker than in short days, but clearly distinguishable from the wild-type, with the strongest defects observed in *eol5* plants and the mildest in *czs-1* plants (Fig. 22). Disregarding cotyledon axils, which are virtually always empty, wild-type exhibited an average of 0.7 ± 1.1 empty leaf axils in the rosette and the mutant alleles *czs-1* 2.8 ± 1.1, *czs-2* 5.1 ± 1.4, and *eol5* 6.8 ± 2.0. The enhancement of the *las* phenotype by *eol5* in long day conditions was minimal. *las* plants still formed 2.3 ± 0.7 buds in the rosette, *eol5 las* 1.6 ± 0.7 buds (Fig. 22), explaining why no phenotypic effect has so far been reported in long days. Furthermore, all *czs* mutants developed more rosette and cauline leaves than the respective wild-type or *las* populations (Fig. 22), the effect on flowering time is described in detail in the following chapter 3.2.3.2.

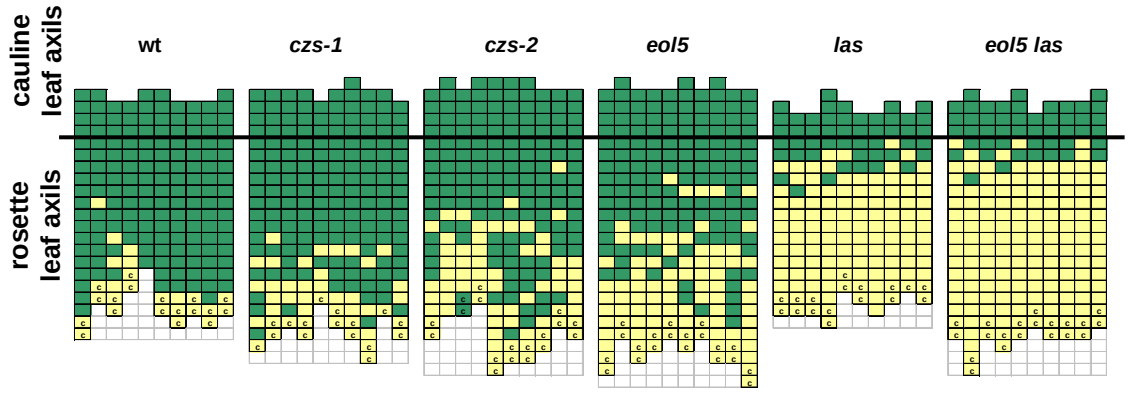


**Figure 22. Analysis of different *czs* mutants under ld conditions.**

Phenotypic analysis of axillary bud formation of indicated genotypes in ld conditions. Each column represents one plant, every box one cauline leaf axil from youngest (top) to oldest. Green indicates an axillary bud, yellow an empty leaf axil, c: cotyledon axil.

#### 3.2.3.2. *eol5* affects flowering time control

To investigate whether *eol5* plants deviate from the wild-type in flowering time, mutants and control plants were grown in short day and long day conditions. Krichevsky *et al.* (2007) reported a moderate delay of flowering in the *czs-1* mutants and a corresponding upregulation of *FLC*. Recent work suggests that in *Arabidopsis* flowering time and side

shoot development defects are to some degree associated, with later flowering plants having stronger defects, possibly linked to the *FLC* locus (X. Huang, B. Schäfer, personal communications).

To assess the flowering time effect of *eol5* under long day conditions, wild-type and *las* control populations were compared to *czs-1*, *czs-2*, *eol5*, and *eol5 las* double mutant plants. As shown in Fig. 23A a mutation in the *CZS* gene causes a delay in flowering of 3 - 4 days in all cases, while the *las* loss-of-function allele does not have an effect on flowering time. The flowering time delay corresponds to the number of formed leaves, illustrated in Fig. 23 B. All *czs* mutant lines produced 2-3 rosette leaves more than the respective control plants, whereas the *eol5* allele seemed to have a stronger effect than the *czs-2* and *czs-1* alleles. Interestingly, also the number of cauline leaves was slightly elevated in all *czs* mutants.

Under short day conditions, however, *eol5* does not have the same effect on floral induction. Two experiments were carried out to determine this, unfortunately both were flawed for different reasons. A first experiment, shown in Fig. 23C, compared different *las* and *eol5 las* lines. These data demonstrated, that the three double mutant lines flowered in fact earlier than the two *las* control populations. However, one *las* line formed less leaves than any double mutant or the other control plants. Even though this line did exhibit an odd growth habit and displayed unusually few leaves compared to the days to flowering, it cannot be definitely decided that the other *las* line represented the normal *las* growth habit.
In another experiment a larger number of genotypes were compared. *eol5 las* plants were again the first to flower, but flowering times varied within these populations. Also some other populations displayed a high variability, the two wild-type populations e.g. exhibited extremely different behavior. A problem that occurred during the growth of these plants was that at a late stage plants suffered from growth inhibitions due to too much watering (Eddy *et al.,* 2008), differing in extent between trays. This delimits comparability between lines and between groups within lines. Also flowering began 5 - 10 days later than in the first experiment (Fig. 23D). Another reason for the observed variation between lines of the same genotype may be that seed batches had not been harvested in parallel. Nevertheless, both experiments suggest that *eol5 las* plants are earlier flowering than *las* controls, hence, no indication was found that *eol5* delays flowering in short days as it does in long days.
Phenotypic analysis of cauline leaf bud formation in *eol5 las* plants showed mostly strong phenotypes in these populations (Fig. 23E, F). Apart from one outlier that also formed

many rosette buds (7th plant in Fig. 23E, population was not genotyped), plants producing more cauline leaf buds were to a higher proportion later flowering. This is a weak indication that a later or slower transition to flowering reduces the phenotypic effect of the *eol5* mutation.

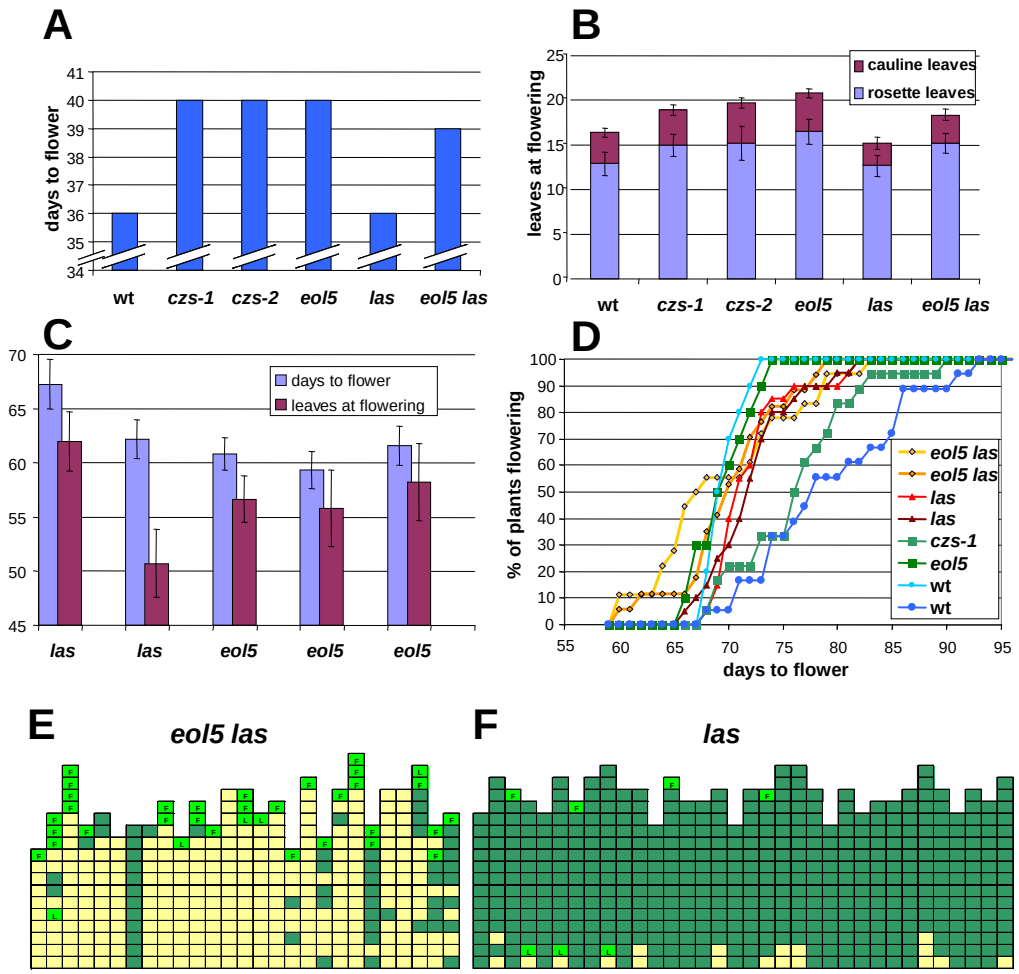


**Figure 23. Flowering time analysis of *czs* mutants under ld and sd conditions.**

**A**, days to flowering (median value) and **B**, leaf formation of populations grown in ld conditions. **A**, n= 14-16, **B**, n= 10. **C**, diagram showing days to flowering (blue) and rosette leaf number (plum) for two *las* lines and three *eol5 las* lines grown under sd.
**D**, development of initiation of flowering in eight populations of indicated genotypes. *eol5* and first wt line n = 10, all others n = 18 – 20.
**E**, **F**, axillary bud formation in cauline leaf axils of *eol5 las* and *las* plants (same data set as in **D**), sorted by flowering times of depicted plants, from earliest (left) to latest. Each column represents one plant, every box one cauline leaf axil from youngest (top) to oldest. Green indicates an axillary bud, yellow an empty leaf axil, light green the following intermediate structures: F: flower in axil, L: leaf in axil.

#### 3.2.3.3. Phenotypic variability of *eol5* mutants

Throughout the project analysis of *eol5* plants was obstructed by the variability of the *eol5* phenotype. The penetrance of the *eol5 las* double mutants ranged from 100 to 0 % empty cauline leaf axils, depending on growth conditions, genetic background composition and other factors. Exemplarily two populations are shown in Fig. 24A and B, both homozygous for *las* and segregating for *eol5* (BC2F2 of backcross to *las*). They originate from the same seed batch and were grown at the same time in Grobanks or Percival growth chambers, respectively. Both fail to show a complete penetrance of the mutant phenotype, but while in the first population only one homozygous mutant does not show the expected phenotype there are four in the second population, which also contains various plants with an intermediate phenotype. Plants grown in Percival growth chambers flowered about 3 weeks later and generally displayed less pronounced alterations between mutant and wild-type. This indicates that environmental conditions play a decisive role in the occurrence of developmental defects, the candidates for which being light quality and quantity, temperature, airflow, humidity, etc.
Fig. 24C and D, and Fig. 24E and F, depict two mapping populations (BC2F4 of Ler cross), which have both been grown at two different time points each. Both segregate for *eol5* as indicated by the marker shown below graphs. Branching defects of plants in Fig. 24C appeared very weak during the first growth, while even non-mutants displayed intermediate phenotypes during second growth (Fig. 24D). In the populations in Fig. 24E and F the co-segregation of the segregating marker with the *eol5* phenotype was not visible in the first population but was suggested by the second one. Variations in the extent of phenotypic deviations were also observed for *eol5* and *czs-1* single mutants. Differences can be observed for *eol5* plants between Fig. 20 and 21 and for *czs-1* plants between Fig. 21 and 31.

There appears to be no seasonal effect as there is no correlation between growing the plants in summer or winter and the magnitude AM defects. At some stage the soil or soil supplements were changed, causing severe growth problems to most plants. *eol5* populations grown during this time generally exhibited more severe *eol5* phenotypes, but also more phenotypic variation. Thus a certain stress level might increase the extent of AM initiation defects. Overall, many different factors, both genetic and environmental, appear to influence the degree of phenotypic alterations observed in *czs* mutants.

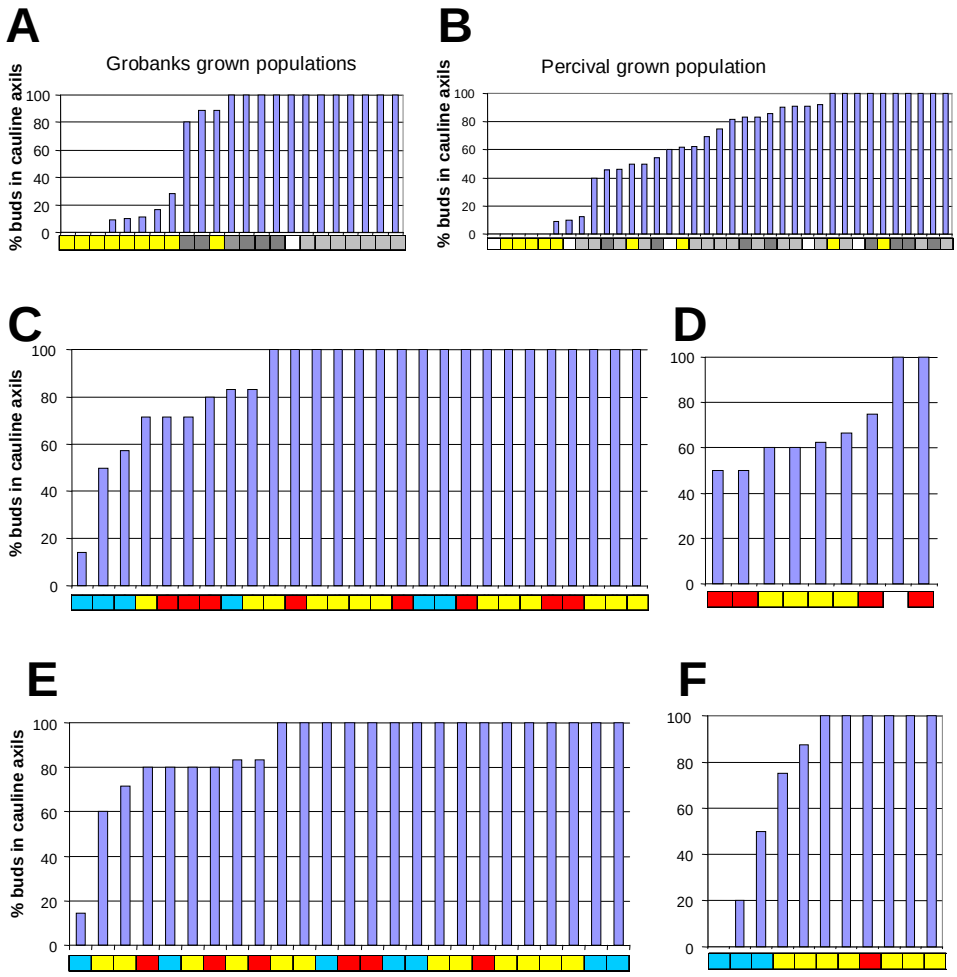


**Figure 24. Variability of *eol5 las* phenotypes observed at different sowings.**

**A**, **B**, phenotypic analysis of axillary bud formation in cauline leaf axils. Same seed batch of an *eol5 las* X *las* backcross F2 population, grown at the same time in a Grobanks (**A**) or Percival (**B**) growth chamber under sd until flowering. Marker indicates genotype at *CZS* locus: homozygous *eol5* mutation: yellow, heterozygous: light grey, wt: dark grey, white: not determined.
**C** and **D**, BC2F4 mapping population (Ler cross) grown at two time points. Marker shown below co-segregates with *eol5* mutation in Col background. Homozygous Col: blue, heterozygous: yellow, homozygous Ler: red. **E** and **F**, additional BC2F4 mapping population (Ler cross) grown at two time points.

### 3.2.4. *CZS* expression profile

Most factors that play an important role in AM development or meristem maintenance have a very defined expression pattern that can be correlated with their function (Schmitz & Theres, 2005). SET domain proteins on the other side are generally expressed constitutively, even though there are also some examples of tissue specific expression (Springer *et al.*, 2003, Venegas & Avramova, 2001).

To determine the expression profile of *CZS*, the relative amount of *CZS* transcript in different tissues was analyzed by real-time PCR. For this purpose RNA was extracted from different tissues of the plant and utilized for cDNA synthesis. The relative expression, determined by the standard curve method (Applied Biosystems, User Bulletin #2, 2001), was normalized with the parallel measured expression of *2PPA* (Czechowski *et al.*, 2005). As illustrated in Fig. 25 the relative expression of *CZS* did not differ strongly between the investigated tissues. Only in case of the root and the stem samples all biological replicates displayed a minor downregulation, with a less than two-fold expression change. Overall, no clear tissue specific *CZS* mRNA accumulation could be observed, indicating constitutive expression.

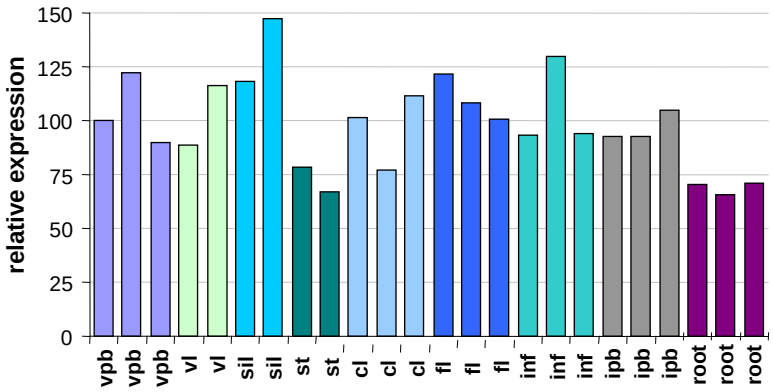


**Figure 25. Expression profile of *CZS* in different *Arabidopsis* tissues.**

*CZS* expression shown in arbitrary units. Results for 2-3 biological replicates are shown in one color for the following tissues: vpb: main body of the vegetative plant without leaves and root harvested after 6 weeks in sd, vl: adult vegetative leaf (~leaf 10) after 6 weeks sd, sil: first fully extended silique, st: part of the lower bolt between nodes, cl: cauline leaf, fl: open flower, inf: inflorescence including apex and all unopened flowers, ipb: main body of the plant without leaves and root harvested after 6 weeks sd + 1 week ld, root: complete root harvested after 6 weeks sd + 1 week ld. Results are averages of 2 technical replicates, normalized with *PP2A* expression.

#### 3.2.4.1. *CZS* expression in mutant alleles

To determine the amount of *CZS* mRNA in the different mutant alleles, the relative expression was determined by real-time PCR. For quantitative PCR analysis primer pairs are usually designed in the 3' region of mRNA sequences to avoid problems arising from inconsistent cDNA synthesis. In this case also a primer pair in the 5' end was utilized, to

measure mRNA quantities of different parts of the mRNA on either sides the of T-DNA insertions (Fig. 26A).

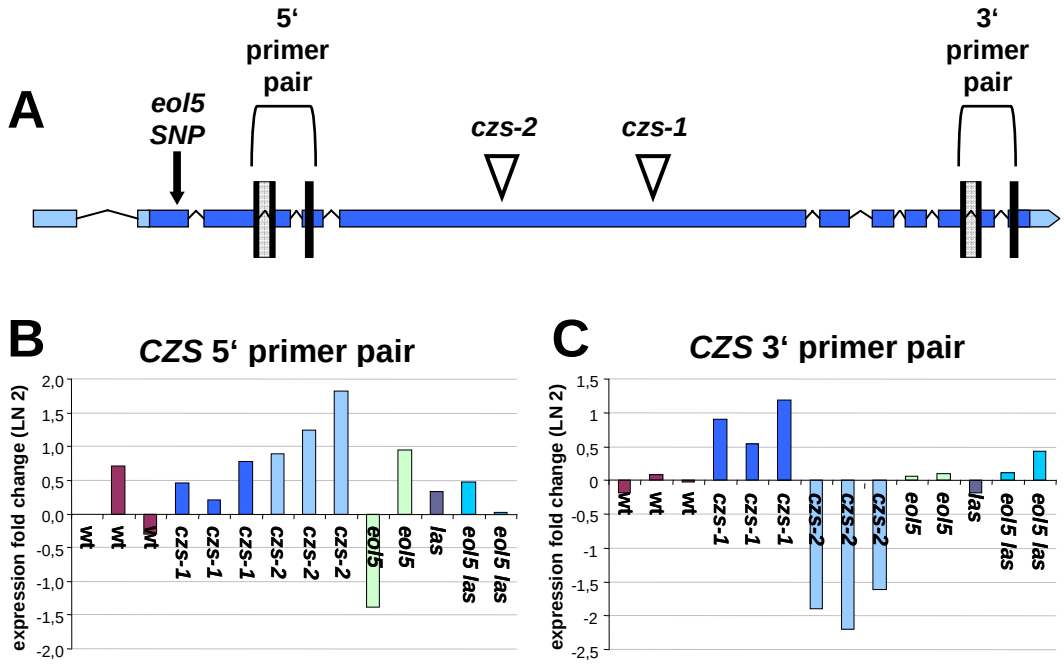


**Figure 26. *CZS* mRNA expression in *czs* mutants.**

**A**, positions of utilized real-time PCR primers and polymorphisms on the *CZS* mRNA. ORF is depicted in blue, UTRs in light blue, gaps indicate introns, primers are shown as black bars.
**B**, **C** *CZS* expression examined with 5’ primers (**B**) and 3’ primers (**C**), in up to three biological replicates of each genotype, displayed as LN2 fold change (1 = 200% expression, 2 = 400%, -1 = 50%, etc.). Values determined by standard curve method, every value represents average of two technical replicates, normalized with *PP2A* expression. RNA extracted from seedlings (roots and leaves removed) grown sterile for 14 days in sd.

The results obtained by amplifications with 5’ primers, shown in Fig. 26B, indicate an upregulation of *CZS* mRNA in the *czs-2* mutants, as all three biological replicates show considerably elevated expression levels compared to all other samples. *czs-2* samples, as all others, exhibit a substantial variation between biological replicates. This is probably due to minor deviations during the delicate synthesis of a 3800 nt cDNA. The first biological replicate of *eol5* e.g. displays largely reduced cDNA levels in the 5’ end compared to the 3’ end, which can only be explained with technical problems.

Results obtained using 3’ primers are a lot more consistent between biological replicates. In *czs-2* plants *CZS* mRNA appears downregulated, in agreement with the expected termination of transcription due to the T-DNA insertion. In contrast, *czs-1* plants display elevated mRNA levels, even in comparison to the start of the transcript. This indicates a promoter activity from the transgene, causing a higher relative expression in the 3’ end in comparison to the 5’ end of the same gene. *CZS* mRNA production or stability does not appear to be affected in the *eol5* mutants.

#### 3.2.4.2. Expression analysis in *eol5* mutants

Histone methyltransferases are assumed to regulate chromatin state, and thereby gene expression of genomic regions. This leads to the question of the target genes that are regulated by *CZS*, and whose deregulation in *czs* mutants causes the observed phenotypes. Various players known to be involved in AM development were examined for histone methylations using the UCSC Genome Browser, which displays the results of genome-wide ChIP chip experiments analyzing the distribution of various histone methylations. A large proportion of these genes were found to have methylated histones in their vicinity, as shown exemplarily for the $me_3$H3K27 marks of *LAS* or *RAX1* in Fig. 27.

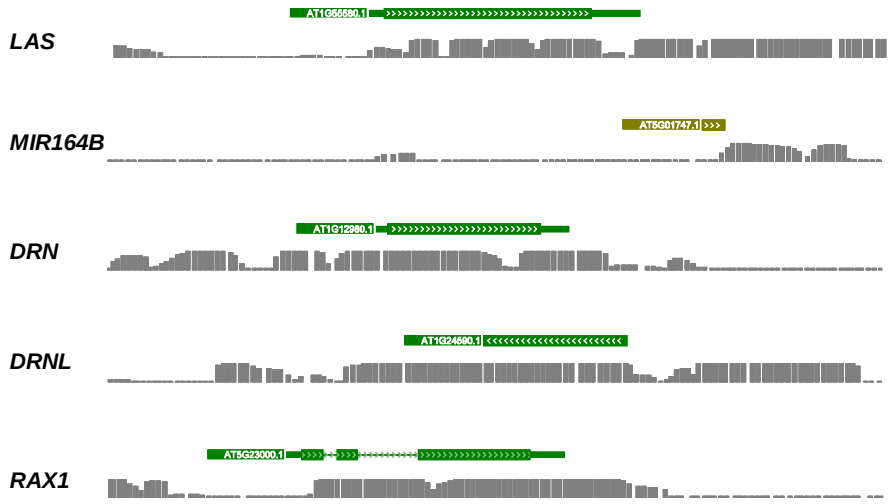


**Figure 27. Traces of histone methylations on selected genes**

Appearance of $me_3$H3K27 histone marks shown as gray bars in a 5 kb window around selected genes, detected by ChIP chip analysis. Data taken from the UCSC Genome Browser (Bernatavichute *et al.,* 2008). Green boxes indicate genes, arrows show direction of transcription.

As *CZS* was reported to be a negative regulator of transcription, thus, its method of action could in the simplest form be the repression of a negative regulator of AM initiation, leading to defects of AM formation in the *czs* mutant. As a matter of fact there are only very few known negative regulators of AM initiation, namely the *MIR171* genes, the *MIR164* genes and possibly *DORNRÖSCHEN* (*DRN*) and *DORNRÖSCHEN-LIKE* (*DRNL*). The *DRN* overexpression allele *drn-D* leads to loss of SAM activity and defects in lateral bud formation (Kirch *et al.*, 2003), and the *drn drnl* double mutant exhibited formation of accessory side shoots at a low frequency (data not shown). *CLV* genes also confer a negative regulation of meristems, but are not expressed near axillary meristem

initiation sites (Brand *et al.*, 2002). *MIR164B*, *DRN*, and *DRNL* genes carry histone methylations according to the UCSC Genome Browser (Fig. 27), thus, represent targets for HMTs.

To identify genes directly or indirectly regulated by *CZS*, the relative expression of numerous candidate genes was analyzed in wild-type and mutant plants by real-time PCR. Primers were designed, when possible spanning intron-exon borders, in the 3' region of the mRNAs. The harvested adult tissue was the vegetative plant body without root or leaves after six weeks of growth in short days and one week induction in long days. At this time point the empty cauline leaf axils, observed in the *eol5 las* double mutant, are assumed to develop. Upon the discovery of a phenotype in the lower rosette of *czs* single mutants, another set of cDNAs was synthesized, using RNA harvested from two week short day grown seedlings, again after removal of leaves and roots.

*STM* mRNA was analyzed as a first candidate because *las stm* double mutants were reported by Oliver Clarenz (2004) to have a leave fusion phenotype, reminiscent to that shown in Fig. 13L. However, no significant alterations in relative expression were found between wild-type and *czs* mutant seedlings (Fig. 28A). The same was observed in adult tissue (data not shown). *RAX1* was considered a likely candidate, as the mutant phenotype was reported to be day length dependent, similar to the *eol5 las* phenotype. *RAX1* transcripts appeared mildly upregulated in most mutant samples (Fig. 28B). Biological replicates displayed some variability, hence, the observed expression increase averaging around 40 % may not be considered significant. In adult tissues no altered expression could be observed (data not shown). Fig. 28C similarly shows a mild downregulation of *MIR164B* in adult *eol5 las* mutants compared to *las* samples, overshadowed by a substantial variability between biological replicates. Analysis of seedling samples did not reveal any significant differential regulation of *MIR164B* transcript levels between *eol5 las* and *las* mutants (Fig. 28D).

A clear effect could be observed for *DRN*. While mRNA abundance was two to four-fold reduced in adult *eol5 las* mutants, there were no major deviations between wild-type and *las* samples (Fig. 28E). *DRNL* transcript, on the other hand, was strongly reduced in *las* samples in comparison to wild-type, but only mildly further repressed in *eol5 las* double

mutants (Fig. 28F). Both, *DRN* and *DRNL* mRNA levels appeared unaffected by *czs* mutations in seedling samples (data not shown).

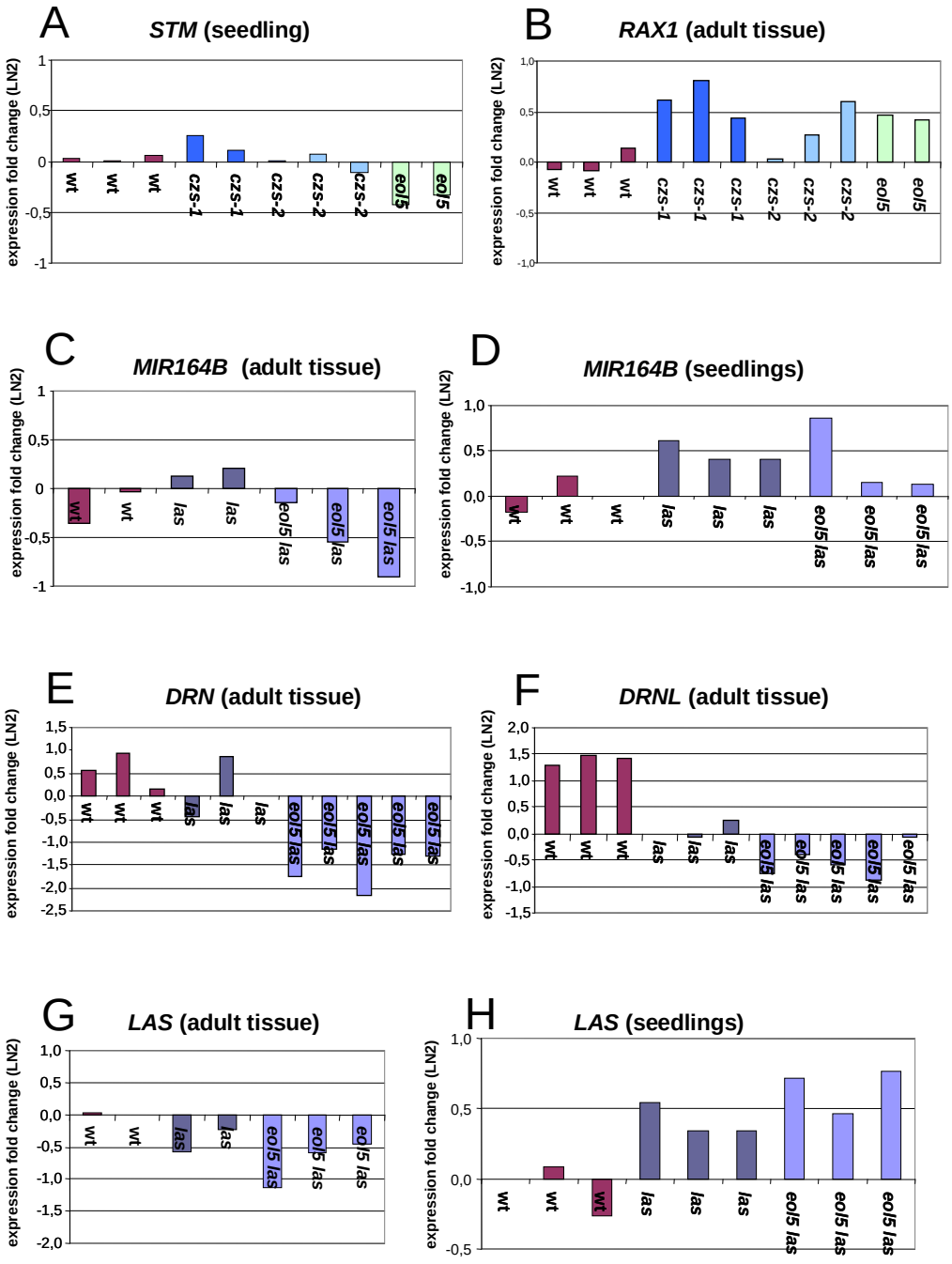


**Figure 28. Real-time PCR analysis of candidate gene expression in *czs* mutants.**

Relative expression of **A**. *STM*, **B**: *RAX1*, **C**-**D** *MIR164B*, **E**: *DRN*, **F**: *DRNL*, **G**-**H**: *LAS*. RNA was harvested from **C**, **E**, **F**, **G**: adult tissue (main body of the plant without leaves and root grown for six weeks in sd + 1 week in ld) or **A**, **B**, **D**, **H**: seedlings (roots and leaves removed, grown sterile for 14 days in sd). Expression values were determined by standard curve method, normalized by 2PPA expression. Every value represents the average of two technical replicates.

To investigate a possible effect of *czs* mutations on the expression of *LAS*, mRNA levels were analyzed in adult and seedling tissue samples. No significant changes between *las* and *eol5 las* double mutants could be observed in either tissue (Fig. 28G and H). Comparing wild-type and *las* mutants no significant deviation in *LAS* transcript were noted in adult tissue. The minor upregulation of *LAS* compared to the wild-type in seedling samples does not exceed 40 % expression change and may not be considered significant. These data are in line with the GUS expression results shown in Fig. 11B, exhibiting similar *LAS* promoter activity (visualized by pES44 construct) in *las* and wild-type plants.

The differential expression in *czs* mutants shown so far for *DRN* and less reliably for *RAX1*, *MIR164B*, and *DNRL*, does not serve to explain the *czs* mutant phenotype, as transcript abundances do not deviate in the right direction. The Citovsky group carried out a microarray experiment using 14 day old *czs-1* seedlings (Krichevsky *et al.*, 2007), of which the data were kindly provided. A list comprising 513 genes showing more than two-fold expression changes was scanned for factors that may be involved in AM development, in order to select new candidates for real-time PCR analysis.

Three genes were chosen to confirm of the microarray results: *LBD25* (*LOB DOMAIN-CONTAINING PROTEIN 25*, at3g27650), *PP2C* (*PROTEIN PHOSPHATASE 2C*, at3g51370), and *ANAC83* (*ARABIDOPSIS NAC DOMAIN CONTAINING PROTEIN 83*, at5g13180). Expression fold changes in *czs-1* mutants were reported to be: *LBD25* + 2.58, *PP2C* – 2.21, *ANAC83* – 3.42. Real-time PCR analysis on seedling samples did not confirm these altered mRNA levels in *czs-1* samples, nor did they reveal any significant deviations between the wild-type and *czs-2* or *eol5* alleles (Fig. 29A, B, C). *LBD25* transcript appeared mildly upregulated in *czs-2* samples, but not consistently in all *czs* mutants. The lack of reproducibility may be due to differences in tissues and growth conditions, as the seedlings used for the microarray were grown in long days and harvested completely.

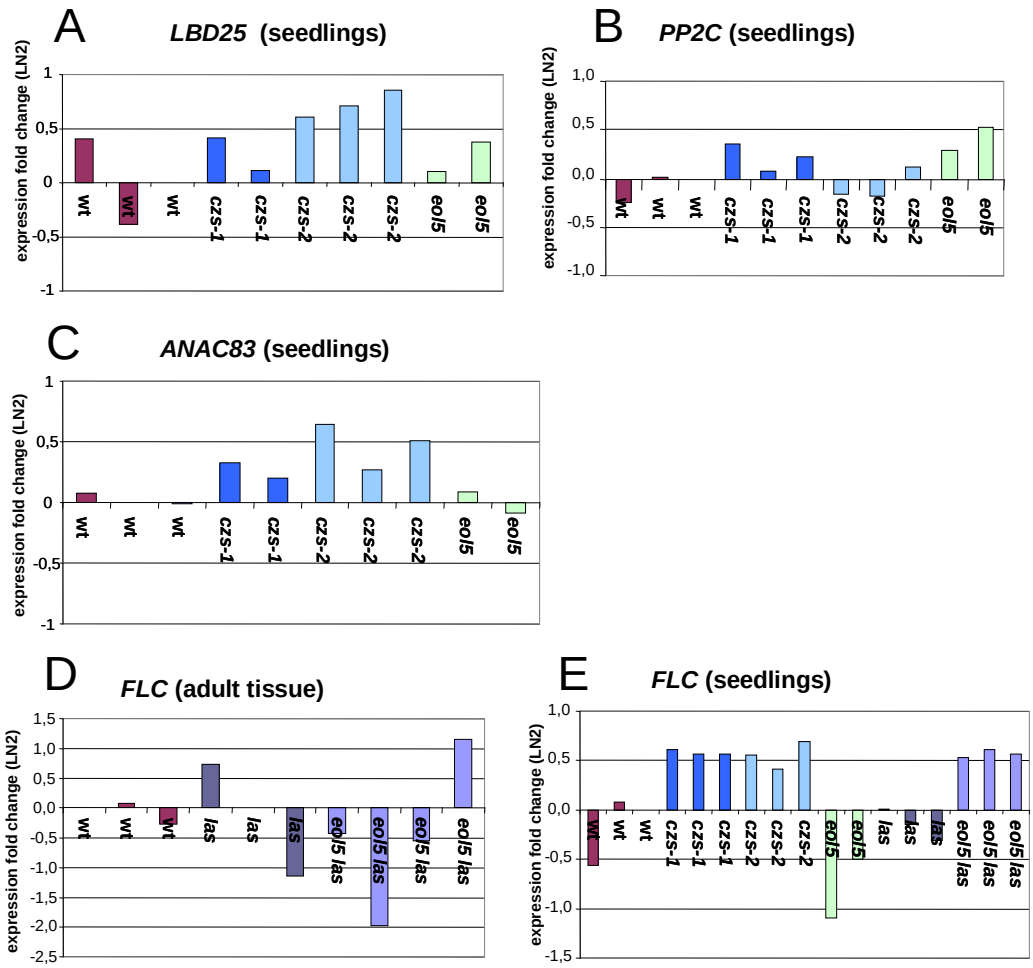


**Figure 29. Real-time PCR analysis of genes indicated to be misexpressed in *czs* mutants by microarray data.**

Relative expression of **A**: *LBD25*, **B**: *PP2C*, **C**: *ANAC83*, **D** and **E**: *FLC* between wt and *czs* mutant alleles, shown as LN2 fold change.
RNA in was extracted from **D**: adult tissue (main body of the plant without leaves and root grown for six weeks in sd + 1 week in ld), or **A**, **B**, **C**, **E**: from seedlings (roots and leaves removed, grown sterile for 14 days in sd). Expression values determined by standard curve method, normalized by *2PPA* expression. Every value represents the average of two technical replicates.

The only gene, for which a differential expression based on real-time PCR data was published, is *FLC* (Krichevsky *et al.*, 2007), reported to be four to five-fold upregulated in *czs-1* seedlings. Analysis of *FLC* transcript abundance in adult tissues only revealed large variations between biological replicates (Fig. 29D). As plants had been shifted to long days seven days prior, this may indicate that *FLC* mRNA levels undergo substantial changes during this time. Analysis of seedling tissue samples demonstrated a robust *FLC* upregulation in *czs-1* and *czs-2* plants. Transcript levels increased only by ~ 50 %, but did so consistently in all biological replicates. The two available *eol5* mutant samples, on the other hand, showed an inconsistent but decisive downregulation of *FLC*. This is contrasting the significant upregulation observed in *eol5 las* samples in comparison to *las*

single mutants, which clearly stated an *eol5* induced increase of *FLC* transcript, comparable to the one observed in *czs-1* and *czs-2* samples. Whether this difference is biologically relevant or due to some technical error needs to be reinvestigated in new cDNA samples.

### 3.2.5. Analysis of *CZS* homologs

In order to investigate a possible general function of SET domain genes in AM formation, mutants of genes homologous to *CZS* were examined for defects in lateral bud formation. T-DNA insertion mutant lines were obtained of the closest *CZS* relative *SUVR3* and of two further members of the same SET domain gene clade, *SUVH1* and *SUVR1*. Ordered lines were designated as homozygous by NASC, but results may be prone to errors as these lines have not been genotyped yet due to time constraints. Patterns of axillary bud formation observed after growth in short days for 6 weeks and subsequent shift to long days were indistinguishable from the wild-type (Fig. 30A). This indicates that these genes have no strong functional homology with *CZS.*

The best studied SET domain genes are the PcG genes: *CLF, SWN,* and *MEA*. *clf* and *swn* mutants were chosen for a first analysis, as they have previously been associated with the control of gene expression in meristematic tissues (Schubert *et al.,* 2005). Based on the observation by Daniel Schubert that *emf2 vrn2* double mutants display defects in AM formation, also these PcG genes were examined, as their gene products act in complexes with the SET domain proteins mentioned above. Plants were grown in short days for 7 weeks and subsequently shifted to long days to induce flowering.
As illustrated in Fig. 31B neither *swn* nor *clf* mutants exhibited a strong defect in lateral bud formation. In the lowest rosette leaf axils *clf* plants displayed more empty axils than wild-type plants, but this result might be due to the early flowering phenotype of *clf*. As the wild-type plants were analyzed some weeks later several of the early leaves, whose axils often do not support bud formation, might have been lost due to senescence and subsequent rotting of leaves. Crossings to *las* plants have been initiated to analyze the effect in the sensitized *las* background.

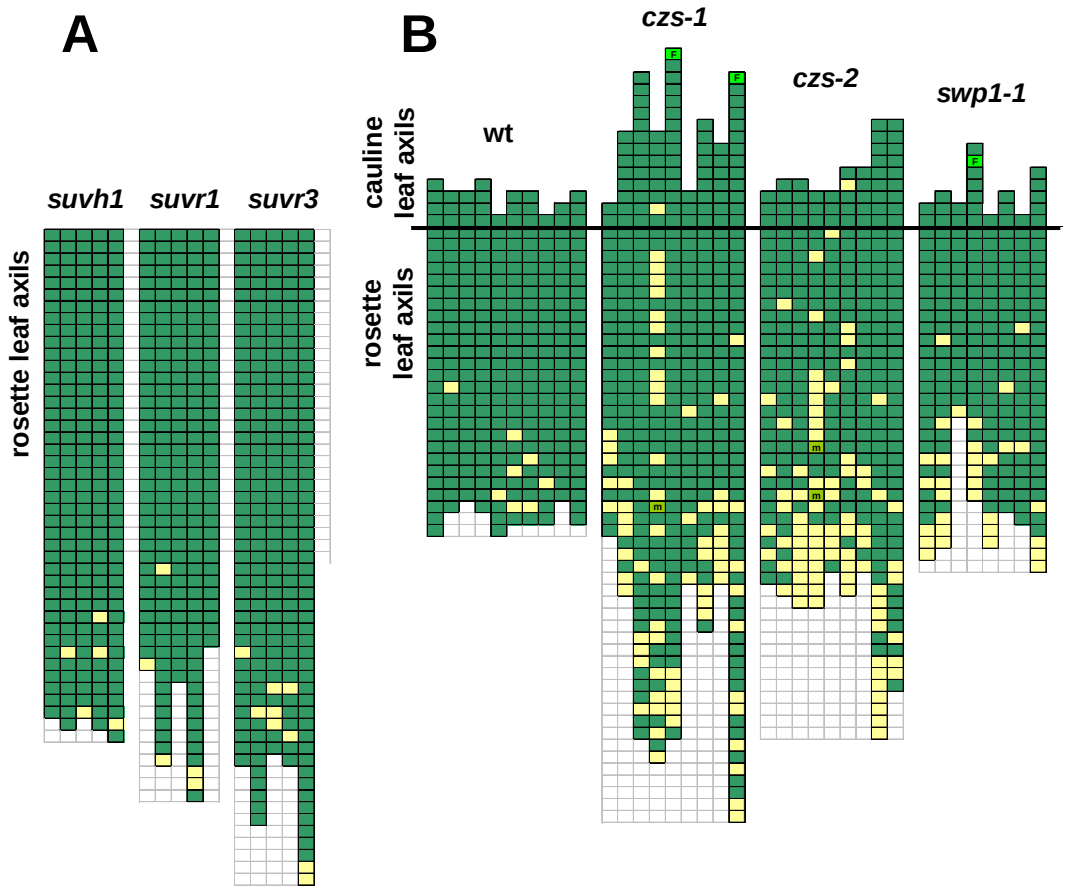


**Figure 30. Phenotypic analysis of homologs and interactors of *CZS***

**A**, analysis of lateral bud formation in rosette leaf axils of *suvh1*, *suvr1*, and *suvr3* T-DNA insertion lines. Plants were grown for 6 weeks in sd and subsequently shifted to ld.
**B**, analysis of lateral bud formation in rosette and cauline leaf axils of *swp1-1* and control plants. All populations shown in B displayed unusual growth habits, probably due to environmental conditions. Each column represents one plant, every box one leaf axil from youngest (top) to oldest. Green indicates an axillary bud, yellow an empty leaf axil, light green the following intermediate structures: F: flower, m: meristem.

In accordance with their name, *emf2* plants flowered extremely early, developing into small, dwarfed plants with narrow leaves. About half of the rosette leaf axils appeared empty but the relevance of this is hard to judge, as there is no morphologically similar wild-type available. *vrn2* plants shown in Fig. 31 exhibited a mild defect in AM development in the upper rosette and an interesting tendency to develop side shoots without subtending leaves, prior to flower formation. Unlike *emf2* mutants, *vrn2* plants were rather late flowering. After the shift to long days, flowers appeared ~ 1 week later than in wild-type Col control plants, though less leaves were formed overall. It has to be noted that the *vrn2* mutant is in the Ler background, so this may be attributed to the different background. However, it is apparent that the *vrn2* mutation does not have the

same effect on flowering as the *emf2* mutation. Plants will be regrown in parallel to Ler wild-type controls to investigate this.

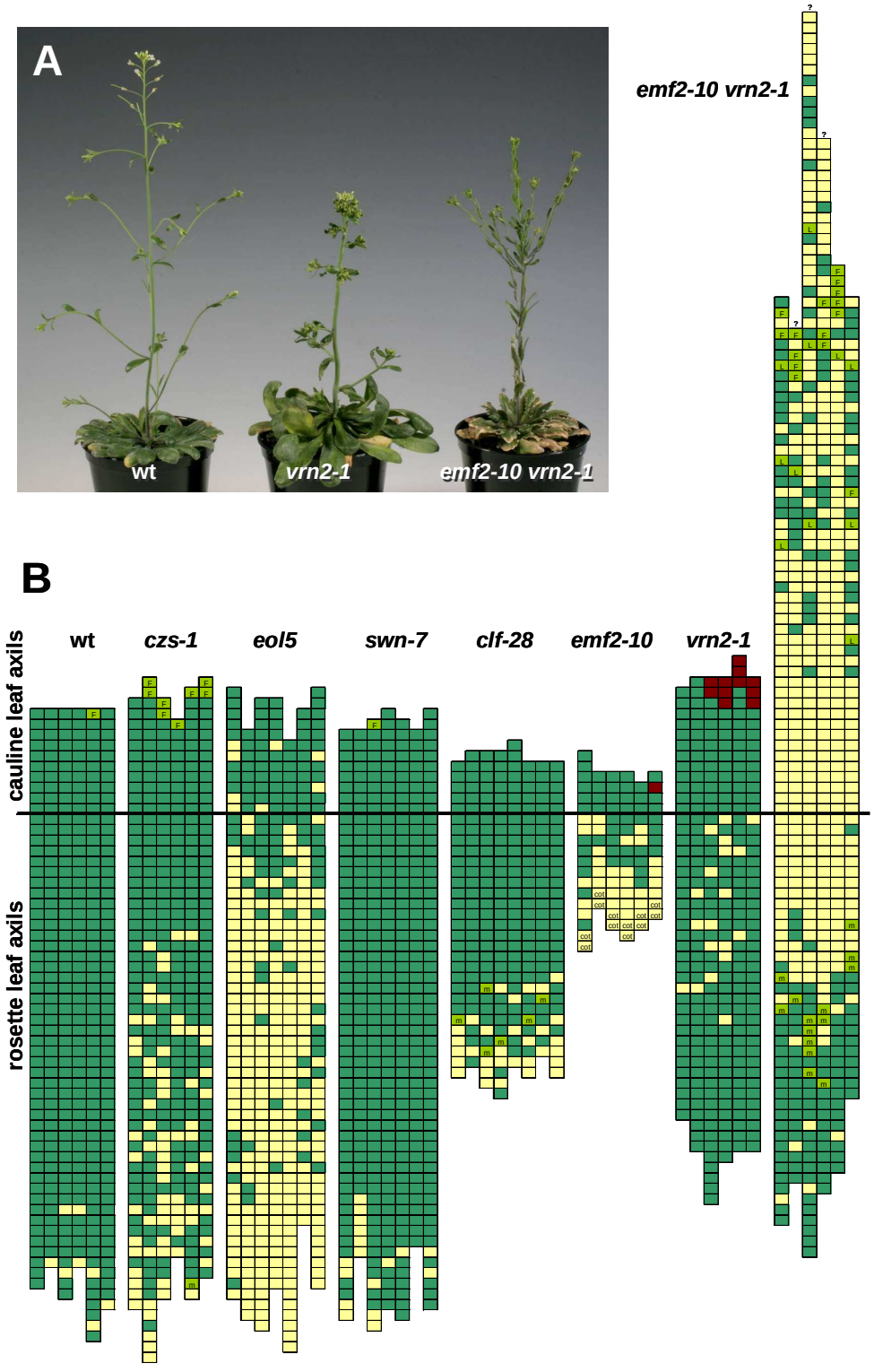


**Figure 31. Lateral bud formation analysis of selected PcG mutants.**

**A**, growth habit of wt Col, *vrn2* (Ler background), and *emf2 vrn2* (mixed background) plants.
**B**, analysis of axillary bud formation in populations with indicated mutant genotypes. Analysis of later cauline leaf axils *emf2 vrn2* double mutants may contain errors, as tissues were in part very

small at time of examination. Question mark on top indicates that a larger, unknown number axils was present. Some plants also reverted back to vegetative development after formation of some flowers. Each column represents one plant, every box one leaf axil from youngest (top) to oldest. Green indicates an axillary bud, yellow an empty leaf axil, light green the following intermediate structures: F: flower in axil, L: leaf in axil, m: meristem. Dark red: shoot without subtending leaf, cot: cotyledon axil. Plants were grown for 7 weeks in sd before shift to ld.

Contrasting the single mutant phenotypes, *emf2 vrn2* plants showed strong and distinct defects in AM development. As illustrated in Fig. 31 bud formation was only supported in the lower rosette and in some later cauline leave axils. Additionally, leaves appeared highly serrated in the double mutant. All analyses of rosettes during this project have been carried out shortly after bolting, because onset of senescence and subsequent rotting of older leaves soon makes analysis impossible. In the case of *emf2 vrn2* plants this meant that the uppermost cauline axils could not be properly analyzed. Due to the small size of organs the exact number of leaves could not be determined in all cases and differentiation between flowers and shoots may not always be correct. Additionally, in some inflorescences reversions to vegetative cauline leaf formation were observed after some flowers had formed.
The flowering time of *emf2 vrn2* mutants is rather dependent on the definition of such, as bolting already started after about four weeks in short days, but subsequent formation of an extremely large number of cauline leaves (Fig. 31A) led to an actual appearance of flowers later than in the wild-type, which had in the meanwhile been shifted to long days.

*CZS* was shown to interact with *SWP1* and mutations in both genes were reported to cause a similar delay in flowering (Krichevsky *et al.,* 2007). A meaningful analysis of *swp1* plants was so far hampered by unusual growths habits, probably due to environmental factors. The results, shown in Fig. 30B, indicate minor defects in AM formation in *swp1* plants that are not clearly significant. In another growing *swp1* plants looked indistinguishable from *czs-1* plants, which on their part appeared indistinguishable from parallel grown wild-type plants. Repetition of this experiment has been initiated to confirm an effect on AM formation.

### 3.2.6. Analysis of potential downstream factors of *CZS*

The bHLH gene *ROB* was shown to be a regulator of AM formation (Yang, 2007). The loss-of-function mutant was reported to lack side shoot formation in the lower rosette and

*ROB* expression was found to increase upon floral transition. To investigate a possible interaction with *CZS* a population homozygous for *rob* and segregating for *eol5* was analyzed. *rob* plants from this population exhibited the previously described phenotype, while *eol5 rob* double mutants showed an intermediate phenotype compared to both parents (Fig. 32). This suggests some interaction between *CZS* and *ROB*, as phenotypes are not additive nor is one mutation epistatic to the other.

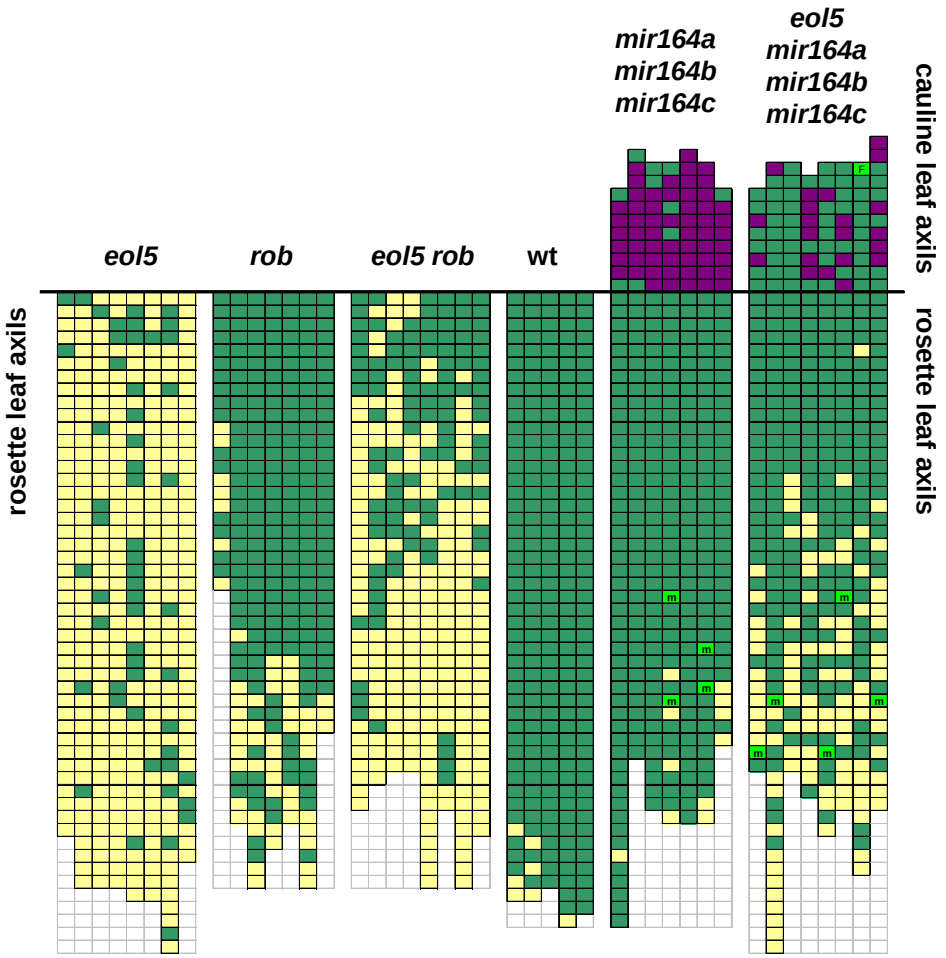


**Figure 32. Phenotypic analysis of *eol5 rob, eol5 mir164a mir164b mir164c* and control plants.**

Axillary bud formation analyzed in the rosette of *eol5, rob, eol5 rob,* and wt plants and of both rosette and cauline leaf axils of *mir164a/b/c* and *eol5 mir164a/b/c* plants. *eol5 rob* and *rob* plants were selected out of one population segregating for *eol5.* Also miR164 mutant plants were selected out of a population segregating for *eol5*.
Each column represents one plant, every box one leaf axil from youngest (top) to oldest. Green indicates an axillary bud, yellow an empty leaf axil, violet an accessory shoot, light green the following intermediate structures: F: flower in axil, m: meristem. Plants were grown for 6 weeks in sd before shift to ld.

The miR164 is a negative regulator of AMs as it targets the genes *CUC1* and *2*. Therefore, it is a possible target of *CZS,* as derepression of miR164 could explain the *czs* mutant phenotype. miR164 is encoded by three genes and the triple mutant (*mir164a b c*) has been described by Raman *et al.,* (2008) to form accessory side shoots in young rosette and most cauline leaf axils. To investigate a possible interaction with *eol5,* a *mir164* triple mutant population segregating for *eol5* was examined. Triple and quadruple mutants shown in Fig. 32 have been selected from this population. While *mir164a/b/c* and *eol5* plants displayed the reported respectively previously shown phenotype, an intermediate level of AM alterations was observed in the quadruple mutant (Fig. 32). A reduced number of accessory shoots was found in the cauline leaf axils and barren leaf axils were observed in the lower rosette combining phenotypes of both parents. Since the *eol5* mutant phenotype is not completely repressed, this indicates that *CZS* does not act via miR164.

As *FLC* was shown to be deregulated in *czs* mutants and other works indicate a link between flowering time and AM formation, the effect of *FLC* on AM development was directly investigated. For this purpose *FRI FLC* plants were examined, which carry an active *FRI* gene, introgressed from San Feliu-2 (Sf-2) accession (Searle *et al.*, 2006). In comparison to Col plants *FLC* expression is strongly upregulated in this line, leading to a substantial delay of flowering. Plants were grown in short days for 6 weeks, subsequently shifted to long days, and analyzed about two weeks after. As most *FRI FLC* plants were not yet flowering at the time of analysis little information was obtained concerning the upper part of the rosette. The time of analysis was chosen to avoid loss of lower rosette axils due to senescence and subsequent rotting, taking place in older plants. As shown in Fig. 33 *FRI FLC* plants revealed a significant defect in AM formation in the lower part of the rosette in comparison to the wild-type. The leaf axils above the juvenile, primary leaves appeared most affected but few barren axils were also observed in the upper half of the rosette. This result suggests and involvement of *FLC* in AM initiation acting as a negative regulator.

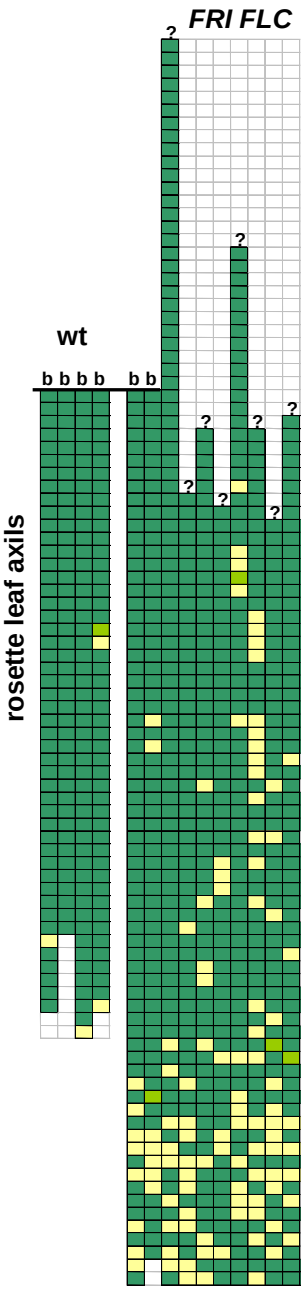


**Figure 33. Analysis of lateral bud formation in *FRI FLC* rosette leaf axils.**

Axillary bud formation in the rosettes of *FRI FLC* plants. Only rosette leaf axils are shown. Plants marked with “b” were bolting at the time of analysis, plants marked with “?” were still in the vegetative growth phase and possessed an unknown, higher number of rosette axils. Analysis of further axils was not feasible due to their small size. Plants were grown in sd for 6 weeks and subsequently shifted to ld. The latter two wt plants were not shifted, but had also initiated flowering at the time of analysis.
Each column represents one plant, every box one leaf axil from youngest (top) to oldest. Green indicates an axillary bud, yellow an empty leaf axil, light green: meristem.

# 4. Discussion

## 4.1. Part I: Towards understanding the *LAS* promoter

*LAS* is a key regulator of AM initiation, as the loss of function mutant exhibits a lack of lateral bud formation during the vegetative growth phase. In order to understand how the specific *LAS* expression pattern is generated, a study to characterize the *LAS* promoter was initiated, to identify important elements and to investigate their contribution to the *LAS* expression profile. These data can provide a basis for later identification of upstream regulators using e.g. yeast one-hybrid studies.

### 4.1.1. Visualization of *LAS* expression by GUS analyses

Complementation of the *las* mutant in previous experiments demonstrated that 820 bp 5' and 3547 bp 3' of the *LAS* ORF are sufficient for complementation. The expression pattern conferred by these promoter regions was visualized by GUS stainings of plants carrying the pBR47 construct (Fig. 12F). Cuttings of apices confirmed that the mRNA accumulation profile resembles that known from RNA in situ hybridization studies (Fig. 1C, D), showing signals in the axils of leaves and flowers and in between floral organs. This is in accordance with the complementation observed in plants transformed with the pBR37 construct, carrying a genomic *LAS* fragment with the same promoter regions (Fig. 10).

Fig. 11 illustrates that the activity of the *LAS* promoter is alike in the wild-type and *las* mutant background. Greb *et al.*, (2003), on the other hand, described observations from RNA in situ hybridization experiments that the *LAS* transcript is reduced in *las* mutants. As GUS lines depicted in Fig. 11 originate from different transformation events, equal signal strength does not represent a strong argument, as the transgene insertion locus may alter expression strength. Real-time PCR, quantifying *LAS*/*las* cDNA levels at different growth stages (Fig. 28G, H) on the other hand, stated that mRNA levels do not differ significantly between wild-type and *las* mutants. Thus, it can be presumed that *LAS* promoter activity is not altered between wild-type and *las* plants, signifying that GUS stainings shown in this work are not skewed by their *las* background.

The expression pattern of *LAS* during later flower development is shown for the first time in Fig. 12H - J. *LAS* is expressed at all organ boundaries separating sepals, petals, stamens, and carpels, respectively, from their neighboring tissues. The observed expression domains may pose an explanation for the loss-of-petals phenotype observed in tomato *ls* mutants, assuming that *Ls* mRNA accumulates in the same way as described in *Arabidopsis*. Even though petal primordia are initiated at the same time as stamens, they first remain minute and develop only later as the last of flower organs (Smyth *et al.,* 1990). Hence, they may rely most on the function of *Ls* to keep cells in an undifferentiated state, required for later development. Therefore, petals are the flower organs expected to be most affected when *Ls* function is lost. In this case close inspection of *ls* flowers should reveal petal primordia arrested at an early stage of development.

### 4.1.2. *LAS* 3`promoter alone is able to confer specific expression

A detailed analysis of plants carrying the pAE70 construct, performed in the course of this work, showed that, contrasting previous preliminary results, 800 bp upstream of the *LAS* ORF are sufficient for complementation in the presence of long 3' promoter regions. The importance of a reanalysis of this line was emphasized by results from additional constructs, featuring deletions of 60 and 100 bp around the area 800 bp upstream of the gene, which were able to confer complete complementation (data not shown). Initial phenotyping problems resulted from time constraints, due to which the line was not analyzed in detail at the time and problems with the construct integrity of some lines were not discovered.

Analysis of additional constructs carrying only 600, 400, or 212 bp ahead of the *LAS* ORF demonstrated that no essential promoter elements are located further upstream of the gene than 212 bp, as all constructs were able to confer complementation (Fig. 4). 95bp of this region are transcribed UTR, which leaves only 117 bp of proximal promoter sequences ahead of the TSS to initiate transcription. Complementation of the shortest construct (pBR59, Fig. 4) came as a surprise, as the T-DNA insertion line SALK_040683 was reported to phenocopy *las* mutant plants (Eicker, 2005). This line was described to carry a T-DNA insertion 696 bp upstream of the ATG, probably harboring a promoter deletion

from position -716 to -265 (Eicker, 2005). Thus, it was assumed that pBR59 would not exhibit any complementation ability, including less promoter sequences than this T-DNA insertion line. As sequencing of its *LAS* ORF revealed no mutations, this line should by all current knowledge confer complementation. One hypothesis explaining such a result is T-DNA induced silencing of surrounding regions.

Experiments in tomato showed that constructs bearing a flower specific *PLENA* 5' promoter, which is not active in vegetative axils, can confer complementation when combined with *Ls* 3' promoter sequences. These results corroborate the idea that the significant elements are located in the 3' region. To uncover whether the *Arabidopsis* 5' promoter contains any specific elements at all, it was exchanged with a 600 bp *PI* promoter fragment (pBR43) or with a -90 35S CaMV minimal promoter (pBR41), while retaining long 3' regulatory sequences.

Analysis of pBR41 plants yielded the striking result that even with the unspecific -90 35S sequences on the 5' side the promoter remains functional. Plants transformed with pBR41 nearly completely complemented the *las* phenotype (Fig. 9), demonstrating clearly that no specific elements upstream of the *LAS* TSS are required. A similar construct without the 3' sequences, on the other hand, did not confer any complementation. Likewise, experiments in tomato demonstrated that complementation of the *ls* mutant can also not be achieved using a complete 35S promoter driving *Ls* (Schmitt, 1999), indicating that the specific expression conferred by the 3' region is essential for gene function. A GUS line carrying the same promoter assembly as pBR41 showed patterns indistinguishable from pBR47 (pBR45, Fig. 12K), revealing that the promoter does not only enable *LAS* function but also confers the specific expression pattern as previously described for the endogenous promoter. This denotes that all important elements required for the establishment of the highly specific RNA accumulation profile are located in the 3' region of *LAS*.

Benfey *et al.*, (1989) reported that the -90 35S promoter was active in the root, especially in the root tip, lateral roots, and in the pericycle, from which lateral roots develop. Expression of pBR45 in root tissue has not yet been analyzed, but signals are observed in outer cell layers of the hypocotyl, intensified around emerging structures that probably represent adventitious roots. This may indicate that the *LAS* 3' promoter is able to redirect 35S expression to lateral organ initiation sites, but this needs to be confirmed by a comparison to -90 35S GUS constructs without the *LAS* regulatory regions. The -90 35S minimal promoter also shows a differential activity in the rosette, as more bud formation

was observed in the lower half of pBR41 plants (Fig. 9). Another only partially complementing pBR41 line only formed lateral buds in the lower rosette (data not shown), a phenotype never observed in other partially complementing lines. This indicates that the usage of -90 35S sequences as a minimal promoter might not always be a good choice, depending on what developmental stage is investigated.

Complementation of the *las* mutant phenotype was also successful when replacing the 5' promoter with a 600 bp *PI* promoter fragment (pBR43, Fig. 9). Honma and Goto (2000) reported that this fragment induces specific expression only in floral primordia but not during the vegetative phase. Without the *LAS* 3' regulatory sequences, again, no complementation was achieved. Analysis of plants carrying a *PI* promoter GUS construct, including *LAS* 3' sequences, displayed all signals expected from an endogenous *LAS* promoter, partially extended by *PI* derived activities. In the flower first signals appeared already in stage 2 flowers (Fig. 12 M) and had an intriguing similarity to the pattern shown by Honma and Goto (2000) for the 500 bp *PI* promoter fragment (Fig. 12 D). This points towards a restrictive activity of the *LAS* 3' regions, overwriting the information supplied by the *PI* element between bp 500 and 600 bp. A similar effect is observed at later stages of flower development, where the promoter does not remain active in developing stamens, as in all *PI* promoter constructs (Fig. 12 E), but is restricted to organ boundaries, similar to the endogenous *LAS* promoter (Fig. 12 N). This denotes that *LAS* 3' regulatory sequences induce additive and also restrictive alterations to the *PI* 5' promoter activity.

The promoter swapping experiments demonstrated that the *LAS* promoter specificity can be determined by the 3' regulatory sequences alone. The importance of 3' sequences for promoter functions has previously been shown for the genes *CLV3* and *DRN*. The weak *clv3-3* allele e.g. carries a T-DNA insertion 175 bp downstream of the polyadenylation site (Fletcher *et al.*, 1999), indicating the disruption/separation of an enhancer element. Brand *et al.*, (2002) showed that the correct *CLV3* expression pattern, known from RNA in situ hybridization studies, could only be generated in GUS experiments if downstream sequences were added. The same applies for the *DRN* promoter, as complementation of the *drn* mutant can only be achieved by including 3' sequences (Wolfgang Werr, personal communication). Cis elements in 3' regions of genes are usually not mentioned in general promoter descriptions and never considered in promoter prediction tools (Pedersen *et al.*, 1999; Shamuradov *et al.*, 2005; Molina & Grotewold; 2005; Abeel *et al.*, 2008). As an

example, Lee *et al.*, (2006) reported an analysis of 61 root TF promoters by GFP constructs. Up to 3 kb of upstream sequences were used and resulted in an 80 % match between observed GFP signals and mRNA accumulation pattern. The remaining 20 % were assumed to be regulated by UTRs, introns, or on mRNA level. As promoter elements in the 3' region seem to appear more frequently than previously anticipated they should be included in the common concept of promoters and subsequently in in silico studies on this topic like promoter prediction tools.

### 4.1.3. Pinpointing important *LAS* 3` promoter regions

Phylogenetic footprinting revealed that 3' regions of various *LAS* orthologs share homologies in two regions termed region A and B (Fig. 6, Fig. 7). Alignment of region A of all available *LAS* orthologs revealed astonishingly high sequence homologies for noncoding sequences of distantly related species. All orthologs investigated so far, including several monocots, display high identities in such a region downstream of the gene.

Nevertheless, the analysis of plants carrying the pBR38 construct (Fig. 10), in which the region A is deleted, discards the expectation that region A is of essential importance for promoter function. The examined plants show complete complementation of the *las* phenotype, just as GUS lines, carrying the same promoter composition (pBR48, Fig. 12G), display the wild-type-like, distinct expression pattern. Thus, the function of the region A remains enigmatic. The high conservation gives strong evidence that this region was subject to positive selection at the DNA sequence level during evolution, giving rise to the hypothesis that necessity for this element might have been lost very recently during evolution of *Arabidopsis*. The only indication that this sequence plays a role as a cis element comes from the analysis of tomato 3' regulatory sequences in *Arabidopsis*. A construct missing the region A confers only partial complementation (pAE123, Fig. 8), whereas a longer construct (pAE127) is able to fully complement the *las* phenotype (pAE127 lacks only the first conserved TGTCTTT element, pAE123 lacks another 70 bp, i.e. the complete region A). This may indicate that the *Arabidopsis* 3' sequence contains a redundant element between bp 488 and 3547, which is able to mask the absence of region A, whereas in pAE123 plants, where the redundant *Arabidopsis* element and the tomato derived region A are missing, defects in side shoot formation are observed. Such a

redundancy, however, could not be detected on sequence level. Similarly unexplained is the molecular function of region A. The absence of an open reading frame, no indication for transcripts, and the constant appearance 3' of all *LAS* orthologs strongly support the notion that this is a cis-regulatory element. Nevertheless, conservation seems too high to be based on the binding of single TFs. A protein complex, whose binding requires all conserved residues, would have to comprise a large number of specific DNA binding factors, an assembly unprecedented for genes controlling meristematic activities.

Furthermore, no evidence could be found for a major function of the promoter region B, which shows homologies only between *Arabidopsis*, *Capsella*, and tomato. The non-complementing construct pAE84 lacks half of the region B, while it is present entirely in the slightly larger construct pBR39. Nevertheless, pBR39 did not exhibit an increased complementation ability compared to pAE84, disproving the expectation that the lack of complementation displayed by pAE84 plants might be due to this sequence. This denotes that an essential promoter element must be located between 3239 bp and 3547 bp of the *LAS* 3' promoter, thereby narrowing down this region of interest from 414 bp to 318 bp, from now on referred to as region *C*.

In contrast to these results, tomato 3' regulatory sequences are able to confer complementation with shorter regions, not even including a complete region B. As illustrated in Fig. 8, pAE127 lacks half this region, just like pAE84 (in both cases the breakpoint is in between the two aligned sequences shown in Fig. 7). However, pAE127 confers full complementation, while pAE84 does not. Functionality of the tomato promoter in *Arabidopsis* demonstrates a strong conservation of non-coding, regulatory sequences between tomato and *Arabidopsis* but also denotes the different activities of these promoter sequences. In all examined cases the tomato sequences appeared to drive gene expression stronger than homologous *Arabidopsis* sequences, as comparable constructs with *Arabidopsis* sequences did not confer complementation. This indicates a different composition and arrangement of promoter elements in tomato regulatory sequences.

Analysis of plants carrying the pBR49 and pAE128 constructs (Fig. 8, Fig. 10) illustrated that the 3' sequences can function independent of their location and orientation in respect to the *LAS* gene. In this light it seems even more intriguing that the conserved region A is in all cases found 3' of the *LAS* orthologs. The complementation observed in pBR49 plants

delivered additional information, namely that the 3' sequence from bp 483 to 1827 does not contain any essential elements, as it is missing in this construct.
In summary, the 3' promoter is alone able to induce a highly specific expression pattern, indistinguishable from the endogenous *LAS* expression, which is dependent on an enhancer-like element located between 3239 bp and 3547 bp downstream of the ORF.

### 4.1.4. Relative importance of 5' and 3' promoter sequences

5' sequences of the *LAS* gene were shown to be replaceable with a -90 35S promoter, i.e. they do not contain any elements essential for promoter function, as long as ample 3' regulatory sequences are present. Nevertheless, partial complementation, with about 60 % of rosette leaf axils supporting bud formation, was reported without long 3' sequences, when 2910 bp of 5' promoter were used (Eicker, 2005). 1447 bp of 5' sequences, on the other hand, were insufficient to complement the *las* phenotype. In tomato a similar construct containing long 5' sequences did not confer any complementation (Schmitt, 1999), further corroborating that promoter elements in tomato are organized differently. However, the *Arabidopsis* promoter appears to have a cis element which is partially able to replace the 3' region, situated between 2910 and 1447 bp upstream of the *LAS* ORF (Fig. 34).

This is supported by data recently published by Goldshmidt *et al.*, (2008), who describe complementation of *las* using a transactivation system, in which a ~3800 bp *LAS* promoter is driving expression of a *LAS*-GFP translational fusion protein. Even though complementation was reported, some empty axils are visible in a published picture of such a plant, leading to the assumption that also here complementation is only partial. Astonishingly the resulting expression pattern is comparable to the endogenous *LAS* mRNA accumulation pattern, showing signals in the axils of flower primordia and sepals. The utilized regulatory sequences show no overlap with those used for e.g. pBR45, yet they result in the same specific expression pattern. This denotes that the redundancy between 5' and 3' cis elements extends to such a degree that both contain all elements necessary for specificity, while only overall activity is slightly decreased in the absence of downstream sequences.

A phylogenetic footprinting analysis of the 5' sequence (bp 1447 – 2910) and region *C* produced various conserved motifs, as could be expected from the comparison of two sequences of this size. Further comparison of these identified motifs to promoter sequences of *LAS* orthologs, using FIMO software, did not reveal any significant homologies.

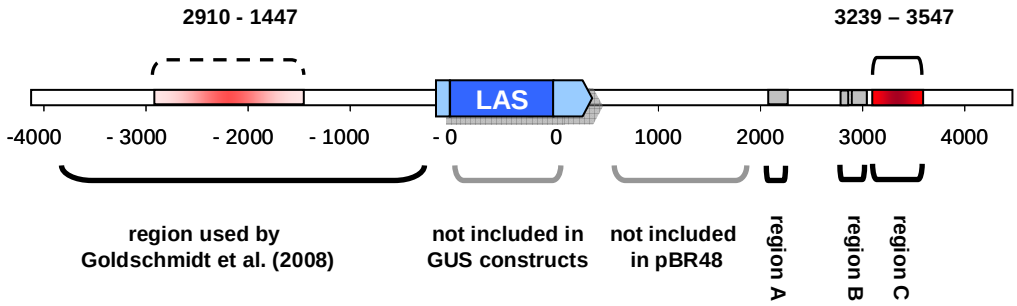


**Figure 34. Summary of current knowledge of the *LAS* promoter**

*LAS* ORF is depicted in blue, UTRs in light blue, regions shown to contain essential promoter elements – functional also in absence of each other - in red. Numbers above parentheses state distances in bp of the indicated regions from the start, respectively stop codon of the *LAS* ORF. Dashed parenthesis indicates region leading to partial complementation in the absence of long 3' sequences. Grey parentheses indicate regions found not to contain essential elements.

In Fig. 34 the current knowledge about the *LAS* promoter is summarized. The two regions, which can independent of each other confer some level of complementation, are depicted in red, sequences shown to be not essential are marked by grey parentheses. The data suggest that at least two copies a major promoter element are present upstream and downstream of the *LAS* ORF.

Another hypothesis states that the pattern is generated by the combined effect of redundant and frequently occurring binding sites, spread throughout all promoter regions and that any general activation of transcription in the presence of more or less any region surrounding the *LAS* gene would result in the described distinct pattern. In initial *LAS* promoter studies, a large promoter region was found to be necessary for correct *LAS* activity. After analysis of various deletion constructs no altered expression pattern could be detected. This contrasts analyses of e.g. the *PI* promoter, where sequential removal of promoter regions caused changes in expression, while different elements could be assigned to specific functions (see Fig. 12B – D, Honma & Goto, 2000). The absence of such findings in the *LAS* promoter dissents the hypothesis of a larger number of dispersed elements. Also both regions of highest interest localize at a large distance from the TSS, suggesting a similar mode of action, pointing towards two confined arrangements of elements.

Overall, it seems likely, yet not proven, that the 5' sequences (bp 1447 – 2910) and region *C*, which are necessary for complementation, also control the specificity of expression. On the further quest to identify upstream regulators of *LAS*, region *C* poses a good starting point for either yeast one-hybrid or DNA affinity purification experiments, as cis-regulatory factors can be expected to bind here. In the case of *LAS* presented in this work, promoter analysis contributes decisively to further analysis, as a standard yeast one-hybrid full promoter analysis, utilizing 1 - 2 kb upstream sequences (Deplancke *et al.*, 2004), would most likely have failed to yield any relevant results.

## 4.2. Part II: Cloning and characterization of the *eol5* mutant

During this work the gene underlying the *eol5* phenotype could be identified by positional cloning to be *CZS*. *eol5* was originally identified in a second-site mutagenesis screen in the *las* background, as it enhances the AM formation defect in *las* plants (Clarenz, 2004). Utilizing a second-site screen, in this case, led to the discovery of a gene that would have otherwise gone unnoticed, as the single mutant phenotype is too weak to be recognized in a conventional screen (Fig. 21).

*CZS* is a putative histone methyl transferase, shown to be involved in chromatin remodeling (Krichevsky *et al.*, 2007). The importance of chromatin structure and epigenetic regulation for plant development is increasingly recognized in recent years (Steimer *et al.*, 2004, Schubert *et al.*, 2005, Reyes, 2006, Henderson & Jacobsen, 2007). With *CZS*, epigenetic regulation enters the stage of AM regulation, a field currently dominated by TFs, as most known players involved in this process are assumed to bind to DNA and regulate transcription (Schmitz & Theres, 2005). Involvement of chromatin remodelers in AM formation does not come as a surprise, as several genes controlling SAM function were reported to be regulated epigenetically (e.g. *KNOX* regulation by *CLF* and *SWN*, Chanvivattana *et al.*, 2004). Nevertheless, control of the constantly, newly arising lateral meristems has so far not been shown to depend on chromatin state. *CZS* is a new regulator of this process and elucidating its mode of action may open the door to understanding a new level of the regulation of AM initiation

### 4.2.1. Positional cloning of *eol5*

#### 4.2.1.1. Determining the correct *CZS* gene structure

Applying a map based cloning strategy, the position of the *eol5* mutation could be located to a 256 kb region on the lower arm of chromosome II. Subsequent sequencing of 39 of 64 genes in this region revealed a mutation in the *CZS* gene (At2g23740). Following the identification of this mutation an annotation problem had to be resolved, as a *CZS* annotation previously published by Krichevsky *et al.,* (2007) places the mutation outside the ORF, whereas, according to the information provided by TAIR, it leads to an early stop codon. *CZS* appears to have a history of incorrect annotations, since first EST based attempts predicted two gene models. This is probably due to the ample length of the mRNA. EST data, obtained by single Sanger reads, led to sequencing of the mRNA ends only, thus resulting in two gene models. The same problem persists for the orthologous gene in rice. The current RefSeq sequence annotates two genes in place of the *CZS* homolog shown in Fig. 18, yet the alignment with various orthologs supports the presence of one large gene. An alignment of the TAIR annotated sequence of *CZS* with mRNA sequences from different sources clearly demonstrated that the complete sequence is transcribed (Fig. 17). A protein alignment of various orthologs of *CZS* shows high homologies even in the N-terminal part of the protein, which is not included in the annotation reported by Krichevsky (2007). High conservation on protein level between distantly related species provides evidence that this sequence is transcribed, translated, and under evolutionary selective pressure.

The experimental evidence for the annotation presented by Krichevsky *et al.,* (2007) is a “RACE” experiment, in which a gene specific reverse primer and a set of genomic forward primers, spaced 200-250 bp apart, were used to amplify PCR products from a cDNA library. The largest PCR product obtained was used to deduce the *CZS* ORF. Such an experimental approach is likely to fail to reveal the correct mRNA sequence, due to the 5 introns that precede the used reverse primer binding site. In summary, the *CZS* mRNA sequence was determined, confirming the TAIR data with the addition of an extra 21 bp ahead of exon 6.

#### 4.2.1.2. Analysis of *eol5* and *czs* mutant alleles reveals common defects

The analysis of *eol5* backcross populations disclosed a discernable *eol5* single mutant phenotype, which had not been reported previously. A comparison of phenotypic deviations caused by *eol5* and the T-DNA insertion alleles *czs-1* and *czs-2* showed defects in AM formation in all cases, supporting the result that *EOL5* and *CZS* encode the same gene. However, AM defects appeared considerably more pronounced in *eol5* plants (Fig. 21). Long day grown plants display the same tendency, with *csz-1* causing the weakest, and *eol5* the strongest phenotypic deviations from the wild-type. Analysis of three segregating *eol5* backcross populations (Fig. 21, others not shown) did not suggest background mutations of the EMS mutagenesis to be responsible for the enhanced phenotype, as no evidence of a second segregating gene affecting the phenotype was seen. Hence, it is assumed that, either in *eol5* or in T-DNA insertion plants, truncated proteins are still produced, impacting on the phenotype.

Apparently an early stop codon at the beginning of the *CZS* gene poses a bigger obstacle for the development of AMs than a T-DNA insertion in the middle of the ORF, even though the insertions are localized well ahead of the conserved SET domain (Fig. 16C). That means either an N-terminal protein fragment or a protein originating from a downstream start codon exerts some kind of function. The next ATG after the SNP in *eol5* still allows the generation of a 1260 AA protein, whereas proteins formed in *czs-1* and *czs-2* reach lengths of at least 906 and 502 AA, respectively.

An allelism test, analyzing F1 plants of *eol5 las* X *czs-1* or *czs-2* crosses, revealed that *CZS* and *EOL5* are indeed allelic, as double heterozygous plants exhibited AM formation defects (Fig. 21). Since these plants rather resemble the T-DNA insertion lines than *eol5* plants, the *czs-1* and *czs-2* alleles appear to have a dominant effect on the phenotype. This points towards an activity of truncated proteins in *czs-1* and *czs-2*. Real-time PCR showed that the 3’ region of *CZS* exhibits an eight fold expression difference between *czs-1* and *czs-2* (Fig. 26B), making it implausible that a C-terminal protein fragment is responsible for the similar defects in *czs-1* and *czs-2*. It seems more likely that a truncated protein, translated from the remaining 5’ mRNA fragment, exerts a partial *CZS* function. This is surprising, as the SET domain, which is assumed to carry the major enzymatic function of producing methyl marks on histones, is not part of such a protein. The truncated *CZS*

fragment could stabilize a repressive complex, which may be able to exert redundant repressive functions, or not make use of the HMT activity in the first place. This hypothesis is in accordance with the slightly stronger phenotype of *czs-2* compared to *czs-1*, observed particularly in long day conditions (Fig. 22), since the N-terminal fragment formed in *czs-2* is shorter than in *czs-1*. However, it cannot be ruled out that a very closely linked second mutation in the *eol5* mutant is enhancing the *eol5* phenotype. Analysis of a new line carrying a T-DNA insertion in the second coding exon may solve this question.

#### 4.2.1.3. Complementation of *eol5* mutants

In order to show that *eol5* is allelic to *CZS*, a complementation experiment was carried out using the native *CZS* promoter in the *las* background. Krichevsky *et al.*, (2007) reported the complementation of the *czs-1* flowering time delay, using slightly shorter promoter sequences. Transgenic plants selected for the *pCZS::CZS* construct regained the ability to form side shoots in many cauline leaf axils in comparison to *eol5 las* control plants. However, complementation only appeared partial, as it did not phenocopy the known *las* single mutant phenotype. The incomplete complementation may be attributed to insufficient promoter sequences or other effects, like growth retardations due to Basta spraying. The experiment will be repeated also phenotyping Basta resistant *las* plants as controls (e.g. pBR44 or pBR47 lines), in order to clarify if complementation is complete or not. It also cannot be ruled out that a truncated protein exerts some function in *eol5*, e.g. actively perturbing a *CZS* containing repressive complex. If this is the case it may not be possible to fully complement an *eol5* mutant. *czs-1* plants transformed with the *pCZS::CZS* construct will also be investigated for complementation.

In summary it could be demonstrated that *eol5* is a mutant allele of *CZS*, by:
(1) map based cloning, (2) at least partial complementation using a *pCZS*::*CZS* construct, showing involvement in the same process, (3) similar defects in *eol5*, *czs-1* and *czs-2* mutants in AM initiation and in flowering time, (4) an allelism test revealing AM formation defects in F1 plants.

#### 4.2.1.4. Phenotypic variability of *eol5*

The positional cloning of *eol5* proved to be challenging due to the constant difficulties with the variability of the *eol5* phenotype. Due to the incomplete penetrance of the *eol5* mutant the phenotype often did not reflect the *eol5* genotype. These problems also hampered mapping of other mutants obtained from this *las* second-site mutagenesis screen, *eol5* is the first to be cloned.

A complete explanation for the observed variability in the *eol5 las* phenotype remains to be identified. Segregating modifiers from the Ler background or the initial EMS mutagenesis are likely to influence the phenotype, evidenced by rough mapping results from *eol3* or *eol5* (Clarenz, 2004; Schulze, 2007). The most variable phenotypes observed during this work have been noted in mapping populations originating from the Ler cross (e.g. Fig. 24E), indicating that modifiers from Ler do play a role.
The first utilized *eol5 las* control plants, which had only been backcrossed once to *las*, always showed a strong mutant phenotype in every sowing (see controls in Fig. 14B). As this line was probably selected out of a segregating F2 population based on a strong phenotype, it may have accumulated a higher number of modifiers from the EMS mutagenesis enhancing the mutant phenotype. As this suggests the presence of such modifiers in the first double mutants, they would also be expected in the Ler cross. However, using later generations, in which most modifiers should not segregate any more, did not solve the problem of phenotypic variation. Between BC2F2 and BC2F5 generations no major improvement of segregation ratios or class discrimination could be observed. Hence, segregating modifiers do not serve as a complete explanation.
Environmental factors have been shown to play a role in the variability of the *eol5 las* phenotype. This was demonstrated by the day length dependent appearance of the *eol5 las* phenotype and also by the different phenotypes observed between populations originating from the same seed batch, grown in parallel in different growth chambers (Fig. 24C - F). Also *eol5* and *czs-1* single mutant populations varied in the extent of AM formation defects in different experiments (Fig. 20 and 21, Fig. 21 and 31). The exact effect of factors like light quality and quantity, temperature, watering, etc., can only be speculated about, as this question has not been addressed in experiments. In any way, not much can be changed to improve growth habits, since in Percival growth chambers environmental conditions are as controlled as feasible for such work. Problems with the cultivation soil causing general

growth inhibitions of *Arabidopsis* led to more intense but also more variable phenotypes, indicating that changing stress levels influence the phenotype.
Fig. 24A, B shows that also *eol5 las* X *las* backcross populations (BC2F2 from original mutant), without Ler background grown in one tray, display incomplete penetrance. Variable penetrance has been shown in many mutants (e.g. *pinhead*: Lynn *et al.,* 1999; *drn*: Chandler *et al.,* 2007). Currently no single explanation can resolve the question of the reason for the phenotypic variation.

### 4.2.2. Phenotypic analysis of *CZS* mutants reveals roles in different processes

The phenotype that led to the discovery of the *eol5* mutant was the lack of axillary buds in cauline leaf axils, in addition to the lateral bud formation defects in the rosette due to *las* (Fig. 13A, C). In *czs* single mutants, on the other hand, mostly rosette leaves are affected. The tendency of upper cauline leaf axils in *eol5 las* plants to occasionally carry flowers or leaves instead of side shoots indicates that meristem identity is coupled with general lateral meristem activity. This may mean that a cell pool, which is not large or undifferentiated or in another way “meristematic” enough, will take up a determinate cell fate producing an organ instead of an indeterminate apical meristem. This is in accord with data reported by Laux *et al.*, (1996).

The failure of axillary organs to correctly execute developmental programs is also evident in the zones of defective flower primordia formation (Fig. 13A, F, G). Flowers appear infertile, sometimes having deranged floral organs, in other cases floral primordia only form reduced structures or are absent. Distortions of phylotaxis occasionally observed in double mutants indicate defects already in SAM organization. *eol5 las* double mutants also exhibited terminations of the main meristem (Fig. 13I, K), affecting up to 75 % of plants of a population, depending on growths conditions. A comparison of sections of terminated and wild-type apices revealed that most terminated apices were devoid of small undifferentiated cells or any organized meristem structure. The last lateral structures formed were often small, without any recognizable shape, consisting of large differentiated cells, pointing at a general loss of meristematic cell identity. *LAS* is not expressed in SAM, yet in tomato *ls* mutants show terminations at a low frequency (G. Schmitz, personal

communication). Occurrence of SAM arrests has not yet been thoroughly investigated in *csz* single mutants, but so far such a phenotype has not been noticed. Thus, the exact contribution *eol5* to this phenotype still has to be investigated. All described phenotypic alterations of SAM and lateral organ development are - again - dependent on growth conditions and were not noticed in all experiments.

Furthermore, detailed analyses of *eol5 las* plants revealed fusions between rosette leaves (Fig. 13L, M). Fusions appeared at the base of lower rosette leaves, with varying degrees, in one experiment affecting in average ~ 7 leaves per plant in short days, and half of that in long day conditions. A role in organ separation had previously been associated with *las*, as the mutant displays concaulescent fusions of lower cauline branches (Greb, 2003). These were not observed in *eol5 las* double mutants due to the lack of such lower cauline branches. Rosette leaf fusions have been reported from *stm las* double mutants (Clarenz, 2004), yet real-time PCR analysis did not reveal any decrease in *STM* transcript in *eol5* mutants. Thus, other genes have to be deregulated in *eol5* mutants, enhancing the organ fusion tendency of *las*, which is involved in organ boundary function.
Overall, *CZS* function appears to be necessary in meristems and all types of lateral organs, as leaves, flowers, and side shoots were shown to be affected. The function that is lost in *czs* mutants looks to be keeping cells in an undifferentiated state.

A role in a different aspect of plant development has previously been shown for *czs-1* plants, which display a moderate delay in flowering. Analysis of long day grown plants revealed an increased time to flowering and a higher leaf number can be observed in all *czs* mutant alleles, also in the *las* background (Fig. 23A, B). The *eol5* line exhibited more pronounced deviations in total leaf number than *czs-1* or *czs-2* (t-test: $p = 0.008$ and $p = 0.179$, respectively), indicating that this result may be due to the same process as the AM formation defect. In contrast to the delay of flowering observed in long days, *czs* mutants grown to flowering in short day conditions rather displayed a converse effect (Fig. 23C, D).
This can be explained with the reported *FLC* upregulation in *czs-1* plants (Krichevsky *et al.*, 2007), which could be confirmed by real-time PCR. *FLC* is a floral repressor, which is itself negatively regulated by the vernalization pathway (e.g. *VRN2*) or by members of the autonomous pathway (e.g. *FLD*), to release repression of floral induction. Upregulation of *FLC* in *czs* mutants explains the delay in flowering in long day conditions, which has been

shown in various other mutants in which *FLC* is derepressed (Simpson, 2004). However, flowering in short days is elicited by the GA-pathway, bypassing *FLC* regulation (Farrona *et al.,* 2008), thereby explaining why *czs* mutants are not late flowering in short days. In summary, *CZS* could be shown to play role in the development of AMs and floral primordia, SAM maintenance, and control of floral transition.

### 4.2.3. Looking into the function of *CZS*

In order to understand the occurrence of the different phenotypes caused by *czs* mutations, the mechanism of *CZS* function has to be investigated in more detail. Protein alignments show that *CZS* is strongly conserved, also in more distant related species like monocots and the moss *Physcomitrella* (Fig. 18). This implies that *CZS* performs an important function that is evolutionary conserved. The domain structure of *CZS* is unique and only appears in plants (Baumbusch *et al.,* 2001). A protein alignment shows a highly conserved protein domain near the N-terminus (Fig. 18, AA 290 to 350), which, according to BLAST searches, is unique for this gene. No function could yet be assigned to this domain, evidence for its importance arises from the comparison of different *czs* alleles. Weaker phenotypes observed in *czs-1* and *czs-2* plants appear to be due to an N-terminal fragment of the *CZS* protein, which is not formed in *eol5* plants. C2H2 zinc finger domains, of which three are found in *CZS*, may bind DNA, but are also known to confer protein protein interactions (SMART, Schultz *et al.,* 1998), hence their exact role cannot be predicted. The molecular function of SET domains has been shown to be the methylation of histones, generating marks that induce changes in chromatin state. *SUVR4*, the closest *CZS* homolog investigated, was shown to have an in vitro HMT activity, generating $me_2$H3K9 with a substrate preference for meH3K9 (Thorstensen *et al.,* 2006).
*CZS* was shown to be a negative regulator of transcription by a reporter gene repression assay in transiently transformed *Arabidopsis* leaves (Krichevsky *et al.,* 2007) and repressive histone marks at the *FLC* locus were shown to be reduced in *czs-1*. Due to the interaction with *SWP1* (see chapter 1.2.1.2) the hypothesis was formulated that *CZS* is part of a co-suppressor complex (Krichevsky *et al.,* 2007b).

This leads to the general concept that *CZS* generates negative histone marks on specific genes or regions, leading to their transcriptional repression. In the mutant, these genes are

deregulated, causing the multitude of phenotypic deviations. Therefore, they are assumed to include repressors of flowering and factors promoting differentiation in the vicinity of the SAM leading to problems in AM formation, primordia development and SAM maintenance. Since pleiotropic effects in *eol5 las* are not severe, deregulation is probably either very restricted to specific genes or generally of minor magnitude.

#### 4.2.3.1. *CZS* expression analysis

As a starting point to elucidate *CZS* function the expression profile was analyzed, since a specific expression pattern may give hints to possible genetic interactors. Most SET domain genes are expressed constitutively (Springer *et al.*, 2003), yet Baumbusch *et al.*, (2001) could also show examples for tissue specific expression of *Arabidopsis* SET domain proteins of the same subfamily as *CZS*. In case of *CZS*, the BAR *Arabidopsis* eFP Browser, integrating micro array data from various experiments, shows constitutive, low expression, slightly reduced in leaves. In agreement with these data, real-time PCR analysis of nine different tissues did not reveal any differential accumulation of *CZS* transcript. The zones of phenotypic deviations observed in *eol5* mutants: (1) single mutant phenotype in rosette, in combination with *las* in (2) cauline leaf axils and (3) SAM termination during flowering, suggest that *CZS* exerts its function during the complete postembryonic development of *Arabidopsis*. Since there is so far no evidence for a specific expression pattern of *CZS*, the question arises how the rather specific phenotype is caused. A likely explanation is that the targets are dependant on other positive or negative regulators.

#### 4.2.3.2. Investigation of candidate targets of *CZS*

The central question that needs to be addressed in order to elucidate the events taking place in *czs* mutants is, which genes are targeted by *CZS*. The second-site mutagenesis screen is expected to identify mutants whose affected genes act in a parallel pathway to *LAS* on the final output AM formation.

Various candidate genes were examined for expression changes in *czs* mutants. Differentiation signals, causing cells to loose meristematic activity, were considered the most likely targets, as their derepression in *czs* mutants might lead to the observed phenotypes. Only few factors promoting loss of meristem identity are known. miR164 and

miR171 repress *CUC1* and *2* and *SCL6, 22,* and *27,* respectively, genes which are necessary for correct meristem function. As miR171 genes do not show negative histone marks (UCSC Genome Browser), focus was first placed on miR164. Other putative promoters of differentiation are *DRN* and *DRNL,* as the *DRN* overexpressing line *drn-D* exhibits empty leaf axils, and accessory bud formation was observed in *drn drnl* double mutants at a low frequency (data not shown). *RAX1* was also considered a good candidate as phenotypic alterations in *rax1* plants are short day dependent and *rax1* has been shown to enhance the *las* phenotype (Müller, 2005). Unfortunately, the described upregulation of *RAX1* and the downregulation of *MIR171*, *DRN*, and *DRNL* (Fig. 28) represent the exact opposite of what would explain the *czs* mutant phenotype. Differentiation signals are expected to be derepressed and factors known to promote AM formation should be downregulated. In this light the observed altered expression levels may represent compensation effects of the plant trying to counter defects in lateral meristem development.

Interaction studies analyzing multiple mutants confirm that *CZS* does not act via miR164, as *mir164* and *eol5* mutant phenotypes appeared additive (Fig. 32). *eol5 rob* double mutants on the other hand displayed intermediate phenotypes (Fig. 32). This result is puzzling as AM formation defects would be expected to be either additive, or the mutation causing the stronger phenotype should be epistatic, if both genes act in one pathway. Yet, double mutants exhibited fewer defects than the *eol5* parent. Further investigations are necessary to provide an explanation for this result. A starting point will be to analyze a population segregating for *rob,* in order to compare plants with an identical, homozygous *eol5* background.

Based on a microarray experiment that was carried out with *czs-1* mutants, further candidates were chosen that might explain the mutant effects. However, mRNA level analysis of *LBD25*, *PP2C*, and *ANAC83* did not reveal any differential expression contradicting the microarray results. This may be due to the different tissue (seedling including leaves and roots) and the different light regime (long day) used to obtain the microarray data. As *CZS* is involved in flowering time regulation, the *czs* mutation may cause different target gene expression levels in long days and short days, respectively. A new microarray experiment has been carried out using the RNA obtained from short day grown seedlings after removal of roots and leaves, data is currently being processed. A

further microarray, utilizing an HA tagged CZS protein for a ChIP chip experiment, is expected to reveal target loci of *CZS*.

*FLC* was reported to be upregulated in a microarray analysis of *swp1* and *czs-1* mutants (Krichevsky *et al.,* 2007). Derepression of *FLC* in *czs-1* and *czs-2* plants could be confirmed in 2 weeks short day grown seedling tissue by real-time PCR (Fig. 29E), even though differential expression was considerably less pronounced than published for long day grown seedlings (50 % increase instead of 400 %). Hence, *CZS* can be formally considered a new member of the autonomous pathway of floral induction, as it represses *FLC* independent of day length conditions or vernalization.
A potential problem appeared in the real-time PCR results depicted in Fig. 29E, which indicate that *FLC* is not upregulated in homozygous *eol5* single mutants. This is in contrast to the results in the *las* background, in which *eol5* plants show the same increase of *FLC* transcript as observed in the T-DNA insertion allele samples. In addition the flowering time delay in *eol5* plants is similar, or even stronger, than in *czs-1* or *czs-2* mutants (Fig. 23A, B). Together with the high variation between the only two available biological *eol5* replicates, this suggests that there might be a technical problem with these samples. The experiment will be repeated with new cDNAs to clarify this matter. Investigation of cDNAs obtained from adult tissues, harvested seven days after shift to long days, did not reveal an upregulation of *FLC* in *czs* mutants. Instead an extremely high variability, also between biological replicates, was observed. This may reflect the big changes in *FLC* levels that occur at the time of floral transition (Searle *et al.,* 2006). Whether *FLC* expression is still upregulated in *czs* mutants at later stages of plant growth, would have to be addressed by analyzing samples that have not been shifted to long days.

#### 4.2.3.3. A method of action hypothesis for *CZS*

A mutation in the *CZS* gene leads to derepression of target genes, causing the described phenotypic alterations in AM initiation and flowering. *FLC* transcript could be shown to be upregulated in *czs* mutants by real-time PCR, thus constituting a direct or indirect target of *CZS*. Recent results suggest that the process of AM formation and flowering time control may be linked. Mutant analysis of *yab1* or *rax1* revealed that AM formation defects only appear in a short day dependent manner (Müller *et al.*, 2006; Yang, 2007). Also crosses with different wild *Arabidopsis* accessions showed lateral bud formation failures coupled

to delayed floral transition, with QTL analyses indicating the involvement of *FRI* and *FLC* loci (X. Huang, B. Schäfer, personal communications). The resulting hypothesis is that *FLC* controls both AM initiation and floral transition.
To test this idea, *FRI* overexpressing plants were analyzed. Because of a deletion in the *FLC* activator *FRI*, *FLC* levels are strongly reduced in Col (Johanson *et al.*, 2000). In contrast, the *FRI FLC* line, carrying an introgression of the active *FRI* allele from the Sf-2 accession, has increased *FLC* levels. Analysis of *FRI FLC* plants revealed defects in lateral bud formation in the lower rosette (Fig. 33), suggesting an involvement of *FLC* in the process of AM formation in *Arabidopsis*.

Taking together all available data the question may be addressed: Can the hypothesized function of *FLC* as a negative regulator of branching explain observed *czs* mutant phenotypes? The repressive factor causing the observed AM defects has to fulfill certain characteristics inferred from mutant phenotypes.
(1) Its level of activity is declining during growth in long days, as *czs* single mutants only exhibit defects in the lower half of the rosette (Fig. 22). Also *eol5 las* double mutants do not show defects in long days, indicating that the repressive factor is not active any more during cauline leaf development in long days.
(2) The repressive factor retains a certain activity during growth in short days and decreases after onset of flowering. This is deduced from the defects of *eol5* plants, which are also observed in younger rosette leaf axils when grown in short days (Fig. 31B). Additionally, if *eol5 las* plants do develop buds leading to intermediate phenotypes, these usually appear in the uppermost cauline leaf axils (Fig. 19). Furthermore, in *eol5 las* populations flowering in short days, the later - or more slowly - flowering plants show a tendency to form more axillary buds (Fig. 23). Hence, after a slow transition to flowering the repressor may have reached lower levels when cauline leaves are formed.
(3) The repressive factor seems to decrease continuously during plant development, as phenotypic deviations in all conditions and zones tend to be stronger in older leaf axils. Also defects in flower development observed in *eol5 las* plants appear in the early phase of flower formation (Fig. 13A).

It has to be added that the extent of phenotypic deviations observed in *eol5 las* mutants is very weak when plants are shifted early. Full penetrance is only achieved when plants are shifted after 5-6 weeks (Clarenz, 2004). Yet *eol5* single mutants do reveal defects in AM

formation during early plant growth. This information is not easily integrated into a model of repressor action and may be a result of slower floral induction in younger plants, leading to a downregulation of the repressor before cauline leaves are formed. However, this hypothesis requires experimental validation.

The description of this repressive factor is to a large degree in accord with previous knowledge about *FLC*. *FLC* activity is generally decreasing during the life of a plant. In long day conditions, *FLC* activity drops after some time (1-2 weeks depending on conditions and ecotype) below a threshold to release repression of floral activators (Searle *et al.,* 2006). Schmid *et al.,* (2003) demonstrated that *FLC* levels decrease after a shift to long days, which is also part of the postulated characteristics of the repressive factor.
On the other hand, *FRI FLC* lines display a much more delayed flowering than *eol5* lines, yet side shoot defects are more pronounced in *eol5*. These results indicate that *FLC* may cause part of the effect but cannot serve to explain the complete phenotypic alterations. Yet, matters are further complicated as *FLC* is strongest expressed in the shoot apex (Searle *et al.,* 2006) but also active in other parts of the plant. The function of *FLC* in leaves or in the apex is to some degree different, inhibiting flowering either by mainly repressing *FT* or *SOC1* (Searle *et al.,* 2006). Hence, a misexpression of *FLC* in the apex could still be alone causative for the observed effects on AMs, without causing a strong delay in flowering.
However, trying to explain all observed phenotypes with the actions of one factor surely does not reflect the complexity of the regulatory networks involved. *FLC* is currently believed to be regulated by more than 20 genes (Farrona *et al.,* 2008). Additionally, there are four *FLC* paralogs (Ratcliffe *et al.,* 2003) and redundancy is also observed in many factors regulating, interacting with, or being regulated by *FLC*. In this light *FLC* may be considered a place holder or an indicator for the complex activities of the network controlling flowering as well as AM development.
Not to forget that the involvement of other deregulated genes is equally likely, even though no candidates have been shown to be deregulated yet. Interactions of *FLC* and *eol5* will be investigated in *eol5 flc* double mutants and *eol5 FRI FLC* plants. Vernalization experiments may also confirm the dependency of the *eol5* phenotype on *FLC*.

### 4.2.4. Findings from the analysis of *CZS* homologs

In order to reveal a possible general role of SET domain proteins or SET containing complexes on branching, homologs of *CZS* were investigated. Mutations in the close *CZS* homologs *SUVH1, SUVR1,* and *SUVR3* did not expose any defects in AM formation. So far no indications for a global role of these related SET domain genes could be found, supporting the idea of a unique function of *CZS,* endorsed by the unique protein domain structure.
Mutant analysis of the interaction partner *SWP1* gave indications for a weak AM formation defect, supporting a common function in a repressive complex. Crosses have been initiated to check whether a mutation in *SWP1* also enhances *las* phenotype.

Furthermore, PcG complex mutants have been investigated for two reasons. Firstly, because CLF, SWN, and MEA are the most studied and understood SET domain proteins, and secondly, due to the observation by Daniel Schubert that *vrn2 emf2* PcG mutants display axillary bud formation defects. Analysis of *clf* or *swn* single mutants did not disclose a specific role in AM development. *vrn2 emf2* double mutants, on the other hand, displayed a strong AM formation defect, as bud formation is only supported in the lower rosette and some later cauline leaves (Fig. 31). This phenotype is somewhat reminiscent of *filamentous flower* mutants (Yang, 2007). *fil-8* plants also show complete bud formation in the lower rosette and increasing defects in older leaf axils. This is in contrast to most other mutants, in which AM formation is compromised most in the lower rosette leaf axils.
*emf2* mutants flower very early leading to small, dwarfed plants (Chanvivattana *et al.*, 2004), while *vrn2* single mutants are rather late flowering. *emf2 vrn2* double mutants display a combination of both single mutant phenotypes. Bolting starts later than in *emf2* plants but earlier than in the wild-type. Intriguingly, bolting and initiation of floral meristems appear uncoupled, demonstrated by the immense number of cauline leaves which are formed (Fig. 31).
A similar uncoupling has been reported from *leafy* (*lfy*) mutants (Schultz & Haughn, 1991). *LFY* acts to confer floral identity in concert with *SOC1,* which is a direct target of *FLC* repression (Farrona *et al.,* 2008). Since *VRN2* has been shown to be necessary for the stable repression of *FLC* upon vernalization, it is tempting to speculate that *VRN2* also negatively influences *FLC* levels in non-vernalized Col plants. The *vrn2* mutation was actually reported not to affect flowering in long days (Gendall *et al.*, 2001), yet *FLC* levels

may still be altered under shift conditions. This could serve to explain the moderate delay in flowering and the minor defects in AM formation in the rosette. In the *emf2 vern2* double mutant, epigenetic regulation is further disrupted resulting in strong defects in AM formation and substantial difficulties in producing floral meristems. This again fits to the hypothesis of *FLC* deregulation and subsequent *SOC1* repression.

The hypothesis of *FLC* being the repressor active in *czs* mutants and also necessary for floral identity is also supported by the observation that plants shifted from short days to long days have more cauline leaves than long day grown plants. As described above, the repressor acting in *czs* mutants is downregulated during vegetative growth in long days. If this repressor is *FLC* and *FLC* is also involved in providing floral identity owing to *SOC1* regulation, this would explain the low number of cauline leaves and absence of AM defects in these cauline leaf axils in long day grown plants. In this case more cauline leaves would be expected to form in *eol5* mutants, which is observed in long days (Fig. 22, Fig. 23B), but not in shift conditions (Fig. 19, Fig. 20).

Preventing further overinterpretations, high *FLC* transcript abundance first has to be experimentally confirmed in *vrn2* and *emf2 vrn2* mutants. As *emf2 vern2* plants show a range of pleiotropic phenotypes many other factors are expected to be deregulated, thus, *FLC* may only play a minor role in the observed phenotypic alterations. The presented “out of *FLC* theory” reducing the multitude of observed phenotypes down to one central regulatory factor, surely does not represent a full explanation. Rather, this first concept is to be expanded and modified and may be used as a starting point to develop hypotheses that can be experimentally validated.

### 4.2.5. Putative biological role of interactions between floral induction pathways and AM formation control

A correlation between late flowering and reduced AM formation has been reported on several occasions (Kalinina *et al.,* 2002; Clarenz, 2004; Müller *et al.,* 2006; Yang, 2007; Wang *et al.,* 2009; B. Schäfer, personal communication; X. Huang, personal communication). Current results indicate that *FLC* may be the missing link connecting AM

development and flowering time control. Hereupon the question arises why is flowering time and lateral bud initiation based on same genetic regulatory pathway?

Plants obviously require active development of axillary meristems upon flowering, as flowers are a type of axillary meristem (Long & Barton, 2000), yet these processes represent an unlikely couple: on the one side flowering time a tightly regulated process with ample adaptive variations between accessions, as it is of vital importance for reproductive success. On the other side: the process of AM initiation, which does not respond to environmental cues and is not varying between accessions, as most wild-type *Arabidopsis* accessions form buds in all relevant axils.

Currently two hypotheses provide a possible explanation why flowering and AM formation are linked.

The first idea interprets this linkage as a relict from a previous perennial plant development. The perennial life history has arisen independently many times (Thomas *et al.,* 2000) and occurs in different genera of the *Brassicaceae* (Beilstein *et al.,* 2006). A recent study by Wang *et al.,* (2009) showed that in *Arabis alpina* the *FLC* homolog *PERPETUAL FLOWERING1* (*PEP1*) regulates flowering and lateral meristem development simultaneously. During vernalization *PEP1* levels decrease causing first: transformation of all vegetative to floral meristems, and second: AM initiation in axils, in which previously no axillary shoot development was visible. These new meristems continue to grow vegetatively, thereby replacing those that switched to floral development, supplying new shoots for the next season. *PEP1* levels increase again with time and the process reiterates upon the next vernalization event, generating new flowers and new lateral meristems. This connection, desired for perennial plants, may still be present in *Arabidopsis*, leading to the observed link between the two traits, mediated by *FLC*. The identification of a recent, perennial ancestor of *Arabidopsis* would provide support for this theory.

Another hypothesis is based on the concept that AM initiation is dependent on a general lateral meristem activity.

The idea originates from an observation from *branched 1* (*brc1*) mutants, published by Aguilar-Martinez *et al.,* (2007). *brc1* mutant plants show no apical dominance, as all lateral buds grow out, but also AMs are formed in axils where they do not appear in Col wild-type, like cotyledons and early true leaves. This indicates that AM initiation and bud

outgrowth are not, as previously assumed, separate mechanisms. This leads to the postulation of a “lateral meristem vigor”, a force controlling AM initiation and the pace of bud development, as well as later bud outgrowth.

Such a lateral meristem vigor could provide an explanation for the *las* mutant phenotype, which exhibits AM initiation during reproductive development but not during vegetative phase. The main function of *LAS* is probably to keep cells in a competent, undifferentiated state. Thereby, *LAS* could provide an extended time window for AM initiation in axil tissues. Lateral meristems formed during the vegetative phase have a low lateral meristem vigor, initiating and developing slowly. Hence, if the time window for this development is closed too early (as in *las*) axillary cells undergo differentiation and AM formation is aborted. The onset of flowering increases the pace of AM formation in *Arabidopsis*, leading to earlier and faster bud development and mostly immediate outgrowth. Therefore these meristems can be assigned a high lateral meristem vigor. As these fast growing meristems do not require a large time window for development they also develop in *las* mutant plants.

Upon transition to flowering *Arabidopsis* requires more active, quickly developing meristems in the axils of late rosette and cauline leaves, explaining why lateral meristem vigor may be under the control of factors regulating floral transition like *FLC*. As the lateral meristem vigor also promotes AM initiation this may serve to explain defects caused by the *FLC* overactivity in *FRI FLC* lines or *czs* mutants. In this light it seems conceivable that *CZS* may act as a repressor of *FLC*, thereby controlling floral transition and AM initiation at the same time.

# 5. Contributions of co-workers to this project

The construct pES44 was cloned by Elisabeth Schäfer, line selection and primary analysis was carried out by Andrea Eicker.

pAE50 and pAE51 have previously been analyzed in detail and were used here as controls (Eicker, 2005).

pAE70 and pAE84 were previously only roughly analyzed by decapitation, followed by examination of side shoot outgrowth (Eicker, 2005).

pAE123, pAE125, pAE127, and pAE128 were designed and cloned by Andrea Eicker, who also produced T1 plants.

# 6. Literature

**Abeel, T., Saeys, Y., Bonnet, E., Rouze, P., and Van De Peer, Y.** (2008). Generic eukaryotic core promoter prediction using structural features of DNA. Genome Research **18,** 310-323.

**Aguilar-Martínez, J.A., Poza-Carrion, C., and Cubas, P.** (2007). *Arabidopsis BRANCHED1* acts as an integrator of branching signals within axillary buds. Plant Cell **19,** 458-472.

**Alonso, J.M., Stepanova, A.N., Leisse, T.J., Kim, C.J., Chen, H.M., Shinn, P., Stevenson, D.K., Zimmerman, J., Barajas, P., Cheuk, R., Gadrinab, C., Heller, C., Jeske, A., Koesema, E., Meyers, C.C., Parker, H., Prednis, L., Ansari, Y., Choy, N., Deen, H., Geralt, M., Hazari, N., Hom, E., Karnes, M., Mulholland, C., Ndubaku, R., Schmidt, I., Guzman, P., Aguilar-Henonin, L., Schmid, M., Weigel, D., Carter, D.E., Marchand, T., Risseeuw, E., Brogden, D., Zeko, A., Crosby, W.L., Berry, C.C., and Ecker, J.R.** (2003). Genome-wide insertional mutagenesis of *Arabidopsis thaliana*. Science **301,** 653-657.

**Alvarez-Venegas, R., and Avramova, Z.** (2001). Two *Arabidopsis* homologs of the animal *trithorax* genes: a new structural domain is a signature feature of the *trithorax* gene family. Gene **271,** 215-221.

**Amaya, I., Ratcliffe, O.J., and Bradley, D.J.** (1999). Expression of *CENTRORADIALIS* (*CEN*) and *CEN*-like genes in tobacco reveals a conserved mechanism controlling phase change in diverse species. Plant Cell **11,** 1405-1417.

**Applied Biosystems** (2001) User Bulletin #2 ABI PRISM 7700 Sequence Detection System.

**Bailey, T.L., and Elkan, C.** (1994). Fitting a mixture model by expectation maximization to discover motifs in biopolymers. Proceedings of the 8th International Conference on Intelligent Systems for Molecular Biology **2,** 28-36.

**Baker, C.C., Sieber, P., Wellmer, F., and Meyerowitz, E.M.** (2005). The *early extra petals1* mutant uncovers a role for MicroRNA *miR164c* in regulating petal number in *Arabidopsis*. Current Biology **15,** 303-315.

**Bannister, A.J., Zegerman, P., Partridge, J.F., Miska, E.A., Thomas, J.O., Allshire, R.C., and Kouzarides, T.** (2001). Selective recognition of methylated lysine 9 on histone H3 by the HP1 chromo domain. Nature **410,** 120-124.

**Bao, N., Lye, K.W., and Barton, M.K.** (2004). MicroRNA binding sites in *Arabidopsis* class IIIHD-ZIP mRNAs are required for methylation of the template chromosome. Developmental Cell **7,** 653-662.

**Barton, M.K., and Poethig, R.S.** (1993). Formation of the shoot apical meristem in *Arabidopsis thaliana* - an analysis of development in the wild-type and in the *shoot meristemless* mutant. Development **119,** 823-831.

**Baumbusch, L.O., Thorstensen, T., Krauss, V., Fischer, A., Naumann, K., Assalkhou, R., Schulz, I., Reuter, G., and Aalen, R.B.** (2001). The *Arabidopsis thaliana* genome contains at least 29 active genes encoding SET domain proteins that can be assigned to four evolutionarily conserved classes. Nucleic Acids Research **29,** 4319-4333.

**BD Biosciensces** (1998) MATCHMAKER One-Hybrid System User Manual, Protocol #1031-1 Version # PR71132. Clontech laboratories, Inc.

**Beilstein, M.A., Al-Shehbaz, I.A., and Kellogg, E.A.** (2006). Brassicaceae phylogeny and trichome evolution. American Journal of Botany **93,** 607-619.

**Benfey, P.N., Ren, L., and Chua, N.H.** (1989). The CaMV S-35 enhancer contains at least 2 domains which can confer different developmental and tissue-specific expression patterns. Embo Journal **8,** 2195-2202.

**Benková, E., Michniewicz, M., Sauer, M., Teichmann, T., Seifertova, D., Jurgens, G., and Friml, J.** (2003). Local, efflux-dependent auxin gradients as a common module for plant organ formation. Cell **115,** 591-602.

**Berger, F., and Gaudin, V.** (2003). Chromatin dynamics and *Arabidopsis* development. Chromosome Research **11,** 277-304.

**Bernatavichute, Y.V., Zhang, X., Cokus, S., Pellegrini, M., Jacobsen, S.E.** (2008) Genome-wide association of histone H3 lysine nine methylation with CHG DNA methylation in Arabidopsis thaliana. PLoS ONE. **9**, 3156.

**Blanchette, M., Schwikowski, B., and Tompa, M.** (2002). Algorithms for phylogenetic footprinting. Journal of Computational Biology **9,** 211-223.

**Bolle, C.** (2004). The role of GRAS proteins in plant signal transduction and development. Planta **218,** 683-692.

**Bradley, D., Carpenter, R., Sommer, H., Hartley, N., and Coen, E.** (1993). Complementary floral homeotic phenotypes result from opposite orientations of a transposon at the *plena* locus of antirrhinum. Cell **72,** 85-95.

**Brand, U., Grunewald, M., Hobe, M., and Simon, R.** (2002). Regulation of *CLV3* expression by two homeobox genes in *Arabidopsis*. Plant Physiology **129,** 565-575.

**Busch, B.** (2009) Genetic and molecular analysis of aerial plant architecture in tomato. Inaugural-Dissertation zur Erlangung des Doktorgrades der Mathematisch- Naturwissenschaftlichen Fakultät der Universität zu Köln.

**Byrne, M.E., Barley, R., Curtis, M., Arroyo, J.M., Dunham, M., Hudson, A., and Martienssen, R.A.** (2000). *Asymmetric leaves1* mediates leaf patterning and stem cell function in *Arabidopsis*. Nature **408,** 967-971.

**Cazzonelli, C.I., Cuttriss, A.J., Cossetto, S.B., Pye, W., Crisp, P., Whelan, J., Finnegan, E.J., Turnbull, C., and Pogson, B.J.** (2009). Regulation of carotenoid composition and shoot branching in *Arabidopsis* by a chromatin modifying histone methyltransferase, SDG8. Plant Cell **21,** 39-53.

**Chan, S.W.L., Henderson, I.R., and Jacobsen, S.E.** (2005). Gardening the genome: DNA methylation in *Arabidopsis thaliana*. Nature Reviews Genetics **6,** 351-360.

**Chandler, J.W., Cole, M., Flier, A., Grewe, B., and Werr, W.** (2007). The AP2 transcription factors DORNRÖSCHEN and DORNRÖSCHEN-LIKE redundantly control Arabidopsis embryo patterning via interaction with PHAVOLUTA. Development **134,** 1653-1662.

**Chanvivattana, Y., Bishopp, A., Schubert, D., Stock, C., Moon, Y.H., Sung, Z.R., and Goodrich, J.** (2004). Interaction of polycomb-group proteins controlling flowering in *Arabidopsis*. Development **131,** 5263-5276.

**Chapman E. J. and Estelle, M.** (2009). Mechanism of Auxin-Regulated Gene Expression in Plants. Annu. Rev. Genet. **43**, 265–85.

**Chaudhury, A.M., Ming, L., Miller, C., Craig, S., Dennis, E.S., Peacock, W.J.** (1997). Fertilization-independent seed development in Arabidopsis thaliana PNAS **94**(8) 4223-4228.

**Clarenz, O**. (2004) Studien zur Rolle des *LATERAL SUPPRESSOR*-Gens bei der Initiation von Achselmeristemen: Analyse von Doppelmutanten und Charakterisierung von Modifikatoren des *las-4*-Phänotyps. Inaugural-Dissertation zur Erlangung des Doktorgrades der Mathematisch-Naturwissenschaftlichen Fakultät der Universität zu Köln.

**Clark, S.E., Running, M.P., and Meyerowitz, E.M.** (1993). *Clavata1*, a regulator of meristem and flower development in *Arabidopsis*. Development **119,** 397-418.

**Clough, S.J., and Bent, A.F.** (1998). Floral dip: a simplified method for *Agrobacterium*-mediated transformation of *Arabidopsis thaliana*. Plant Journal **16,** 735-743.

**Czechowski, T., Stitt, M., Altmann, T., Udvardi, M.K., and Scheible, W.R.** (2005). Genome-wide identification and testing of superior reference genes for transcript normalization in *Arabidopsis*. Plant Physiology **139,** 5-17.

**Deplancke, B., Dupuy, D., Vidal, M., and Walhout, A.J.M.** (2004). A gateway-compatible yeast one-hybrid system. Genome Research **14,** 2093-2101.

**Dong, G.F., Ma, D.P., and Li, J.X.** (2008). The histone methyltransferase SDG8 regulates shoot branching in *Arabidopsis*. Biochemical and Biophysical Research Communications **373,** 659-664.

**Ebbs, M.L., and Bender, J.** (2006). Locus-specific control of DNA methylation by the *Arabidopsis* SUVH5 histone methyltransferase. Plant Cell **18,** 1166-1176.

**Edgar, R. C.** (2004) MUSCLE: multiple sequence alignment with high accuracy and high throughput. Nuc. Acids Res., **32**(5), 1792-1797.

**Edwards, K., Johnstone, C., and Thompson, C.** (1991). A simple and rapid method for the preparation of plant genomic DNA for PCR analysis. Nucleic Acids Research **19,** 1349-1349.

**Eicker, A.** (2005) Studien zur Charakterisierung der regulatorischen Elemente des *LATERAL SUPPRESSOR* Gens in *Arabidopsis thaliana.* Inaugural-Dissertation zur Erlangung des Doktorgrades der Mathematisch-Naturwissenschaftlichen Fakultät der Universität zu Köln.

**Elliott, R.C., Betzner, A.S., Huttner, E., Oakes, M.P., Tucker, W.Q.J., Gerentes, D., Perez, P., and Smyth, D.R.** (1996). *AINTEGUMENTA*, an *APETALA2*-like gene of *Arabidopsis* with pleiotropic roles in ovule development and floral organ growth. Plant Cell **8,** 155-168.

**Farrona, S., Coupland, G., and Turck, F.** (2008). The impact of chromatin regulation on the floral transition. Seminars in Cell & Developmental Biology **19,** 560-573.

**Fleet, C.M., and Sun, T.P.** (2005). A DELLAcate balance: the role of gibberellin in plant morphogenesis. Current Opinion in Plant Biology **8,** 77-85.

**Fletcher, L.C., Brand, U., Running, M.P., Simon, R., and Meyerowitz, E.M.** (1999). Signaling of cell fate decisions by *CLAVATA3* in *Arabidopsis* shoot meristems. Science **283,** 1911-1914.

**Florquin, K., Saeys, Y., Degroeve, S., Rouze, P., and Van de Peer, Y.** (2005). Large-scale structural analysis of the core promoter in mammalian and plant genomes. Nucleic Acids Research **33,** 4255-4264.

**Gendall, A.R., Levy, Y.Y., Wilson, A., and Dean, C.** (2001). The *VERNALIZATION 2* gene mediates the epigenetic regulation of vernalization in *Arabidopsis*. Cell **107,** 525-535.

**Goldshmidt, A., Alvarez, J.P., Bowman, J.L., and Eshed, Y.** (2008). Signals derived from *YABBY* gene activities in organ primordia regulate growth and partitioning of *Arabidopsis* shoot apical meristems. Plant Cell **20,** 1217-1230.

**Goodrich, J., Puangsomlee, P., Martin, M., Long, D., Meyerowitz, E.M., Coupland, G.** (1997). A polycomb-group gene regulates homeotic gene expression in Arabidopsis. Nature **386** 44-51.

**Greb, T.** (2003) Untersuchungen zur Rolle des Gens *LATERAL SUPPRESSOR* in der Seitentriebentwicklung von *Arabidopsis thaliana* H. und der Tomate (*Lycopersicon esculentum* M.). Inaugural-Dissertation zur Erlangung des Doktorgrades der Mathematisch-Naturwissenschaftlichen Fakultät der Universität zu Köln.

**Greb, T., Clarenz, O., Schafer, E., Muller, D., Herrero, R., Schmitz, G., and Theres, K.** (2003). Molecular analysis of the *LATERAL SUPPRESSOR* gene in *Arabidopsis* reveals a conserved control mechanism for axillary meristem formation. Genes & Development **17,** 1175-1187.

**Grossniklaus, U., Vielle-Calzada, J.P., Hoeppner, M.A., Gagliano, W.B.** (1998). Maternal control of embryogenesis by MEDEA, a polycomb group gene in Arabidopsis. Science **280**, 446-450.

**Hanahan, D.** (1983). Studies on Transformation of *Escherichia coli* with Plasmids. Journal of Molecular Biology **166,** 557-580.

**Heisler, M.G., Ohno, C., Das, P., Sieber, P., Reddy, G.V., Long, J.A., and Meyerowitz, E.M.** (2005). Patterns of auxin transport and gene expression during primordium development revealed by live imaging of the *Arabidopsis* inflorescence meristem. Current Biology **15,** 1899-1911.

**Helariutta, Y., Fukaki, H., Wysocka-Diller, J., Nakajima, K., Jung, J., Sena, G., Hauser, M.T., and Benfey, P.N.** (2000). The *SHORT-ROOT* gene controls radial patterning of the *Arabidopsis* root through radial signaling. Cell **101,** 555-567.

**Henderson, I.R., and Jacobsen, S.E.** ***(2007).*** Epigenetic inheritance in plants. Nature **447,** 418-424.

**Hindemitt, T., and Mayer, K.F.X.** (2005). CREDO: a web-based tool for computational detection of conserved sequence motifs in noncoding sequences. Bioinformatics **21,** 4304-4306.

**Honma, T., and Goto, K.** (2000). The *Arabidopsis* floral homeotic gene *PISTILLATA* is regulated by discrete cis-elements responsive to induction and maintenance signals. Development **127,** 2021-2030.

**Hughes, J.D., Estep, P.W., Tavazoie, S., and Church, G.M.** (2000). Computational identification of cis-regulatory elements associated with groups of functionally related genes in *Saccharomyces cerevisiae*. Journal of Molecular Biology **296,** 1205-1214.

**Jackson, J.P., Johnson, L., Jasencakova, Z., Zhang, X., PerezBurgos, L., Singh, P.B., Cheng, X.D., Schubert, I., Jenuwein, T., and Jacobsen, S.E.** (2004). Dimethylation of histone H3 lysine 9 is a critical mark for DNA methylation and gene silencing in *Arabidopsis thaliana*. Chromosoma **112,** 308-315.

**Jackson, J.P., Lindroth, A.M., Cao, X.F., and Jacobsen, S.E.** (2002). Control of CpNpG DNA methylation by the KRYPTONITE histone H3 methyltransferase. Nature **416,** 556-560.

**Jepsen, K., Rosenfeld, M.G.,** (2002). Biological roles and mechanistic actions of corepressor complexes. J Cell Sci **115**, 689-98.

**Johanson, U., West, J., Lister, C., Michaels, S., Amasino, R., and Dean, C.** (2000). Molecular analysis of *FRIGIDA*, a major determinant of natural variation in *Arabidopsis* flowering time. Science **290,** 344-347.

**Kalinina, A., Mihajlovic, N., and Grbic, V.** (2002). Axillary meristem development in the branchless Zu-0 ecotype of *Arabidopsis thaliana*. Planta **215,** 699-707.

**Kent, W.J., Sugnet, C.W., Furey, T.S., Roskin, K.M., Pringle, T.H., Zahler, A.M., and Haussler, D.** (2002). The human genome browser at UCSC. Genome Research **12,** 996-1006.

**Koncz, C., Schell, J.** (1986). The promoter of TL-DNA gene 5 controls the tissue-specific expression of chimaeric genes carried by a novel type of Agrobacterium binary vector. Mol Gen Genet **204**, 383-396.

**Krichevsky, A., Gutgarts, H., Kozlovsky, S.V., Tzfira, T., Sutton, A., Sternglanz, R., Mandel, G., and Citovsky, V.** (2007). C2H2 zinc finger-SET histone methyltransferase is a plant-specific chromatin modifier. Developmental Biology **303,** 259-269.

**Krichevsky, A., Kozlovsky, S.V., Gutgarts, H., and Citovsky, V.** (2007b). *Arabidopsis* co-repressor complexes containing polyamine oxidase-like proteins and plant-specific histone methyltransferases. Plant Signaling & Behavior **2,** 174-177.

**Laux, T., Mayer, K.F.X., Berger, J., and Jurgens, G.** (1996). The *WUSCHEL* gene is required for shoot and floral meristem integrity in *Arabidopsis*. Development **122,** 87-96.

**Lee, J-Y., Colinas, J., Wang, J. Y., Mace, D., Ohler, U., Benfey, P. N.** (2006). Transcriptional and posttranscriptional regulation of transcription factor expression in Arabidopsis roots. PNAS **15**, 6055–6060.

**Li, J.J., and Herskowitz, I.** (1993). Isolation of ORC6, a component of the yeast origin recognition complex by a one-hybrid system. Science **262,** 1870-1874.

**Lister, R., O'Malley, R.C., Tonti-Filippini, J., Gregory, B.D., Berry, C.C., Millar, A.H., and Ecker, J.R.** (2008). Highly integrated single-base resolution maps of the epigenome in *Arabidopsis*. Cell **133,** 523-536.

**Long, J. and Barton, M.K.** (2000). Initiation of Axillary and Floral Meristems in Arabidopsis. Developmental Biology **218**, 341–353.

**Luo, M., Bilodeau, P., Koltunow, A., Dennis, E.S., Peacock, W.J., Chaudhury, A.M.** (1999). Genes controlling fertilizationindependent seed development in Arabidopsis thaliana. Proc. Natl. Acad. Sci. USA **96**, 296-301.

**Lynn, K., Fernandez, A., Aida, M., Sedbrook, J., Tasaka, M., Masson, P., and Barton, M.K.** (1999). The *PINHEAD/ZWILLE* gene acts pleiotropically in *Arabidopsis* development and has overlapping functions with the *ARGONAUTE1* gene. Development **126,** 469-481.

**Molina, C., and Grotewold, E.** (2005). Genome wide analysis of *Arabidopsis* core promoters. BMC Genomics **6**.

**Morgenstern, B.** (1999). DIALIGN 2: improvement of the segment-to-segment approach to multiple sequence alignment. Bioinformatics **15,** 211-218.

**Morgenstern, B., Prohaska, S.J., Pohler, D., and Stadler, P.F.** (2006). Multiple sequence alignment with user-defined anchor points. Algorithms for Molecular Biology **1,** 6.

**Muller, D., Schmitz, G., and Theres, K.** (2006). *Blind* homologous *R2R3 Myb* genes control the pattern of lateral meristem initiation in *Arabidopsis*. Plant Cell **18,** 586-597.

**Murashige, T., and Skoog, F.** (1962). A revised medium for rapid growth and bio assays with tobacco tissue cultures. Physiologia Plantarum **15,** 473-497.

**Ng, D.W.K., Wang, T., Chandrasekharan, M.B., Aramayo, R., Kertbundit, S., and Hall, T.C.** (2007). Plant SET domain-containing proteins: Structure, function and regulation. Biochimica Et Biophysica Acta-Gene Structure and Expression **1769,** 316-329.

**Ohad, N., Yadegari, R., Margossian, L., Hannon, M., Michaeli, D., Harada, J.J., Goldberg, R.B., Fischer, R.L.** (1999). Mutations in FIE, a WD polycomb group gene, allow endosperm development without fertilization. Plant Cell **11**, 407-416.

**Pedersen, A.G., Baldi, P., Chauvin, Y., and Brunak, S.** (1999). The biology of eukaryotic promoter prediction - a review. Computers & Chemistry **23,** 191-207.

**Pluthero, F.G.** (1993). Rapid purification of high-activity Taq DNA polymerase. Nucleic Acids Research **21,** 4850-4851.

**Raman, S.** (2006) Genetic analysis of axillary meristem development in *Arabidopsis*: roles of *MIR164, CUC1, CUC2, CUC3* and *LAS*, and identification of novel regulators. Inaugural–Dissertation zur Erlangung des Doktorgrades der Mathematisch-Naturwissenschaftlichen Fakultät der Universität zu Köln. 101 p.

**Raman, S., Greb, T., Peaucelle, A., Blein, T., Laufs, P., and Theres, K.** (2008). Interplay of miR164, *CUP-SHAPED COTYLEDON* genes and *LATERAL SUPPRESSOR* controls axillary meristem formation in *Arabidopsis thaliana*. Plant Journal **55,** 65-76.

**Ratcliffe, O.J., Kumimoto, R.W., Wong, B.J., and Riechmann, J.L.** (2003). Analysis of the *Arabidopsis MADS AFFECTING FLOWERING* gene family: *MAF2* prevents vernalization by short periods of cold. Plant Cell **15,** 1159-1169.

**Reyes, J.C.** (2006). Chromatin modifiers that control plant development. Current Opinion in Plant Biology **9,** 21-27.

**Rhoades, M.W., Reinhart, B.J., Lim, L.P., Burge, C.B., Bartel, B., and Bartel, D.P.** (2002). Prediction of plant microRNA targets. Cell **110,** 513-520.

**Rozen, S., and Skaletsky, H.** (2000). Primer3 on the WWW for general users and for biologist programmers. Methods in Molecular Biology **132,** 365-386.

**Sabatini, S., Heidstra, R., Wildwater, M., and Scheres, B.** (2003). *SCARECROW* is involved in positioning the stem cell niche in the *Arabidopsis* root meristem. Genes & Development **17,** 354-358.

**Sambrook, J. and Russel, D.W.** (2001) "Molecular Cloning: A Laboratory Manual," 3rd Edition. Cold Spring Harbor Laboratory Press, NY.

**Schmid, M., Uhlenhaut, N.H., Godard, F., Demar, M., Bressan, R., Weigel, D., and Lohmann, J.U.** (2003). Dissection of floral induction pathways using global expression analysis. Development **130,** 6001-6012.

**Schmitt, T.** (1999) Isolierung und Charakterisierung des *Lateral suppressor*-Gens aus *Lycopersicum esculentum* M. Inaugural-Dissertation zur Erlangung des Doktorgrades der Mathematisch-Naturwissenschaftlichen Fakultät der Universität zu Köln.

**Schmitz, G., and Theres, K.** (2005). Shoot and inflorescence branching. Current Opinion in Plant Biology **8,** 506-511.

**Schoof, H., Lenhard, M., Haecker, A., Mayer, K.F.X., Jurgens, G., and Laux, T.** (2000). The stem cell population of *Arabidopsis* shoot meristems is maintained by a regulatory loop between the *CLAVATA* and *WUSCHEL* genes. Cell **100,** 635-644.

**Schubert, D., Clarenz, O., and Goodrich, J.** (2005). Epigenetic control of plant development by Polycomb-group proteins. Current Opinion in Plant Biology **8,** 553-561.

**Schubert, D., Primavesi, L., Bishopp, A., Roberts, G., Doonan, J., Jenuwein, T., and Goodrich, J.** (2006). Silencing by plant Polycomb-group genes requires dispersed trimethylation of histone H3 at lysine 27. Embo Journal **25,** 4638-4649.

**Schultz, E.A., and Haughn, G.W.** (1991). *LEAFY*, a homeotic gene that regulates inflorescence development in *Arabidopsis*. Plant Cell **3,** 771-781.

**Schultz, J., Milpetz, F., Bork, P., and Ponting, C.P.** (1998). SMART, a simple modular architecture research tool: Identification of signaling domains. Proceedings of the National Academy of Sciences of the United States of America **95,** 5857-5864.

**Schulze, S.** (2007) Charakterisierung *HAIRY MERISTEM*-ähnlicher Gene und Identifizierung neuer Regulatoren der Seitentriebentwicklung in *Arabidopsis thaliana.* Inaugural-Dissertation zur Erlangung des Doktorgrades der Mathematisch-Naturwissenschaftlichen Fakultät der Universität zu Köln

**Schumacher, K.** (1995) Markergestützte Klonierung von Kandidaten für das *Lateral suppressor* Gen der Tomate *Lycopersicum esculentum* M. Inaugural-Dissertation zur Erlangung des Doktorgrades der Mathematisch-Naturwissenschaftlichen Fakultät der Universität zu Köln.

**Schumacher, K., Schmitt, T., Rossberg, M., Schmitz, C., and Theres, K.** (1999). The *Lateral suppressor* (*Ls*) gene of tomato encodes a new member of the VHIID protein family. Proceedings of the National Academy of Sciences of the United States of America **96,** 290-295.

**Searle, I., He, Y.H., Turck, F., Vincent, C., Fornara, F., Krober, S., Amasino, R.A., and Coupland, G.** (2006). The transcription factor FLC confers a flowering response to vernalization by repressing meristem competence and systemic signaling in *Arabidopsis*. Genes & Development **20,** 898-912.

**Sessions, A., Weigel, D., and Yanofsky, M.F.** (1999). The *Arabidopsis thaliana MERISTEM LAYER 1* promoter specifies epidermal expression in meristems and young primordia. Plant Journal **20,** 259-263.

**Shahmuradov, I.A., Gammerman, A.J., Hancock, J.M., Bramley, P.M., and Solovyev, V.V.** (2003). PlantProm: a database of plant promoter sequences. Nucleic Acids Research **31,** 114-117.

**Shahmuradov, I.A., Solovyev, V.V., and Gammerman, A.J.** (2005). Plant promoter prediction with confidence estimation. Nucleic Acids Research **33,** 1069-1076.

**Simpson, G.G.** (2004). The autonomous pathway: epigenetic and post-transcriptional gene regulation in the control of *Arabidopsis* flowering time. Current Opinion in Plant Biology **7,** 570-574.

**Smyth, D.R., Bowman, J.L., and Meyerowitz, E.M.** (1990). Early flower development in Arabidopsis. Plant Cell **2,** 755-767.

**Springer, N.M., Napoli, C.A., Selinger, D.A., Pandey, R., Cone, K.C., Chandler, V.L., Kaeppler, H.F., and Kaeppler, S.M.** (2003). Comparative analysis of SET domain proteins in maize and *Arabidopsis* reveals multiple duplications preceding the divergence of monocots and dicots. Plant Physiology **132,** 907-925.

**Steimer, A., Schob, H., and Grossniklaus, U.** (2004). Epigenetic control of plant development: new layers of complexity. Current Opinion in Plant Biology **7,** 11-19.

**Stuurman, J., Jaggi, F., and Kuhlemeier, C.** (2002). Shoot meristem maintenance is controlled by a *GRAS*-gene mediated signal from differentiating cells. Genes & Development **16,** 2213-2218.

**Thijs, G., Lescot, M., Marchal, K., Rombauts, S., De Moor, B., Rouze, P., and Moreau, Y.** (2001). A higher-order background model improves the detection of promoter regulatory elements by Gibbs sampling. Bioinformatics **17,** 1113-1122.

**Thomas, H., Thomas, H.M., and Ougham, H.** (2000). Annuality, perenniality and cell death. Journal of Experimental Botany **51,** 1781-1788.

**Thompson, J.D., Higgins, D.G., and Gibson, T.J.** (1994). CLUSTALW: Improving the sensitivity of progressive multiple sequence alignment through sequence weighting, position-specific gap penalties and weight matrix choice. Nucleic Acids Research **22,** 4673-4680.

**Thorstensen, T., Fischer, A., Sandvik, S.V., Johnsen, S.S., Grini, P.E., Reuter, G., and Aalen, R.B.** (2006). The *Arabidopsis* SUVR4 protein is a nucleolar histone methyltransferase with preference for monomethylated H3K9. Nucleic Acids Research **34,** 5461-5470.

**Uberlacker, B., and Werr, W.** (1996). Vectors with rare-cutter restriction enzyme sites for expression of open reading frames in transgenic plants. Molecular Breeding **2,** 293-295.

**Völkel, P., and Angrand, P.O.** (2007). The control of histone lysine methylation in epigenetic regulation. Biochimie **89,** 1-20.

**Wang, R.H., Farrona, S., Vincent, C., Joecker, A., Schoof, H., Turck, F., Alonso-Blanco, C., Coupland, G., and Albani, M.C.** (2009). *PEP1* regulates perennial flowering in *Arabis alpina*. Nature **459,** 423-U138.

**Winter, D., Vinegar, B., Nahal, H., Ammar, R., Wilson, G.V., and Provart, N.J.** (2007). An "electronic fluorescent pictograph" browser for exploring and analyzing large-scale biological data sets. PLoS One **2,** e718.

**Yang, F.** (2007) Identification and characterization of interactors of *RAX1* controlling shoot branching in *Arabidopsis thaliana.* Inaugural-Dissertation zur Erlangung des Doktorgrades der Mathematisch-Naturwissenschaftlichen Fakultät der Universität zu Köln.

**Yoshida, N., Yanai, Y., Chen, L., Kato, Y., Hiratsuka, J., Miwa, T, Sung, Z.R., Takahashi, S.** (2001). EMBRYONIC FLOWER2, a novel polycomb group protein homolog, mediates shoot development and flowering in Arabidopsis. Plant Cell **13**, 2471-2481.

# Abstract

Aerial architecture of flowering plants is largely based on the activities of the shoot apical meristem and axillary meristems (AM), which are initiated in the axils of leaves. The *LATERAL SUPPRESSOR* (*LAS*) loss-of-function mutant is characterized by a lack AM development during the vegetative growth phase, identifying *LAS* as a key regulator of this process. *LAS* is expressed in a very specific band-shaped domain at the adaxial side of leaf primordia, the site of later formation of AMs. In order to understand how this specific expression pattern is established, and to be able to subsequently address the question which factors control *LAS*, the *LAS* promoter was analyzed in detail in this work.

Complementation of the *las-4* phenotype with various promoter deletion constructs revealed that less than 117 bp 5' of the transcription start are necessary for gene function. However, the ability to complement is lost when constructs harbor less than 3547 bp of 3' sequences. The importance of the 3' region is emphasized by results showing that complementation is still achieved if the 5' promoter is replaced by a minimal 35S promoter or a *PISTILLATA* (*PI*) promoter fragment, which does not confer expression in the apex. In both cases visualization of expression profiles using promoter GUS constructs showed specific expression in axils of leaves and flowers, alike the endogenous *LAS* promoter activity. In summary an *LAS* 3' promoter element, extending from bp 3239 to 3547 behind the ORF, was found to be necessary for complementation. It is tempting to speculate that it is this element, which causes the highly specific *LAS* expression pattern.

A previous *las-4* second site modifier screen led to the identification of the new regulator of AM development *ENHANCER OF LATERAL SUPPRESSOR 5* (*EOL5*). The *eol5 las-4* double mutant was identified owing to the lack of AM formation in cauline leaf axils. Additionally, *eol5 las-4* plants could be shown to exhibit leaf fusions and defects in meristem maintenance and floral primordia development. The gene underlying the *eol5* mutation could be identified by map based cloning as *CZS*, a putative histone methyl transferase, previously shown to be involved in the epigenetic regulation of *FLOWERING LOCUS C* (*FLC*) and displays a mild delay of flowering. Complementation with an endogenous *pCZS::CZS* construct led to a recovery of the ability to form axillary shoots in cauline leaf axils, likewise an allelism test showed that the T-DNA insertion alleles *czs-1* and *czs-2* are allelic to *eol5*. However, the single mutant phenotype of *eol5* is more

pronounced, leading to a lack of AM formation in most rosette leaf axils, whereas *czs-1* and *czs-2* plants only exhibited few barren axils in the lower rosette. Accordingly, the delay of flowering observed in long day conditions was most distinct in *eol5* plants.

To address the question which genes are regulated by *CZS*, the expression of various candidates was compared between mutants and wild-type by real-time PCR. *FLC* could be shown to be upregulated in *czs* mutants. Analysis of *FRI FLC* plants, which strongly express *FLC*, revealed side shoot development defects, suggesting that *FLC* is involved in the process of AM formation. This indicates that similar mechanisms regulate lateral meristem development and flowering, thus the AM initiation defects observed in *czs* mutants are likely to be caused by the upregulation of *FLC*.

# Zusammenfassung

Die oberirdische Architektur von Samenpflanzen wird durch die Aktivitäten des Sprossapikalmeristems und der Achselmeristeme bestimmt, die in den Achseln aller Blätter angelegt werden. Die *lateral suppressor (las)*-Mutante in *Arabidopsis* ist gekennzeichnet durch das Ausbleiben der Achselmeristemanlage während der vegetativen Entwicklung. Dies zeigt, dass *LAS* eine zentrale Rolle in der Regulation von Lateralmeristemen spielt. *LAS* wird in einer sehr spezifischen Domäne an der adaxialen Seite von Blattprimordien exprimiert, wo später Achselmeristeme gebildet werden. Um zu verstehen wie dieses Expressionsmuster entsteht, und um später Regulatoren von *LAS* identifizieren zu können, wurde in dieser Arbeit eine detaillierte Promotoranalyse durchgeführt.

Eine Komplementation des *las-4* Phänotyps mit verschiedenen Promotor-Deletionskonstrukten zeigte, dass weniger als 117 bp im 5'-Bereich des Transkriptionsstarts für die Genfunktion notwendig sind. Es wurde jedoch keine Komplementationsfähigkeit mehr festgestellt, wenn die Konstrukte weniger als 3547 bp der 3'-Sequenzen enthielten. Die Bedeutung der 3'-Region wird dadurch verdeutlicht, dass eine Komplementation auch dann erreicht werden kann, wenn der 5'-Promotor vollständig durch einen 35S CaMV Minimalpromotor oder durch ein *PISTILLATA* (*PI*)-Promotorfragment ersetzt wird, welche selbst keine Expression im Apex hervorrufen. In beiden Fällen zeigte eine Visualisierung des Expressionsprofils mittels Promotor-GUS-Konstrukten eine spezifische Expression in den Achseln von Blättern und Blüten, vergleichbar mit der endogenen *LAS*-Promotoraktivität (RNA *in situ* Hybridisierung). Zusammenfassend konnte ein *LAS*-Promotorbereich identifiziert werden, der 3235 bis 3547 bp hinter dem offenen Leseraster des *LAS*-Gens liegt und für die Komplementationsfähigkeit notwendig ist. Die Vermutung liegt nahe, dass dieses Promotorelement, unabhängig von anderen Promotoren in der Umgebung, das spezifische *LAS*-Expressionsmuster hervorruft.

In einer früheren Durchmusterung einer Population mutagenisierter *las-4*-Pflanzen konnte der neue Regulator der AM-Entwicklung, *ENHANCER OF LATERAL SUPPRESSOR 5* (*EOL5*), gefunden werden. Die *eol5 las-4* Doppelmutante hat die Fähigkeit Seitentriebe in den Achseln von Stängelblättern anzulegen verloren und zeigt Fusionen von Blättern sowie

Defekte in der Erhaltung des Sprossapikalmeristems and der Bildung von Blütenprimordien. Das der *eol5*-Mutation zugrunde liegende Gen konnte durch markergestützte Kartierung als *CZS* identifiziert werden. Vorangegangene Arbeiten zeigten, dass *CZS* wahrscheinlich eine Histonmethyltransferase kodiert, die an der epigenetischen Regulation von *FLOWERING LOCUS C* (*FLC*) beteiligt ist.

Eine Transformation der *eol5 las-4*-Mutante mit einem *pCZS::CZS*-Konstrukt führte zu einer partiellen Komplementation des Defektes der Seitentriebbildung. Außerdem konnte in einem Allelietest festgestellt werden, dass *eol5* und die T-DNA-Insertionsallele *czs-1* und *czs-2* allelisch sind. Allerdings zeigte die *eol5*-Einzelmutante, mit dem Fehlen fast aller AM in der vegetativen Phase, einen deutlich stärker ausgeprägten Phänotyp als *czs-1* und *czs-2*-Pflanzen, in denen nur einzelne Achseln im unteren Bereich der Blattrosette betroffen waren. Ebenso konnte in *eol5*-Pflanzen die deutlichste Verschiebung des Blühzeitpunktes beobachtet werden.

Um die Frage zu beantworten, welche Gene von *CZS* reguliert werden, wurde die Expression verschiedener Kandidatengene in Wildtyp und Mutanten mit Hilfe von Echtzeit-PCR verglichen. Hier konnte gezeigt werden, dass die *FLC*-Transkription in *czs*-Mutanten erhöht ist. Eine Analyse von *FRI FLC*-Pflanzen, in denen die *FLC*-Expression deutlich verstärkt ist, offenbarte Defekte in der Achselmeristemanlage, die belegen, dass *FLC* eine Rolle in der Achselmeristementwicklung spielt. Dies führt zu der Hypothese, dass die Lateralmeristementwicklung und die Regulation des Blühzeitpunktes einem gemeinsamen Mechanismus unterliegen. Daraus ergibt sich, dass die in *czs*-Mutanten beobachteten Defekte der AM-Initiation möglicherweise auf eine Deregulierung von *FLC* zurückzuführen sind.

# Erklärung

Die vorliegende Arbeit wurde am Max-Planck-Institut für Züchtungsforschung in Köln-Vogelsang durchgeführt.

Ich versichere, dass ich die von mir vorgelegte Dissertation selbständig angefertigt, die benutzten Quellen und Hilfsmittel vollständig angegeben und die Stellen der Arbeit – einschließlich Tabellen, Karten und Abbildungen –, die anderen Werken im Wortlaut oder dem Sinn nach entnommen sind, in jedem Einzelfall als Entlehnung kenntlich gemacht habe; dass diese Dissertation noch keiner anderen Fakultät oder Universität zur Prüfung vorgelegen hat; dass sie noch nicht veröffentlicht worden ist sowie, dass ich eine solche Veröffentlichung vor Abschluss des Promotionsverfahrens nicht vornehmen werde. Die Bestimmungen dieser Promotionsordnung sind mir bekannt. Die von mir vorgelegte Dissertation ist von Professor Dr. Klaus Theres betreut worden.

Köln, 4.10.2009

Bodo Raatz